Structure-Property Relationships and Salt Selection for Functional Organic Materials

Aiden Walls

University of Strathclyde

Department of Pure and Applied Chemistry

Structure-Property Relationships and Salt Selection for Functional Organic Materials

Aiden Walls

Thesis submitted to the Department of Pure and Applied Chemistry, University of Strathclyde, in fulfilment of the requirement for degree of Master of Philosophy.

This thesis is the result of the author's original research. It has been composed by the author and has not been previously submitted for examination which has led to the award of a degree.

The copyright of this thesis belongs to the author under the terms of the United Kingdom Copyright Act as qualified by the University of Strathclyde Regulation 3.49. Due acknowledgement must always be made of the use of any material contained in, or derived from, this thesis.

Signed:

Date:

Acknowledgements

First I would like to thank my supervisor, Dr A Kennedy for his continued guidance and support throughout this research project. His help and encouragement has greatly contributed to making this experience both enjoyable and invaluable to my development in research.

I would also like to thank the academic staff within the R6.17 office; Dr C. Dodds, Dr M. Rodgers and Dr M. Spicer for their advice and support. I also thank the students I have worked with during my studies for making my time in the office and the laboratory enjoyable.

Finally, I would like to thank my family and friends for their support throughout my studies.

Abstract

Eleven salt forms of salicylic acid were prepared, all of which contained strontium or calcium as counterions with nine of the eleven samples containing a mix of both metals which occupied the same crystallographic site. Ten of these forms were successfully characterised by single crystal diffraction, these shared the formula $[Ca_{(1-x)}Sr_x(C_7H_5O_3)_2(OH_2)_2]$ with x having the following values: 0, 0.041, 0.083, 0.165, 0.306, 0.529, 0.632, 0.789, 0.835 and 1. The calcium to strontium ratios of each sample was also measured using atomic absorption spectroscopy and reported. The aqueous solubility of each sample was also measured. Systematic changes to structure and to solubility with changing metal ratio are reported.

Thirteen previously unpublished organic complexes of 4-nitrophenol (NPOH or 4-nitrophenolate NPO) were prepared and had their crystal structures elucidated. These were: 1S2R-(+)-methylephedrine-NPO, 2-amino-3-pyridinecarboxaldehyde - NPOH, 4-acetylpyridine-NPOH, 2-aminobenzylamine-NPO, dimethylpiperidine-NPO(H_2O), dipropylenetriamine-NPO, 1S2R-(+)-ephedrine-NPO$(MeCN)_2$, ethanolamine-NPO, n-methylpyrollidine-NPO-NPOH, Rhodamine B-NPOH$(MeCN)_2$, tris-2-amino-ethylenetriamine-NPO$(H_2O)_2$, isopropylamine-NPO(H_2O) and 1,4-diaminobutane-NPO. These 13 structures were compared to 50 structures containing NPOH or NPO found on the Cambridge Structural Database (CSD).

Hydrogen bonding and other intermolecular interactions were studied extensively in an attempt to find common interactions which could be linked to the apparent tendency for 4-nitrophenol materials to crystallise in non-centrosymmetric space groups. This included a study of packing analysis and graph set notations. Two separate isostructural groups of cocrystal of salt structures were found to share packing similarities. Potential links between non-centrosymmetric packing and hydrogen bonding, chemical type and pKa values are evaluated.

Table of Contents

Acknowledgements i

Abstract ii

Table of Contents iii

1. Introduction…… 1

1.1 The use of amorphous materials…….. 3

1.2 Polymorphism…… 4

1.2.1 Examples of polymorphism in industry…… 4

1.3 The use of co-crystalline materials…….. 8

1.3.1 Hydrates and solvates…… 10

1.4 Salt screening…… 12

1.5 Mixed metal salt forms…… 15

1.6 Non Linear Optically active materials…… 17

1.7 Aims…… 22

2. Experimental…… 23

2.1 Mixed metal salt forms…… 23

2.1.1 Mixed metal salts of salicylic acid…… 23

2.1.2 Solubility tests…… 25

2.2 NLO materials…… 26

2.3 Attempted synthesis of Ca/Sr mixed metal salts of NPOH…… 45

2.4 X-ray diffraction experiments…… 45

3. Results…… 47

3.1 Mixed metal solid state solutions…… 47

3.2 NLO 4-nitrophenol materials…… 57

3.2.1 Analysis of pKa values of coformers…… 59

3.2.2 Molecular structures of coformers studied…… 61
3.2.3 Structural evaluation of 4-nitrophenol complexes…… 72
3.2.4 Overview of intermolecular interactions……. 73
3.2.5 Overview of hydrogen bonding…….. 74
3.2.6 Analysis of NPOH-NPO planar angles…… 75
3.2.7 Analysis of hydrogen bond acceptor-donor ratios…….. 78
3.2.7.1 Analysis of hydrogen bond acceptor-donor ratios of hydrate structures…… 79
3.2.8 Crystal structure analysis……. 80
3.2.9 Crystal packing similarity analysis……. 82
3.2.10 Graph set analysis……. 89
3.2.10.1 Comparison of isostructural crystal packing groups to all cocrystal of salt structures…… 96
3.3 Summary of NPOH material structural analysis…… 101

4. Conclusion…….. 104
Further work……. 115
References…….. 108
Appendix…….. 115
Publications arising during MPhil year…… 124

1. Introduction

For solid state materials it is becoming increasingly apparent that material properties governing delivery and use of a material is often as important to successfully commercialising its use as is the material's capacity to perform the prime functionality that it was originally designed for. This is especially well appreciated in the pharmaceutical industry. Aakeroy et. al [1] claimed only 1 % of drug molecules undergoing trial reach the final market with many failing due to problems associated with physicochemical properties. Problems such as low aqueous solubility or lack of manufacturability [1]. With an increasing number of poorly soluble drug molecules undergoing trials in recent years [2] the ability to improve the linked properties of solubility, dissolution rate and hence bioavailability would be highly desirable.

Other material properties are also highly important during manufacturing of both pharmaceuticals and other fine chemicals. Properties such as material strength (influencing behaviour during grinding and tableting), habit, morphology and crystal size (effecting material transport during manufacture) and melting point and general reactivity such as hygroscopicity (effecting the stability of the material during manufacturing and storage) can all influence the success of a product. Due to this, there is a high demand for the ability to alter the physicochemical properties of a solid material without changing its prime functionality.

Many of the properties of a solid material are determined by the intermolecular interactions which constitute the solid state structure [3-15]. Therefore the properties of a solid can be influenced by changing the intermolecular interactions which influence the solid state structure [3-15]. Changing the target molecule itself can often change the functionality of a molecule and computational systems have been developed to attempt to calculate these changes [16]. However testing the physicochemical properties of a material for manufacture often happens late in the development process where a change in functionality is undesirable [5]. When

attempting to tune the properties of a material it is often favourable to change the solid state structure rather than the molecule itself.

When attempting to alter the solid state of a material four methods are commonly investigated:

- The use of amorphous versus crystalline materials
- Polymorphism
- The use of co-crystalline materials
- The use of salt materials

The use of amorphous materials and polymorphism involves changing purely the solid form of the material and the use of co-crystals and salts involves changing the chemical form.

1.1 The use of amorphous materials

There may be advantages to using an amorphous form of a material rather than the crystalline form during formulation [17]. The amorphous form of a solid is generally the kinetic form and typically is formed much quicker than the thermodynamically favoured crystalline form by ensuring that molecules joining a growing solid are not given time to arrange in such a way to maximise attractive interactions and minimise repulsive interactions. The kinetic amorphous form thus lacks the long range order that the crystalline form contains. Its molecules can be thought to pack in a random order with at most only short range order present [6, 11, 18-19]. Thus for example, an amorphous form of a drug has improved dissolution rate and hence potentially enhanced bioavailability compared to the crystalline equivalent of the same material [6, 20-23].

An example of amorphous material used within the pharmaceutical industry is the use of “fast acting” insulin [24] where the enhanced solubility of the amorphous form allows dissolution into the recipient as quickly as possible. Another example is the use of salbutamol inhalers containing amorphous product where the dissolution rate of the crystalline form is too low for this method of administration to be viable [25].

While the use of the amorphous form presents an interesting way of greatly improving a materials physicochemical properties it is not commonly used due to concerns over product stability [26] (one of the benefits of solid state materials is typically their stability allowing for safe long term storage). Amorphous solids have a tendency to crystallise to the thermodynamic form over time [18, 26, 27]. This spontaneous transformation leads to both legal and practical issues. Further concerns can even arise from the potential for the material to crystallise in the gastrointestinal tract [28].

1.2 Polymorphism

Polymorphism can be defined as the ability for a substance to form different crystalline packing arrangements in 3D space [29]. As the material has packed in a different 3D arrangement we can assume the intermolecular interactions between molecules are different, which leads to potentially different physicochemical properties [8-11, 30, 31]. McCrone once stated “Every compound has different polymorphic forms and that, in general the number of forms for a given compound is proportional to the time and money spent in research on that compound” [32].

Polymorphism can be difficult to control and thorough screening is required to identify all potential metastable forms and the stable thermodynamic form [12, 33, 34]. Due to this, polymorphism can be considered an area of interest as well as an area of concern to a number of industries including; the pharmaceutical industry [20, 35-41], the dyes and pigments industry [15, 42-44] and in the manufacture of explosives [50].

1.2.1 Examples of polymorphism in industry

Three drug molecules which show polymorphism within the pharmaceutical industry include; carbamazepine, ritonavir and paracetamol. Carbamazepine [figure 1] is an anticonvulsant drug used in the treatment of epilepsy that has four known polymorphs as well as a dihydrate form. As is typical, to avoid stability issues it is the most stable form that is commercially used [37-41].

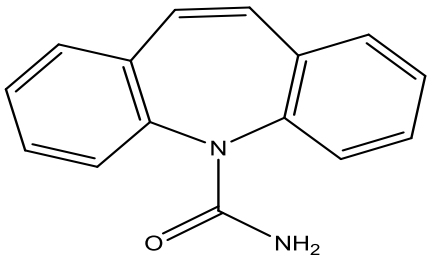

Figure 1: Molecular structure of the anticonvulsant drug carbamazepine.

Ritonavir [FIGURE 2] now has multiple known polymorphs [20, 45]. Form I was originally used as a treatment for HIV delivered as a mixed solvent slurry. This odd formulation was needed as the solid form had relatively low solubility and bioavailability. However, manufacturing problems arose when later batches were found to have even lower solubility. This was later found to be caused by the formation of a previously unknown, second more stable polymorph with lower bioavailability than form I. This suggests that Ritonavir follows Ostwald's rule of stages where a less stable polymorph forms before the thermodynamically stable one [46]. For a time, manufacturing the active form I polymorph became difficult, with the inactive Form II consistently made instead. The financial and reputational damage of this late discovery of a new polymorphic form is what drives much of the pharmacy industry's current interest in understanding polymorphic phase space of their products.

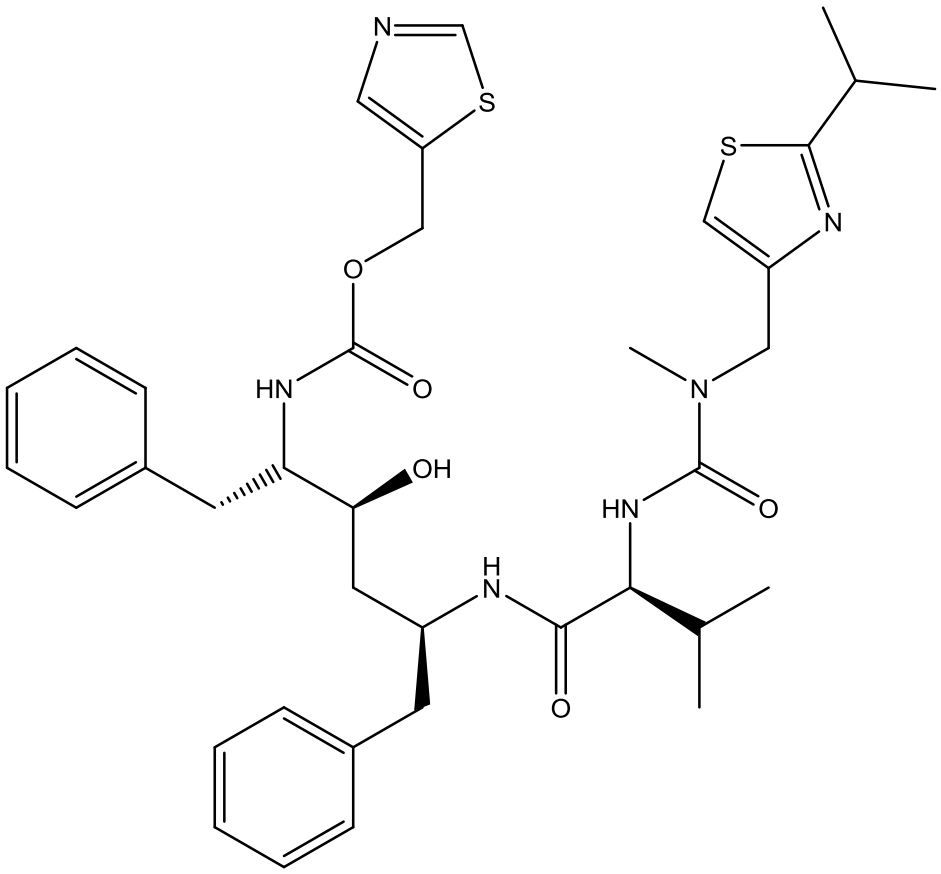

Figure 2: Molecular structure of the HIV treatment drug Ritonavir.

Finally, paracetamol is a common “over the counter” pain relief drug with 3 known polymorphic forms [37-41] where form I is the thermodynamic form and the others are classed as metastable. Paracetamol forms I and II can be seen in figure 3 where form I can be seen to display a “herring bone” packing arrangement and form II appears to form layers which propagate along the crystallographic *b* axis. During manufacture form I has been noted to display low compressibility leading to difficulties manufacturing the pill form while form II shows improved compressibility due to its layered structure. In contrast to the Ritonavir example, this is a case where the variability in polymorphic form may be useful rather than problematic.

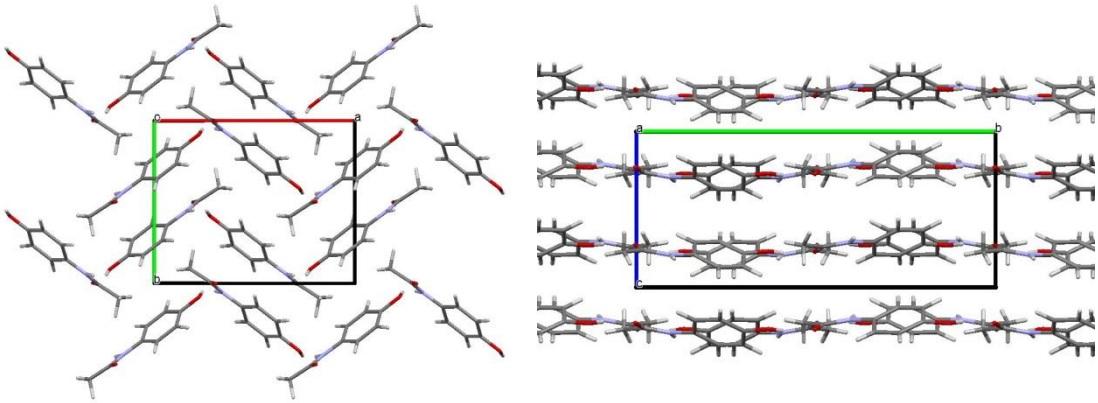

Figure 3: Packing diagrams for Form I (left) of paracetamol and for Form II (right) of paracetamol.

Polymorphism is also an area of interest in other fields, such as for example the dye and pigment industry with polymorphs not only influencing solubility but properties which are more uniquely significant to dyes and pigments such as “fastness” and colour. Polymorphism may not be significant with respect to colour, for example the dye maize 1 displays three polymorphic forms [47] and very little difference in colour is noted between these three forms. However, the highly coloured compound 5-methyl-2-[(2-nitrophenol)amino]-3-thiophenecarbonitrile (ROY) (as seen in figure 4) is an excellent example of colour change due to polymorphism. The compound is known as ROY due to the red, orange or yellow colour of its polymorphs [48].

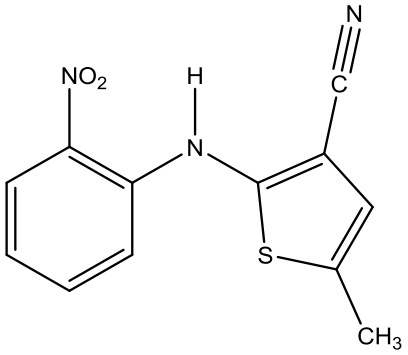

Figure 4: Structure of 5-methyl-2-[(2-nitrophenol)amino]-3-thiophenecarbonitrile (ROY.)

Six crystal structures of polymorphic forms of ROY have been solved making it the most polymorphic organic compound found on the Cambridge Structural Database [48]. McHugh et al. also discuss a chlorinated diketopyrrolepyrrole colourant which is shown to form two polymorphs, one yellow and one red in colour [49].

An interesting study of polymorphism involves the explosive compound 2,4,6-trinitrotoluene (TNT). TNT is one of the most widely used explosive compounds due to its stability over a wide range of temperatures, though concern has arisen from the tendency to form a metastable form from both the melt and growth from solution which converts to the stable form over time [50]. Macroscopic changes such as cracks and voids can form during phase changes, which can lead to unwanted sensitivity of the material to detonation and to general unpredictability of properties. The unit cells of the two TNT polymorphs discussed are seen in figure 5.

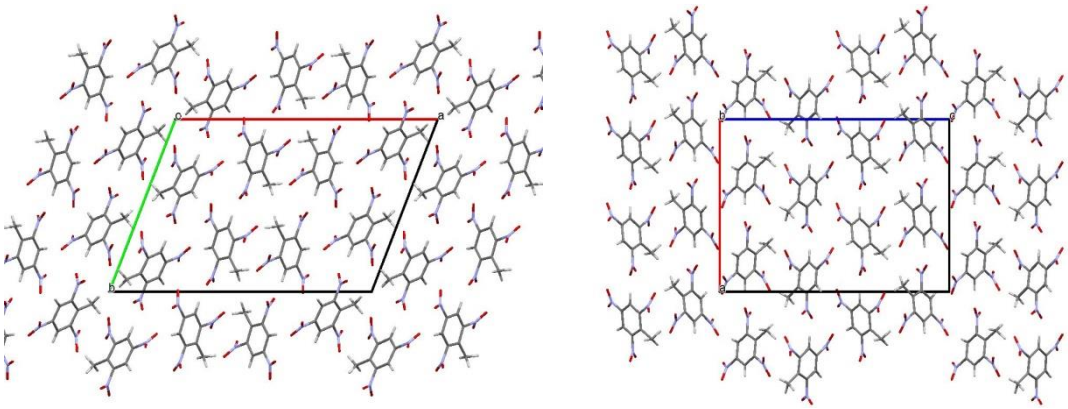

Figure 5: Packing structures of two polymorphic forms of 2,4,6-trinitrotoluene.

While polymorphism offers potential to improve physicochemical properties it is often not studied as a solution but as a problem, with typically the most stable form being used in applications [30]. If a metastable form is used there can be concerns about long term stability and storage with the potential of the material undergoing a phase change to a more stable form with different properties.

1.3 The use of Co-crystalline materials

The definition of a co-crystal is one that is widely debated within the scientific community [5, 29, 51-54]. The official definition described by the Food and Drug Administration (FDA) is given as follows: “solids that are crystalline materials composed of two or more molecules in the same crystal lattice” [55]. This definition sparked controversy at the meeting on the “Evolving Role of Solid State Chemistry in Pharmaceutical Science” where over 70 industrial and academic researchers discussed this matter in attempt to provide a more appropriate definition, the result was the following definition which will be used in this discussion: “Co-crystals are solids that are crystalline single phase materials composed of two or more different molecular and/or ionic compounds generally in a stoichiometric ratio” [5]. This definition would also classify hydrates and solvates as co-crystals and so these will also be discussed in this section. An example of a cocrystal elucidated in this study is the cocrystal formed from 4-nitrophenol and 2-amino-3-pyridinecarboxaldehyde, seen in figure 6.

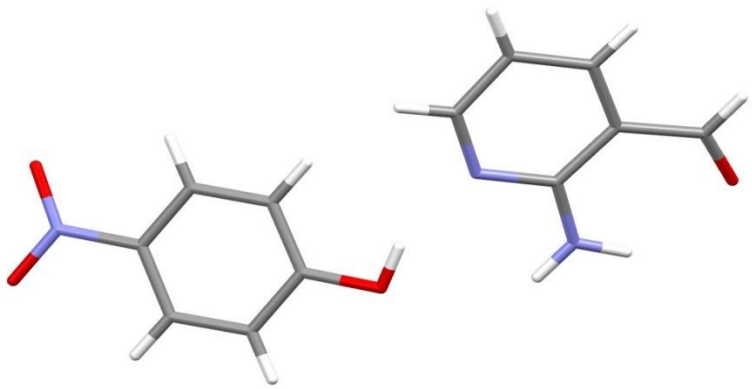

Figure 6: Asymmetric unit of 4-nitrophenol – 2-amino-3-pyridinecarboxaldehyde. Here and throughout, grey = C, red = O, blue = N and white = H.

Co-crystals present an interesting method for potentially changing the physicochemical properties of a material where a new form can be generated through the use of a relatively simple procedure [7]. The use of co-crystals has been of interest to a number of industries, for example the use of co-crystalline materials for gas storage and transport[57], the development of room temperature ferroelectronics[58], production of non-linear optically active (NLO) materials[59] and also pharmaceutical co-crystals[7].

While pharmaceutical co-crystals are a class of material that has been acknowledged for a long time they have not been heavily studied until relatively recently [5]. However, pharmaceutical co-crystals present an opportunity to potentially generate a large spectrum of new Active Pharmaceutical Ingredient (API) forms due to the abundance of potential co-crystallising agents available [1]. While the FDA consider new co-crystalline forms to be novel and therefore can be patented [60] there are still numerous concerns that follow their development and use. For example temperature dependent proton transfer which would change the definition of a solid form from co-crystal to salt upon changing temperature or the potential for the co-crystalline form to recrystallize as the pure API during dissolution [7]. In a recent review of pharmaceutical co-crystals Steed is quoted “No commercial pharmaceutical co-crystal has yet been approved for sale as a drug substance and it will perhaps be a brave drug company with deep pockets that undertakes the first ‘test case’” [7]. Outside of the pharmaceutical industry there is an even larger pool of potential co-crystallising agents such as materials that contain aromatic rings which have the potential to form co-crystals through π stacking [61].

1.3.1 Hydrates and solvates

Under the definition of co-crystals mentioned above, hydrates and solvates can be considered to be co-crystalline forms. A hydrate can be considered an organic compound that contains water as a component of its crystalline structure and a solvate is an organic form that contains non-water solvent molecules as part of its structure (see figure 7 for an example solvate elucidated in this study). Both of these forms can also be considered pseudopolymorphic forms under an older classification scheme [18].

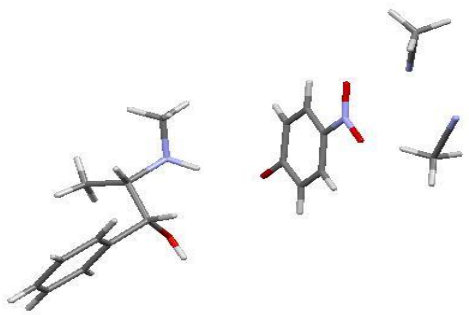

Figure 7:Acetonitrile solvate of Ephedrine Nitrophenolate.

Hydrates are found to be the most common solvate form of organic crystals (for example asparagine hydrate [Figure 8]) with approximately 6.6 % of organic structures uploaded to the Cambridge Structural Database[62] containing water molecules as part of their structure (for structures that met the following criteria: R1>10 %, no disorder, 3d coordinates available, as of January 2002) [63]. Due to the nature of water molecules, they can be considered to stabilise the crystal lattice through the presence of reliable hydrogen bond donors and acceptors [64].

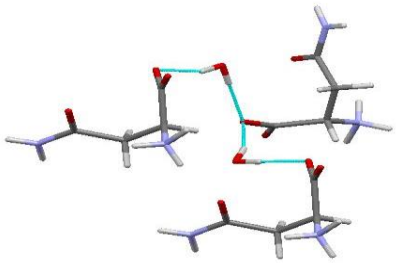

Figure 8: Hydrogen bonding within the hydrate form of asparagine.

In a study of the function of water molecules in the crystal lattice less than 5 % of water molecules in almost 700 examined hydrate structures were found to not form hydrogen bonds with reliable hydrogen bond donors or acceptors [65]. In another study which reviewed hydrate formation it was shown that the presence of formally charged/ionic groups increased the probability of hydrate formation (62 % of Ca^{2+} compounds and 35 % of compounds containing carboxylate groups were found to form hydrates [67]).

While hydrate and solvate formation can be considered a way to change the physicochemical properties of a material, a number of problems can be associated with this method. One problem is the stability of a structure containing water molecules, as the material may undergo dehydration during storage. Another problem related to hydrates, is hygroscopicity where additional water is adsorbed onto the surface of the material leading to potential phase changes and formation of higher hydration states [63]. Both of these could potentially change the material's properties during storage, leading to problems with both licensing and material effectiveness.

It should be noted that generally organic hydrates are less water soluble than their anhydrous equivalents due to the difference in free energy change between the two forms [64].

1.4 Salt screening

The most commonly utilised method for altering problematic material properties found in APIs or other ionisable fine chemicals is salt formation [65-69]. The formation of API salts is typically attempted to improve solubility (and therefore bioavailability and dissolution rate) [67]. Salt forms have been used consistently for over70 years with Nelson reporting a number of pharmaceutical salts in the 1950s [70-71]. Due to the large number of potential salt formers available salt screening has become an important stage in drug development [66] with modern high throughput salt screening methods being developed over the past decades [72-74].

A wide variety of salt formers are available and the property that is widely agreed to be the limiting factor for salt formation is the difference in dissociation constant (pKa) of the anion and cation formers. A ΔpKa of 2 is generally considered enough to assume salt formation will occur between an acid and a base [66]. Pfannkuch et. al proposed a number of different categories to classify API salt formers, with the following description used for their first class of salt formers “First class salt formers can be used more or less without restriction as they represent physiologically ubiquitous ions or occur as metabolites in biochemical pathways” [66]. The salt formers that fit under this classification are those that would be approved for salt formation of APIs and the salt forms found on the FDA orange book database [75].

The most commonly used salt formers in the pharmaceutical industry are chloride and sodium for basic drugs and acidic drugs respectively [68, 76]. An example of a drug molecule where the sodium salt is used is the nonsteroidal anti-inflammatory drug diclofenac. The free acid form is not found on the FDA approved drug list however the sodium and potassium salts are [76].

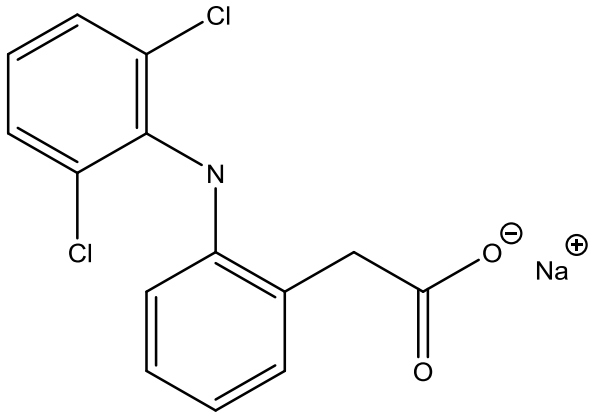

Figure 9: Sodium salt of diclofenac.

The formation of salts displays numerous advantages over the use of the free acid/base form such as a high amount of control over the product formed leading to the ability to produce a consistent solid form [66]. Salt forms tend to show greatly enhanced physicochemical properties such as solubility (a summary of the solubility of a number of drug molecules and their salt forms is given by Weidman et. al. [69]) while also displaying a high level of stability.

Another advantage of salt formation is the simple preparation generally associated with their manufacture and the relatively cheap reagents (HCl and NaOH for chloride and sodium salts respectively). With the wide variety of salt formers available and the simple preparation method, this gives the potential to generate a large number of new API solid forms with pharmaceutically safe counterions such as chlorine and sodium [67, 68, 75, 77].

While salt formation has a number of advantages, there are potential problems. One problem associated with the use of salt forms is the common ion effect. The common ion effect describes a reduction in solubility of an ionic material when added to a solution containing a common ion to the material due to Le Chatelier's principle [78]. The equilibrium associated with the dissociation of an ionic material is described below:

$$CA_{(s)} \rightleftharpoons A^{-}_{(aq)} + C^{+}_{(aq)}$$

And the equilibrium expression for the dissolution is as follows:

$$K_{eq} = \frac{[C^{+}_{(aq)}][A^{-}_{(aq)}]}{CA_{(s)}}$$

An example of the common ion effect in drug manufacture and dosage is the reduction in solubility of chloride salt forms in the $HCl_{(aq)}$ containing gastrointestinal tract [79-80]. From the use of Le Chatelier's principle we can see that the addition of chloride ions to the system (anions) would shift the equilibrium for dissolution of a hydrochloride salt form to the left side, reducing the amount of drug material in solution.

One problem associated with sodium and other s-block metal salts is their hygroscopicity and tendency to form high hydration states. As discussed above, this leads to potential for phase changes and a lower stability.

Of the above mentioned methods of altering the solid state, salt formation is of particular interest to this body of work. While examining structures single crystal X-ray diffraction will be required to fully elucidate and compare solid state structure and properties. With the information obtained from such analyses it would potentially be possible to look at correlations between structure and properties, however information on a series of systematically related structures would be required to do this.

1.5 Mixed metal salt forms

As discussed above, salt selection is the most commonly used method for altering the solid state – both in the pharmaceutical industry and in other industries such as the dye and pigments industry [65-69, 81-83]. This involves choosing a suitable counterion to optimise physicochemical properties. As this also involves changing the solid state interactions and therefore structure, it should in theory be possible to predict any changes to the properties of a material through our understanding of solid state chemistry. However, there is a lack of systematic structural data sets available to support this goal. This is due to the fact that the possibility of analysing large numbers of crystalline samples through single crystal XRD has only been made possible in the last 20 years due to development and increased availability of modern day diffractometers [84]. Another common method to predict the properties of a material is simply by studying/considering its molecular structure, though this is often not as simple a process as might be expected. Frequently unforeseen issues appear while utilising this strategy due to solid state structural interactions. For example it is commonly believed that increasing the number of polar groups present in a molecular structure will increase its solubility in polar solvents, however this is often not true. An increase in polar groups present in a molecular structure can also lead to the formation of strong intermolecular interactions increasing the stability of the solid state and therefore lowering solubility. Such phenomena were seen in a comparative study of salt forms of benzoic and salicylic acid derivatives [85], the molecular structures of such compounds are seen in Figure 10.

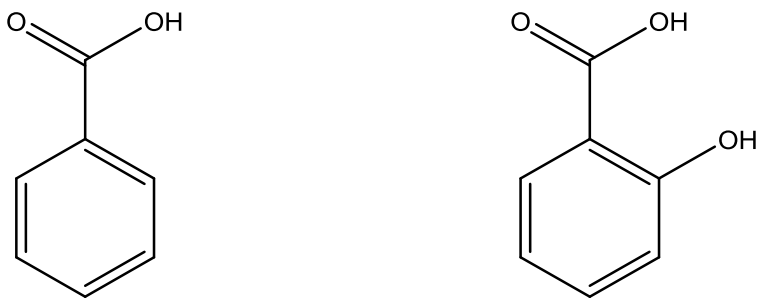

Figure 10: Molecular structure of benzoic acid (left) and salicylic acid (right).

Another problem is the apparent lack of a common trend in solubility for salt forms when ascending or descending a particular periodic group. Kennedy et. al. [85] report a large data set of 36 group 2 *s*-block metal salts of benzoic acid species and the trend in solubility was found to differ for each acid studied. In no cases were the periodic trends Mg > Ca > Sr > Ba or indeed Ba > Sr > Ca > Mg found. Our current inability to explain the trends observed, further reinforces the need for increased availability of large systematic structural studies in the future to identify and explain trends in physicochemical properties from changes in solid state structure.

Salt selection is typically carried out using a single counter ion, however it is possible to use a mix of counter ions as seen by Bock et. al. who produced a number of mixed caesium/rubidium salts of an imido-disophosphate compound[86]. Such mixed cation species (or solid solutions) are common in inorganic systems but only a small number of examples of mixed metal salt forms of organic materials which contain group 1 and group 2 metals were found when searching the CSD [86-90]. Matsui et. al. reported a small series of calcium/strontium mixed salts of the simple organic formate anion, they report a total of three intermediate mixed salts with unit cell data [90]. This study perhaps is most relevant to the study presented within this body of work.

Upon examining the unit cell parameters of the calcium and strontium salts of salicylic acid they are found to be isostructural and therefore according the Hume-Rothery rules [91-92] are more likely to form mixed metal salts. The Hume-Rothery rules also state that the similar ionic radii of calcium and strontium (100 and 118 pm respectively) also favour formation of mixed metal salts. These rules are usually applied to inorganic systems (e.g. alloys, minerals) but here we postulate an opportunity to study a series of mixed salt forms of a commonly used model API and report trends in physicochemical properties.

1.6 Non Linear Optically active materials

When light interacts with a material it typically displays linear behaviour, which means that input radiation is of the same frequency and wavelength as the output radiation. However, under certain conditions light can be shown to behave non-linearly i.e. input frequency does not equal output frequency. Materials that allow such behaviour are known as non-linear optically active materials (NLO) and significant interest has been shown in the development of these materials [93, 94]. NLO materials have been studied since the 1960s, [95] however interest in these materials has increased greatly in the past few decades due to increased availability of the high field laser sources required for non-linear activity to occur [93-94, 96]. With the ability to alter the properties of a light source NLO materials have found a wide variety of practical applications such as the generation of green light (532 nm) from a neodymium (yttrium aluminium garnet)(Nd-(YAG) laser operating at 1064 nm wavelength. Their uses also include optical frequency conversion, integrated photonics and high speed information signalling [97-101].

A wide variety of materials have been tested for NLO activities such as; inorganic materials [102], organometallics [103], liquid crystals [104] and organic molecules [105]. The use of organic materials gives an interesting option for the generation of NLO materials due to the ability to tune the solid state structure to influence properties as mentioned above. The use of organic materials also has the potential of producing high quality single crystals allowing full structural analysis to gain a full understanding of the material. A number of benefits are also gained from use of single crystal materials such as material stability as well as a highly aligned and stable orientation of chromophores required for NLO activity. Through the use of salt screening there is the potential to generate a large number of new materials from a vast pool of potential salt formers. Variation of counterions can be a route to small changes in the solid state structure, thus enabling tuning of properties without changing the main electronic structure of the functional material [96, 106].

When a field is applied to a molecule it may result in a change in polarisation within the chemical structure. As the material has been polarised it can be classified as a

dielectric and therefore the material will have a relative permeability (ε_r). The degree of polarizability of a material is known as its susceptibility (χ). Linear susceptibility and relative permeability can be related as follows [107]:

$$\chi = \varepsilon_r - 1$$

Polarisation can be considered to be a linear process for most materials, this linear response can be shown as:

$$P = \varepsilon_0 \chi E$$

Where P is the polarisation and E is the applied field and ε_0 is the permittivity of free space.

However under certain criteria the molecule may behave non-linearly, this adds additional terms to the above equation (where $\alpha = \varepsilon_0\chi$):

$$P_m = \alpha E + \beta E^2 + \gamma E^3 + \ldots$$

Where Pm is the polarisation of a single molecule, αE is the linear term ($\varepsilon_0\chi$) and β and γ are the non-linear terms. βE is the first molecular hyperpolarisability which is responsible for second order non-linear optical processes such as second harmonic generation (SHG) [93]. Further non-linear terms are possible (third order and fifth order) however they have not reached the maturity second order non-linear optics have in terms of application [93] and as such will not be further considered for this body of work.

As mentioned above, one second order non-linear effect of particular interest to this body of work is the second harmonic generation effect. This effect involves production of light of frequency twice that of the input frequency. For this effect to be expressed mathematically we must consider the optical field to be a time dependent function of the frequency ω, as follows:

$$E(t) = E_0 \cos(\omega t)$$

Combining with the first molecular hyperpolarisability we can now evaluate the polarisation which arises from a second order response through:

$$P^{(2)} = \varepsilon_0 \chi^{(2)} [{E_0}^2 cos^2(\omega t)]$$

Upon expansion of the expression $\cos^2(\omega t)$ the following is obtained:

$$P^{(2)} = \frac{1}{2} \varepsilon_0 \chi^{(2)} [{E_0}^2 + {E_0}^2 cos(2\omega t)]$$

It can be seen from the above equation that this polarisation can be split in to two separate terms, the latter term ($2\omega t$) is responsible for the frequency doubling observed through SHG.

In order for non-linear behaviour to occur a high field laser is required to give a large value of E (which will also increase the values of the first and second terms of molecular hyperpolarisability). Molecules with high polar susceptibilities can also give large non-linear responses by having high non-linear hyperpolarisability. As well as polarizability, good NLO materials must also have a number of structural features. The material must crystallise in a non-centrosymmetric space group as this allows a net dipole to be present in the structure. This factor is central to this thesis as investigating the possibility of designing structures that favour non-centrosymmetric packing is the main aim of this work. Other factors are that materials containing large amounts of π conjugation are typically favoured as well as those containing electron donor and electron acceptor moieties. A notable example of an NLO material with structure like this is 4-nitrotoluene which displays very high 2nd order susceptibility [108-110]. Examples of good NLO material molecular structures can be seen in Figure 11. Where examples of donor groups include hydroxyl and amine substituents and examples of withdrawing groups include nitro groups and sulfonates.

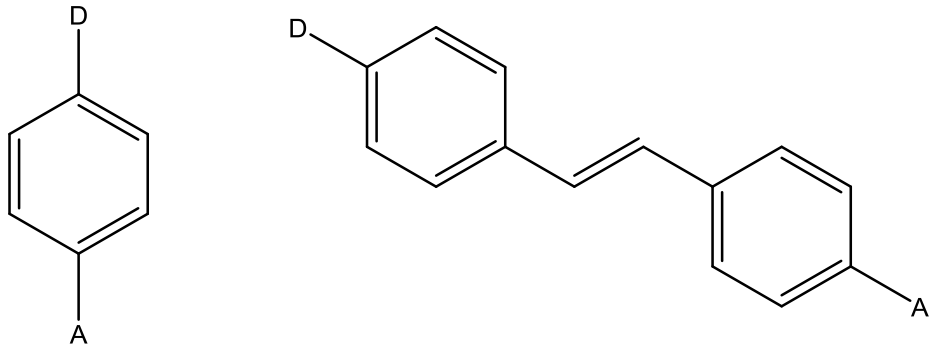

Figure 11: Examples of suitable NLO structures.

The central investigative line of the current crystallographic based work is based on the observation mentioned above that for β and χ to be a non-zero value the material must crystallise in a non-centrosymmetric space group. This can be considered problematic as only 22 % of materials [111] on the Cambridge Structural Database (CSD)[62] were found to crystallise in non-centrosymmetric space groups. It should also be noted that for achiral materials there will in practice be less than a 22 % chance of crystallising in a non-centrosymmetric space group. The figure will be lower due to the inclusion of enantiopure materials, which can only crystallise in the non-centrosymmetric Sohncke space groups, in the above study of space group frequencies within the CSD. Indeed, Etter and Huang estimate that only 11 % of achiral materials crystallise in non-centrosymmetric space groups [112].

4-Nitrophenol is a material of potential interest for the manufacture of NLO materials. The simple molecule consists of an aromatic system with substitution consisting of an electron donor and an electron withdrawing group *para* substituted to each other with extensive resonance possible within the structure. This is a classic push-pull structure. While the known anhydrous forms of 4-nitrophenol crystallise in centrosymmetric space groups a number of salt forms and co-crystals have been found to crystallise in non-centrosymmetric and therefore SHG active space groups. A total of 27 structures of salt forms of 4-nitrophenol are found on the CSD of which 15 belong to non-centrosymmetric space groups (55.6 %) [113-132]. Salt forms of 4-nitrophenol thus appear initially to have a much higher than

average tendency to crystallise in non-centrosymmetric space groups. Indeed, statements that 4-nitrophenol does have a special propensity to crystallise in non-centrosymmetric space groups have been made by various authors [129, 132]. This observation opens up the potential for an interesting study on the factors which influence the packing arrangements of molecules and therefore the space group which the material tends to crystallise in. If such factors can be identified, then they would allow the deliberate design of non-centrosymmetric, SHG active materials. Interactions such as the hydrogen bonding between hydroxyl groups have previously been shown to influence the orientation of molecular dipoles [133]. Magnitude of response is also of interest. As a long term goal, it may also be possible to measure the SHG response of a material and relate these to structural features within the crystal packing.

1.7 Aims

The aim of this project is to develop the knowledge of the relationship between structural factors and material properties through increasing the availability of data sets of crystal structures. Two sets of crystalline materials are presented and structural features are investigated to relate them to material properties. These observations are compared to previous structural observations made in the literature enhancing the understanding of the relationship between structural properties and material properties.

The objectives of this project are as follows:

- Synthesise barium, calcium, magnesium and strontium mixed metal salts of salicylic acid.
- Grow suitable single crystals of mixed metal salicylate salts for single crystal x-ray diffraction.
- Carry out x-ray diffraction analysis
- Attempt synthesis of mixed metal salts of 4-nitrophenol and enrofloxican.
- Carry out solubility tests on mixed metal salt forms.
- Solve and refine crystal structures of mixed metal salts.
- Synthesise salt forms of 4-nitrophenol with organic coformers.
- Grow suitable single crystals of 4-nitrophenol salts for single crystal x-ray diffraction.
- Solve and refine crystal structures of 4-nitrophenol salt forms
- Search Cambridge Structural Database for previously published 4-nitrophenol structures.
- Carry out comparative analysis of 4-nitrophenol structures including both those produced within this project and those in literature,

2. Experimental

2.1 Mixed metal salt forms

2.1.1 Mixed metal salts of salicylic acid

Salicylic acid, calcium carbonate and strontium carbonate were added to warm water and dissolved with stirring over a period of 30 minutes. The resultant solution was then allowed to evaporate slowly to produce crystals. The mass of reactants and mole equivalents used for individual samples are given in table 1. This procedure was also repeated for Ca/Mg and Ba/Sr mixed metal salts of salicylic acid using magnesium and barium carbonate respectively.

Each sample was analysed using atomic absorption spectroscopy (AAS) to measure the calcium to strontium ratio of the bulk sample, as measured by a Thermo Scientific iCE 3300 Series AA spectrometer. For AAS each sample solution was diluted to contain approximately 4 mgl^{-1} strontium content. Lanthanum solution was added to prevent complex formation in the sample. Reference samples containing 1, 2, 2.5, 3, 4 and 5 mgl^{-1} were prepared using a strontium standard, these were used to produce a calibration graph.

Table 1: Mass of reactants used (ratio X:Y is the ratio of calcium and strontium used respectively).

Sample name	Mass of salicylic acid added (g)	Mass of calcium carbonate added (g)	Mass of strontium carbonate added (g)
CaSal	1.6242 (11.7593mmol)	0.5832 (5.8269 mmol)	-
CaSrSal 90.1 : 9.9	1.6672 (12.0706 mmol)	0.5494 (5.4892 mmol)	0.0896 (0.6069 mmol)
CaSrSal 80.1 : 19.9	1.6421 (11.8889 mmol)	0.4752 (4.7479 mmol)	0.1743 (1.1807 mmol)
CaSrSal 69.8 : 30.2	1.6638 (12.0460 mmol)	0.4139 (4.1354 mmol)	0.2643 (1.7903 mmol)
CaSrSal 60.3 : 39.7	1.6299 (11.8006 mmol)	0.3520 (3.5169 mmol)	0.3425 (2.3199 mmol)
CaSrSal 50.5 : 49.5	1.6121 (11.6717 mmol)	0.2966 (2.9634 mmol)	0.4296 (2.9099 mmol)
CaSrSal 39.7 : 60.3	1.6284 (11.7897 mmol)	0.2349 (2.3469 mmol)	0.5256 (3.5603 mmol)
CaSrSal 30.2 : 69.8	1.6461 (11.9178 mmol)	0.1798 (1.7964 mmol)	0.6138 (4.1577 mmol)
CaSrSal 19.3 : 80.7	1.6528 (11.9664 mmol)	0.1138 (1.1370 mmol)	0.7043 (4.7707 mmol)
CaSrSal 11.2 : 88.8	1.6561 (11.9903 mmol)	0.0676 (0.6754 mmol)	0.7943 (5.3803 mmol)
SrSal	1.6433 (11.8976 mmol)	-	0.8830 (5.9812 mmol)

2.1.2 Solubility tests

Solubility tests were carried out on each sample. Each sample (1 g) was added to a sample vial containing deionised water (8 cm^3) and the resultant slurry was then placed in an incubator at 25 °C and stirred for 10 days. The slurry was then filtered through syringe filters (0.2 µm pore size) and diluted to suitable concentration for UV-Vis analysis, all UV-Vis analysis was measured with an Agilent Technologies Cary 60 UV-Vis instrument at 295 cm^{-1}. Calibration graphs were also obtained using Sr-salicylate solutions with the following concentrations: 20 mgl^{1}, 15 mgl^{-1}, 10 mgl^{-1}, 5 mgl^{-1} and 2 mgl^{-1} (note molarity in this scenario refers to the molarity of salicylate in each sample). Each solubility test was carried out in duplicate.

To calculate the mass of salt required for 40 mg (0.000457 mol) Sr first the molecular weight of the salt was calculated:

For CaSrSal 90:10 (CaSal M.W = 314 $gmol^{-1}$ SrSal M.W = 361.5 $gmol^{-1}$)

$$M.W = (0.9 \times 314) + (0.1 \times 361.5) = 318.75$$

$$Mass\ of\ salt\ required = \left(\frac{318.75}{0.1}\right) * 0.000457 = 1.4567\ \mathrm{g}$$

This was then diluted to the required concentration of 4 mgl^{-1}.

The strontium values were measured through AAS and the absorption values from the two calibrations above were averaged and plotted to obtain the straight line equation required to calculate strontium concentration present in each analysed sample. This gave the following equation:

$$y = 3534.3x + 0.0345$$

This gives us the concentration in mgl^{-1} we can divide this value by 10 to give the concentration in mg/100 ml, as each sample was made to a 100ml solution this gives us the mass of strontium present in the sample.

$$\frac{Mass\ Sr}{atomic\ mass\ Sr} = number\ of\ mols\ Sr$$

$$Mass\ SrSal_2.H_2O = n \times atomic\ mass\ SrSal_2.H_2O$$

$$\%Sr = \frac{Mass\ SrSal_2.H_2O}{Mass\ of\ sample}\ x\ 100$$

2.2 NLO materials

General procedure: A solution of nitrophenol was prepared by dissolving 4-nitrophenol in hot solvent. Each base was then added to this solution with heating and stirring. The resulting solid-free solution was then decanted into sample vials, and each vial was then sealed with parafilm and pierced to allow slow evaporation to occur. Full details of sample preparation can be seen in table 3.

Table 2: Experimental details for NLO salt preparation.

Base	Mass of base (g)	No. mols base (mmol)	Mass 4-nitrophenol (g)	Mols 4-nitrophenol (mmol)	Solvent	Time	Result
(1R,2S)-(-)-Ephedrine	0.1674	1.0131	0.1385	0.9956	Acetonitrile	3 days	Crystalline product formed
(1R,2S)-(-)-methylephedrine	0.1791	0.9911	0.1407	1.0114	Acetonitrile	7 days	No crystalline material formed
(1R,2S)-(-)-methylephedrine	0.08910	0.4970	0.1399	1.0057	Acetonitrile	7 days	No crystalline material formed
(1S,2R)-(+)-methylephedrine	0.1776	0.9907	0.1411	1.0143	Acetonitrile	4 days	Crystalline product formed
(1S,2R)-(+)-methylephedrine	0.0889	0.4959	0.1398	1.0049	Acetonitrile	4 days	Crystalline product formed

Base	Mass of base (g)	No. mols base (mmol)	Mass 4-nitrophenol (g)	Mols 4-nitrophenol (mmol)	Solvent	Time	Result
(R)-(+)-α methylbenzylamine	0.0613	0.5059	0.1393	1.0014	Acetonitrile	7 days	No crystalline material formed
(R)-(+)-α methylbenzylamine	0.1217	1.0043	0.1401	1.0071	Acetonitrile	7 days	No crystalline material formed
(s)-(-)-α methylbenzylamine	0.0601	0.4959	0.1402	1.0078	Acetonitrile	7 days	No crystalline material formed
(s)-(-)-α methylbenzylamine	0.1231	1.0016	0.1413	1.0157	Acetonitrile	7 days	No crystalline material formed
1,2-diaminodecane	0.1286	0.7463	0.1052	0.7562	Acetonitrile	7 days	No crystalline material obtained

Base	Mass of base (g)	No. mols base (mmol)	Mass 4-nitrophenol (g)	Mols 4-nitrophenol (mmol)	Solvent	Time	Result
1,3-diaminopropane	0.0745	1.0051	0.1406	1.0107	Water	7 days	No crystalline material obtained
1,4-diaminobutane	0.4415	5.0085	0.6941	4.9896	Water	4 days	Crystalline product formed
1,8-diaminonaphthalene	0.1593	1.0069	0.1417	1.0186	Acetonitrile	14 days	No crystalline material formed
1-adamantyl amine	0.1541	1.0188	0.1422	1.0222	Acetonitrile	7 days	Crystallised as nitrophenol starting material
2,3-diaminophenol	0.1279	1.0303	0.1436	1.0322	Water	5 days	Crystallised as nitrophenol starting material

Base	Mass of base (g)	No. mols base (mmol)	Mass 4-nitrophenol (g)	Mols 4-nitrophenol (mmol)	Solvent	Time	Result
2,3-diamino-pyridine	0.1162	1.0648	0.1437	1.0329	Acetonitrile	7 days	Crystalline product formed
2-Acetylpyridine	0.1219	1.006	0.1393	1.001	acetonitrile	7 days	Crystallised as nitrophenol starting material
2-amino benzophenone	0.1978	1.0028	0.1413	1.0157	Acetonitrile	2 days	Crystallised as amino benzophenone starting material
2-amino nicotinic acid	0.1412	1.0222	0.1379	0.9913	Acetonitrile	14 days	Crystallised as 4-nitrophenol starting material

Base	Mass of base (g)	No. mols base (mmol)	Mass 4-nitrophenol (g)	Mols 4-nitrophenol (mmol)	Solvent	Time	Result
2-amino-3-methyl-pyridine	0.1105	1.0218	0.1384	0.9949	Acetonitrile	7 days	Crystalline material formed, problems collecting strong data.
2-amino-5-nitro-6-methylpyridine	0.1518	0.9912	0.1396	1.0035	Acetonitrile	7 days	No crystalline material formed
2-amino-5-nitropyridine	0.0694	0.49889	0.0701	0.5039	Acetonitrile	7 days	No crystalline material formed
2-amino-nicotinaldehyde	0.1227	1.0047	0.1398	1.005	Acetonitrile	7 days	Crystalline product formed
2-aminophenol	0.1149	1.0528	0.1378	0.9906	Acetonitrile	14 days	No crystalline material formed

Base	Mass of base (g)	No. mols base (mmol)	Mass 4-nitrophenol (g)	Mols 4-nitrophenol (mmol)	Solvent	Time	Result
2-aminophenylamine	0.2942	1.0132	0.1423	1.0229	Acetonitrile	7 days	No crystalline material formed
2-aminopyridine	0.0952	1.0116	0.1400	1.0063	Acetonitrile	5 days	Crystalline product formed
3,3 diamino-N-methyldipropylamine	0.1475	1.0154	0.1403	1.0085	Acetonitrile	14 days	No crystalline material formed
3,5-dimethylpyrazole	0.0733	0.7625	0.1016	0.7304	Acetonitrile	7 days	No crystalline material obtained
3-acetyl-2,6-bis(tert butyl amino)-4-methyl pyridine	0.2059	0.7422	0.1048	0.7534	Acetonitrile	14 days	No crystalline material obtained
3-Acetylpyridine	0.1213	0.1001	0.1387	0.9971	acetonitrile	7 days	Starting material

Base	Mass of base (g)	No. mols base (mmol)	Mass 4-nitrophenol (g)	Mols 4-nitrophenol (mmol)	Solvent	Time	Result
3-aminopropanol	0.0763	1.0156	0.1391	0.9999	Water	14 days	Crystallised as nitrophenol starting material
4,4'-bipyridyl	0.1572	1.0065	0.1397	1.0042	Acetonitrile	2 days	No crystalline material obtained
4-Acetylpyridine	0.1221	1.008	0.1401	1.0071	acetonitrile	7 days	Crystalline product formed
4-amino-3-bromo-2-methylpyridine	0.0889	0.4753	0.0694	0.4988	Acetonitrile	7 days	Amorphous material formed
4-aminopyridine	0.0915	0.9722	0.1396	1.0035	Acetonitrile	7 days	Crystalline product formed

Base	Mass of base (g)	No. mols base (mmol)	Mass 4-nitrophenol (g)	Mols 4-nitrophenol (mmol)	Solvent	Time	Result
4-dimethyl aminopyridine	0.0931	0.7621	0.1039	0.7468	Acetonitrile	5 days	Crystalline product obtained
4-methyl morpholine	0.1015	1.0038	0.1412	1.0150	Water	7 days	Crystallised as nitrophenol starting material
5-aminobenzotriazole	0.1363	1.0161	0.1399	1.0057	Acetonitrile	7 days	No crystalline material obtained
6-amino-3-bromo-2-methylpyridine	0.1931	1.0324	0.1419	1.0201	Acetonitrile	7 days	No crystalline material obtained
8-hydroxyquinoline	0.1473	1.0149	0.1398	1.0049	Acetonitrile	7 days	Crystallised as nitrophenol starting material

Base	Mass of base (g)	No. mols base (mmol)	Mass 4-nitrophenol (g)	Mols 4-nitrophenol (mmol)	Solvent	Time	Result
9,10 diamino phenanthrene	0.1041	0.4999	0.1415	1.0172	Acetonitrile	7 days	No crystalline material formed
Allyl amine	0.0589	1.0259	0.1400	0.1006	Acetonitrile	7 days	No crystalline material formed
Amino benzylamine	0.1238	1.0133	0.1408	1.0121	Acetonitrile	7days	Crystalline product formed
Aminoacetaldehyde dimethylacetal	0.5062	4.814	0.6933	4.9838	Water	5 days	Crystallised as nitrophenol starting material
Aniline	0.4669	5.013	0.6971	5.0111	Water	7 days	Crystallised as nitrophenol starting material

Base	Mass of base (g)	No. mols base (mmol)	Mass 4-nitrophenol (g)	Mols 4-nitrophenol (mmol)	Solvent	Time	Result
Benzyl amine	0.0511	0.4768	0.1385	0.9956	Acetonitrile	4 days	Crystalline product formed
Creatine	0.7445	5.6771	0.6961	5.0039	Water	4 days	Crystallised as nitrophenol starting material
D-(+)-Neoptarin	0.0126	0.0498	0.0141	0.0101	Acetonitrile	7 days	Crystallised as nitrophenol starting material
Diallyl amine	0.0998	1.0278	0.1388	0.9978	Acetonitrile	7 days	No crystalline material formed
Diaminobenzoic acid	0.1537	1.0102	0.1401	1.0071	Acetonitrile	7 days	Crystallised as nitrophenol starting material

Base	Mass of base (g)	No. mols base (mmol)	Mass 4-nitrophenol (g)	Mols 4-nitrophenol (mmol)	Solvent	Time	Result
Diaminomethyl dipropylamine	0.1509	1.0391	0.1399	1.0056	Water	7 days	No crystalline material formed
Diethylenetriamine	0.5117	4.9598	0.6933	4.9839	Water	4 days	Crystalline product formed
Di-isopropylethylamine	0.6482	5.0151	0.6931	4.9824	Water	7 days	No crystalline material formed
N,N dimethyl ethanolamine	0.0904	1.0148	0.1394	1.0021	Water	7 days	No crystalline material obtained
Tetramethyl piperidine	0.1426	1.0097	0.1374	0.9877	Acetonitrile	7days	Crystalline product formed

Base	Mass of base (g)	No. mols base (mmol)	Mass 4-nitrophenol (g)	Mols 4-nitrophenol (mmol)	Solvent	Time	Result
Dipropylenetriamine	0.1324	1.0089	0.1415	1.0171	Water	7 days	Crystalline product formed
Ethanol amine	0.3066	5.0196	0.6941	4.9896	Water	7 days	Crystalline product obtained
Ethylene diamine	0.0299	0.4975	0.1403	1.0086	Acetonitrile	2 days	Crystalline product formed
Hexamine	0.1061	0.7568	0.1084	0.7792	Acetonitrile	7 days	Crystalline product obtained, however difficulty was found elucidating structure

Base	Mass of base (g)	No. mols base (mmol)	Mass 4-nitrophenol (g)	Mols 4-nitrophenol (mmol)	Solvent	Time	Result
Indole	0.0873	0.7451	0.1050	0.7548	Acetonitrile	7 days	Crystallised as nitrophenol starting material
Isopropylamine	0.2763	4.6743	0.6920	4.9745	Water	4 days	Crystalline product obtained
Methyl amine	0.1559	5.0189	0.6914	4.9701	Water	7 days	Crystalline product formed
Methyl phenethylamine	0.1473	1.0894	0.1423	1.0229	Water	7 days	Not crystalline material formed
Methyl pyrollidine	0.0365	0.4287	0.1389	0.9985	Acetonitrile	7 days	Crystalline product formed

Base	Mass of base (g)	No. mols base (mmol)	Mass 4-nitrophenol (g)	Mols 4-nitrophenol (mmol)	Solvent	Time	Result
N-benzyl methylamine	0.6084	5.0206	0.6927	4.9795	Water	7 days	No crystalline material formed
N-naphthylethylene diamine	0.1364	0.7323	0.1060	0.7621	Acetonitrile	7 days	No crystalline material obtained
Nonylamine	0.1447	1.0103	0.1388	0.9977	Water	7 days	No crystalline material formed
o-phenylenediamine	0.1136	1.0501	0.1394	1.0021	Acetonitrile	7 days	No crystalline material formed
Phenethyl amine	0.0597	0.4926	0.1383	0.9942	Acetonitrile	4 days	Crystalline product formed

Base	Mass of base (g)	No. mols base (mmol)	Mass 4-nitrophenol (g)	Mols 4-nitrophenol (mmol)	Solvent	Time	Result
Picoline	0.0962	1.0329	0.1411	1.0143	Acetonitrile	7 days	Crystalline product formed
Pyrazole	0.0741	1.0897	0.1392	1.0006	Acetonitrile	5 days	Crystalline product formed
Pyridine	0.4065	5.1390	0.6982	5.0190	Water	7 days	Crystallised as nitrophenol starting material
Pyridine-2-aldehyde	0.1077	1.006	0.1398	1.0050	acetonitrile	7 days	Nitrophenol starting material
Pyridine-3-aldehyde	0.1074	1.003	0.1403	1.0086	acetonitrile	7 days	Nitrophenol starting material

Base	Mass of base (g)	No. mols base (mmol)	Mass 4-nitrophenol (g)	Mols 4-nitrophenol (mmol)	Solvent	Time	Result
Pyridine-4-aldehyde	0.1068	0.9975	0.1397	1.0042	Acetonitrile	7 days	Nitrophenol starting material
Pyrrole	0.0327	0.4874	0.1399	1.0057	Acetonitrile	7 days	Crystallised as nitrophenol starting material
Pyrrole	0.0674	1.0046	0.1406	1.0107	Acetonitrile	7 days	Crystallised as nitrophenol starting material
R-(-)-phenylephrine	0.1011	0.6047	0.8468	0.6087	Acetonitrile	7 days	Crystallised as nitrophenol starting material

Base	Mass of base (g)	No. mols base (mmol)	Mass 4-nitrophenol(g)	Mols 4-nitrophenol (mmol)	Solvent	Time	Result
Rhodamine B	0.4811	1.0043	0.1373	0.9869	Acetonitrile	3 days	Crystalline product formed
Sulfadiazine	0.2578	1.0301	0.1429	1.0272	Water	7 days	No crystalline material formed
Tetramethyl ethylenediamine	0.1169	1.0059	0.1401	1.0071	Water	7 days	Crystalline product formed
Theophylline	0.1825	1.0129	0.1418	1.0193	Water	2 days	Crystallised as theophylline starting material
Triethylamine	0.5057	4.9975	0.6917	4.9723	Water	7 days	No crystalline material obtained
Triethylene tetramine	0.1466	1.0022	0.1382	0.9935	Water	7 days	Crystalline product formed

Base	Mass of base (g)	No. mols base (mmol)	Mass 4-nitrophenol (g)	Mols 4-nitrophenol (mmol)	Solvent	Time	Result
Tri-isopropylamine	0.1499	1.0461	0.1416	1.0179	Acetonitrile	14 days	No crystalline material formed
Trimethylamine	0.2963	5.0127	0.6915	4.9709	Water	7 days	Crystalline product obtained
Tris(2-amino) ethyleneamine	0.1477	1.0101	0.1417	1.0186	Acetonitrile	7days	Crystalline product formed
Urea	0.0654	1.0866	0.1424	1.0237	Acetonitrile	3 days	Crystallised as nitrophenol starting material

2.3 Attempted synthesis of Ca/Sr mixed metal salts of NPOH

General procedure:

Nitrophenol was dissolved in water with stirring and heating, calcium hydroxide and strontium hydroxide were then added and the solution was stirred until all solid had dissolved. The resultant solution was then decanted to an evaporating dish and left to evaporate. A summary of experimental information can be seen in table 4.

Table 3: Experimental details for CaSr NP experiments.

Sample ID	Mass of nitrophenol (g)	No. of mols of nitrophenol (mmol)	Mass of calcium hydroxide (g)	No. of mols of calcium hydroxide (mmol)	Mass of strontium hydroxide (g)	No. of mols of strontium hydroxide (mmol)
SrNP	0.1407	1.0114	-	-	0.1362	0.5125
CaSrNP 10:90	0.1413	1.0157	0.0010	0.0553	0.1218	0.4583
CaSrNP 20:80	0.1399	1.0057	0.0018	0.1005	0.1084	0.4078
CaSrNP 30:70	0.1434	1.0308	0.0028	0.1552	0.0956	0.3596
CaSrNP 40:60	0.1429	1.0272	0.0037	0.2056	0.0819	0.3083

Each calcium containing sample formed a pale yellow precipitate, recrystallization in DMF was attempted for each sample. Any single crystal formed was isolated for single crystal diffraction.

2.4 X-Ray diffraction experiments

Single crystal diffraction measurements were carried out with Oxford Diffraction Gemini S or Xcalibur E instruments. Measurements were made with graphite monochromated Cu or Mo radiation. Structures were solved using the programs SHELXS or SIR92. [134-135]. All structures were refined to convergence using all unique reflections and against F^2. The refinement programs came from the SHELX suit. [134] WinGX was used to edit models and prepare files. [136] All non-hydrogen atoms were refined anisotropically. Hydrogen atoms bonded to C were refined in riding modes. Where possible, hydrogen atoms bonded to O or N were refined isotropically, but often some restraint on the X-H bond lengths were required and in a small number of cases a riding mode was required. Details of these treatments and of disorder models and twinning treatments are given in the cif files of the appendix. Selected crystallographic and refinement details for each structure are given in table 5.

3. Results

3.1 Mixed metal solid state solutions

As stated in section 1.7 there is a need for expanded data sets of crystal structures to relate structural features to physicochemical properties. To further develop the understanding of mixed metal salt forms (also known as solid state solutions) a series of Calcium-Strontium salts are presented. The crystal structures of these species are described and the subtle changes observed are related to changes in the content of each metal in relation to the other. The solubility of each species was measured and this property is related to the ratio of calcium and strontium present.

A total of eleven isostructural Ca:Sr mixed cation salt forms of salicylic acid were synthesised, ten of which produced crystalline materials which were successfully analysed using single crystal X-ray diffraction. These salt forms all share the general formula $[Ca_{(1-x)}Sr_x(C_7H_5O_3)_2(OH_2)_2]$ with all mixed-metal crystal structures containing both metals on the same disordered crystallographic site. For the 10 structures elucidated in this body of work x had the following values: 0, 0.041, 0.083, 0.165, 0.306, 0.529, 0.632, 0.789, 0.835 and 1. An additional isostructural salt form was elucidated, this being the Sr/Ba mixed cation salt of salicylic acid $[Sr_{0.729}Ba_{0.271}(C_7H_5O_3)_2(OH_2)_2]$ [Figure 12]. The synthesis of the Sr/Ba salt form involved equimolar amounts of Sr and Ba coformers however the resultant salt did not contain a 50:50 ratio of Sr/Ba cations, this suggests that the larger ionic radii of Ba is not as good of fit for the crystal lattice as Ca or Sr. As mentioned in section 1.5 the Humes-Rothery rules suggest that both the isostructural nature of the complexes and similar ionic radii (table 6) favour mutual substitution. Ba has a “more different” ionic radii compared to Sr than does Ca and the known structure of barium salicylate is considerably different (in terms of metal coordination, coordination polymer nature and hydration state) than the mutually isostructural structures of the Ca and Ba salts. So it is perhaps unsurprising that Ba is a less good fit to this structure.

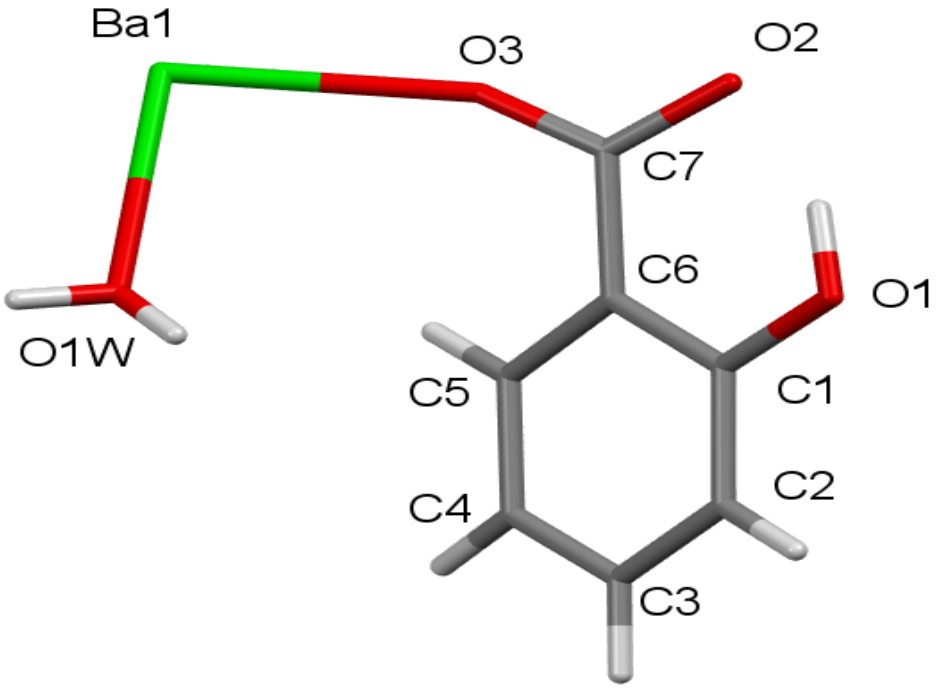

Figure 12: Asymmetric unit of Ba/Sr salicylate. Atom site marked Ba1 is a mix of Sr and Ba cations.

Table 4: Ionic radii of Mg2+, Ca2+, Sr2+ and Ba2+ ions.

Ion	Ionic radii (pm)
Mg^{2+}	72
Ca^{2+}	100
Sr^{2+}	118
Ba^{2+}	135

While the ten Ca/Sr samples share similar unit cell parameters, expansion can be seen along the crystallographic *a* and *c* axes with increasing Sr content (by 1.80 and 3.18 % respectively) [Figure 13] and slight contraction can be seen along the crystallographic *b* axis. This expansion is also observed in the Sr/Ba structure to a greater extent. This can possibly be explained when we examine M-O bond

distances which are shown to increase with increasing Sr content. (The observed M-O distances are of course averages of the Ca-O and Sr-O bonds distances actually present in the crystal). Of the 4 M-O interactions present in the structure the interaction between the metal centre and the neutral water species shows the largest increase with increasing Sr content (6.39 % increase for M1-O1W compared to 4.37, 4.63 and 5.40 % for bonds from M1 to O2^{ii}, O3 and O3^{ii} respectively). This greater expansion in bond length can be expected due to the previously reported greater affinity of Ca for neutral water ligands compared to that of Sr [85] and fits with the general concept of Ca having less ionic bonding characteristics than Sr.

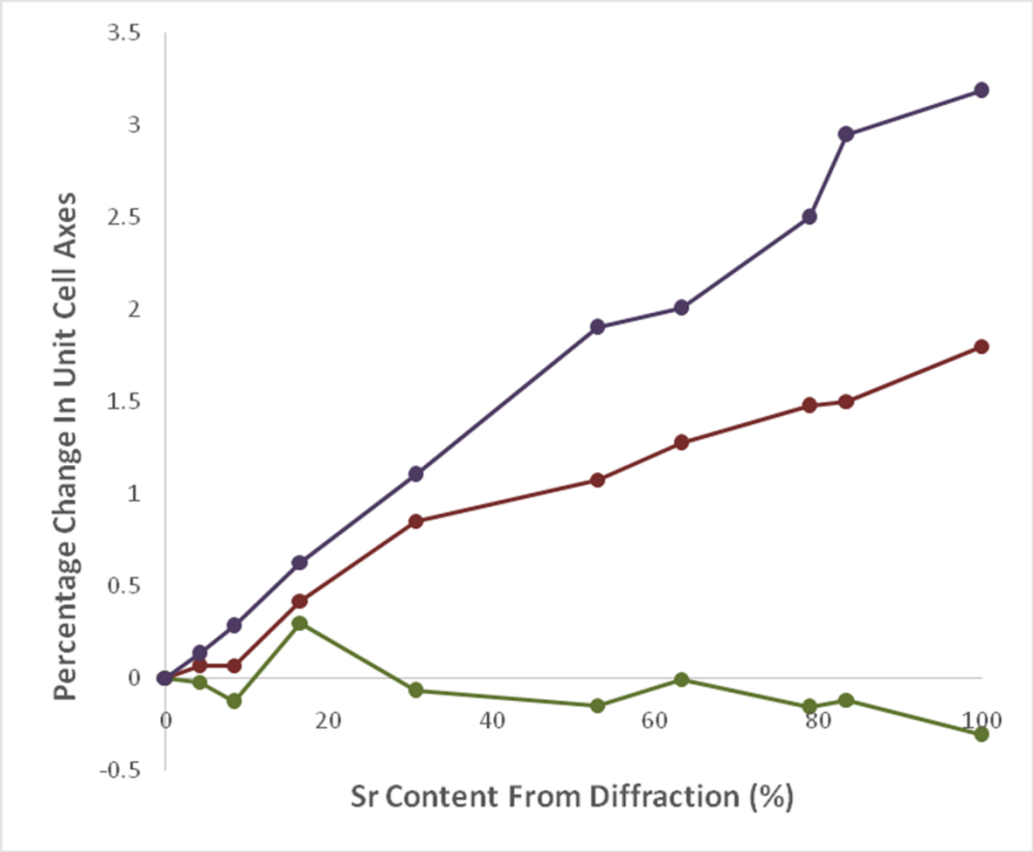

Figure 13: Plot of percentage change in each unit cell axes (for CaSr salicylate structures) vs. percentage Sr content Purple represents the a axis, green the b axis and red the c axis.

In structures with higher Ca content the shortest M-O contact occurs between the metal centre and the neutral water ligand however with high Sr content the shortest

contact is found between the carboxylate and the metal centre. The switching of the identity of the shortest bond length occurs at 50 % Ca/Sr incorporation.

Upon examining the structure further we can observe that the 1-dimensional coordination polymer propagates along the crystallographic *c* axis through M-O interactions. This could be a potential explanation for the larger expansion observed along this axis [Figure 14].

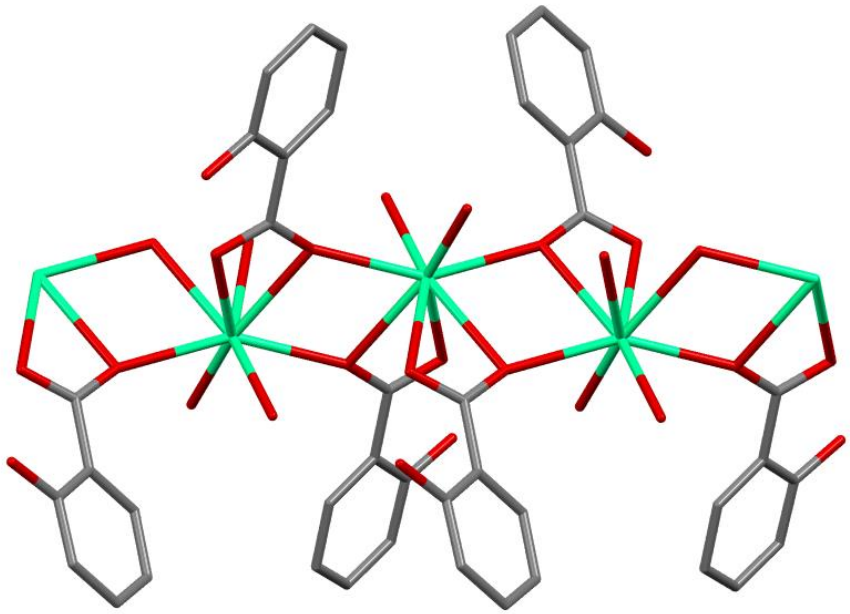

Figure 14: Propagation of calcium salicylate coordination polymer through M-O contacts along the crystallographic c axis (c direction left to right).

As can be seen in figure 14 the O ligands form an 8 coordinate complex with the metal centre. Each 8 coordinate metal centre is linked by M-O-M-O rings allowing the coordination polymer to propagate along the crystallographic *c* axis. The M-O-M-O rings have side lengths of approximately 2.4005(9) Å and 2.4781(9) Å with internal angles of 70.90(3) and 109.10(3)° (all given exact values for 100 % Ca species). Expanding these distances by increasing the Sr content, obviously increases the

average M···M distance in the polymeric chain and hence increases the length of the *c* axis.

It is not obvious why the a axis also increases in length but the b axis contracts slightly. Figure 15 shows that in plan the 1-dimensional polymeric chains run along each corner of the unit cell (at (0,0,z), (0,1,z), (1,0,z) and (1,1,z)) and through the centre of the cell (0.5, 0.5, z). The chains thus stack in both the *a* and *b* directions, with the shortest M to M inter-chain separations corresponding to the short *b* axis. The chains are connected by hydrogen bonding that runs diagonally with respect to *a* and *b*. The hydrogen bonds link coordination polymer chains along the diagonals through water-phenol-water interactions which lengthen as the M-O contacts lengthen with increasing Sr content. However, this does not result in any overall increase in the *b* dimension. A significant difference may be that hydrophobic π-π contacts are also seen along the *b* direction (shortest C···C contact 3.2354 (19) Å) between aromatic rings. These π interactions are highlighted in Figure 15, it may be these interaction zones that buffer expansion along this axis by allowing extra interdigitation of organic fragments.

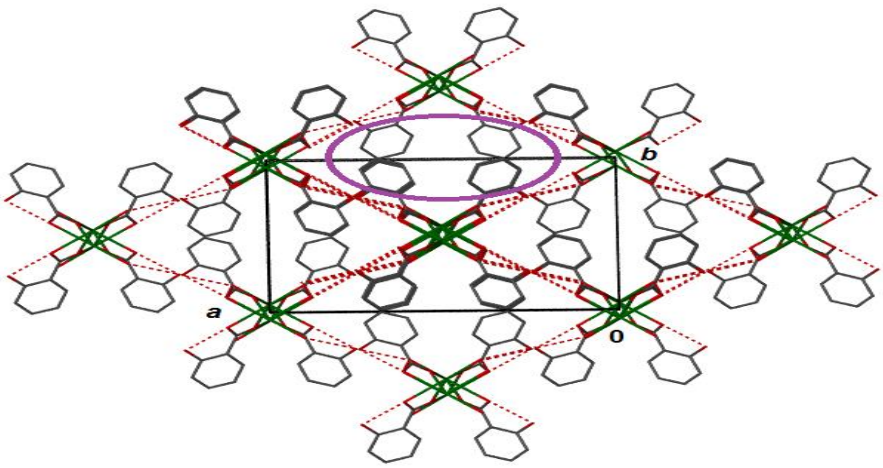

Figure 15: Expanded crystal structure of CaSal with hydrophobic interactions highlighted. View is down the c axis and hence along the length of the coordination polymers.

It should be noted that unit cell expansion for a CaSal sample was measured at a range of temperatures varying from 150 K to 298 K, see figure 16. Thermal expansion was seen in all three crystallographic axes and therefore displays different expansion mechanics to those observed above.

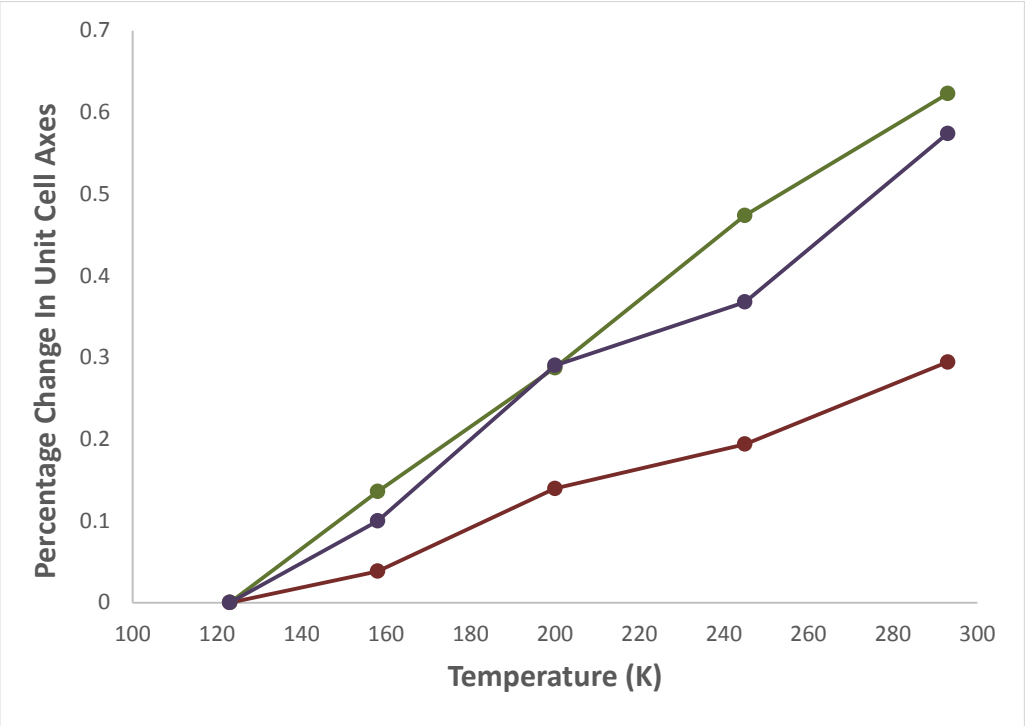

Figure 16: plot of percentage change in the unit cell axes of CaSr salicylate with varying temperature. Red = a axis, green = b axis and purple = c axis.

The solubility of 11 Ca/Sr salt forms of salicylic acid were measured, 2 of these were the pure Ca and Sr salts and 9 were mixed cation salts. As mentioned in section 1.5 the solubilities of calcium and strontium salicylate were previously reported by Kennedy et. al [85] with an increase in solubility observed when moving from the calcium to the strontium salt. This trend is also seen when moving from the pure calcium salicylate salt through increasing amounts of incorporation of strontium into the crystal lattice [Table 7] [Figure 17].

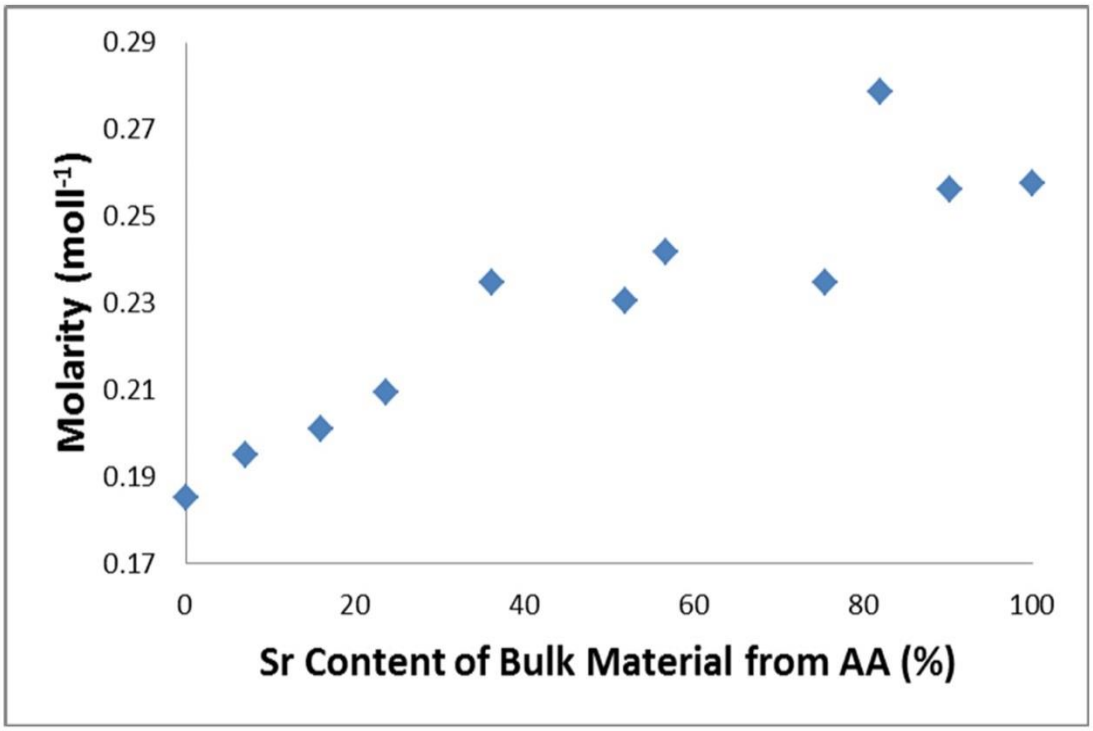

Figure 17: Plot of molar concentration of salicylate in solution vs Sr content of bulk material.

It should be noted that for these measurements the %Sr present is calculated by atomic absorption analysis using a bulk powder sample and is not reliant on single crystal diffraction analysis (the %Sr present in each bulk sample is given in table 7 which is calculated from the calibration data and graph shown in table 6 and figure 18 respectively). A general trend of increasing solubility with increasing Sr content can be seen with a maximum increase of approximately 50 % when compared to CaSal. Most values lie between the two end points which can be defined as the pure calcium and strontium salts, thus giving rise to the possibility of fine tuning the solubility of the model API salicylate through the use of mixed cation salt formation.

Table 5: UV-Vis results for calibration graphs.

SrSal (1)			
Concentration (gl^{-1})	Molarity (M)	$\lambda_{max}(cm^{-1})$	Abs.
0.020	$10x10^{-5}$	295	0.404
0.015	$7.5x10^{-5}$	295	0.315
0.010	$5x10^{-5}$	295	0.212
0.005	$2.5x10^{-5}$	295	0.128
0.002	$1x10^{-5}$	295	0.070
SrSal (2)			
Concentration (gl^{-1})	Molarity (M)	$\lambda_{max}(cm^{-1})$	Abs.
0.020	$10x10^{-5}$	295	0.403
0.015	$7.5x10^{-5}$	295	0.307
0.010	$5x10^{-5}$	295	0.234
0.005	$2.5x10^{-5}$	295	0.128
0.002	$1x10^{-5}$	295	0.068

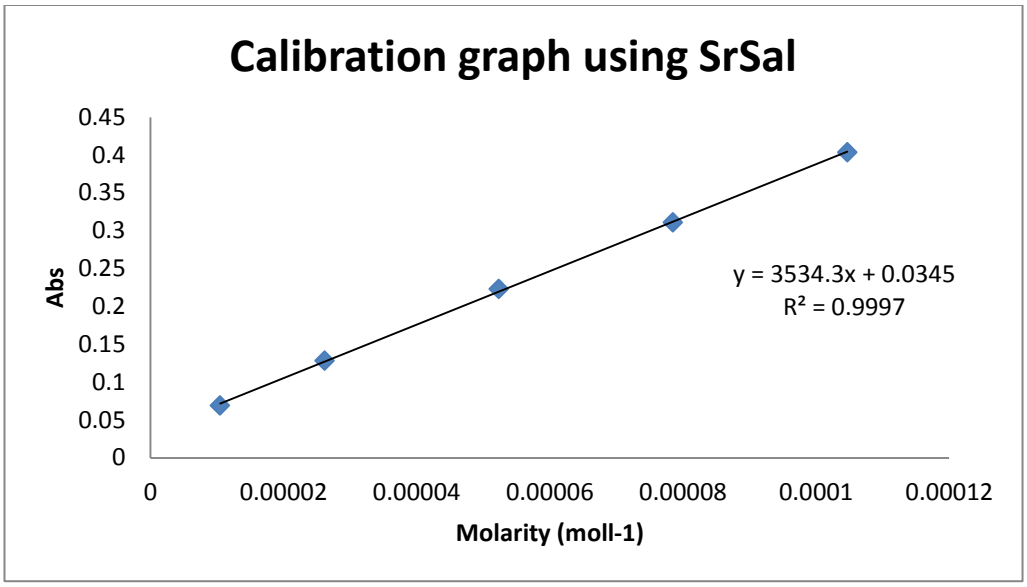

Figure 18: UV-vis Calibration graph obtained using Strontium standards

Table 6: Solubility data and Ca/Sr ratios.

%Sr bulk (from AA)	Solubility (mol dm^{-3})
0	0.185 (4)
7.01	0.195 (2)
16.04	0.201(2)
23.67	0.209 (2)
36.13	0.235 (10)
51.88	0.231 (4)
56.67	0.242 (8)
75.59	0.235 (6)
82.01	0.279 (20)
90.28	0.257 (8)
100	0.257 (10)

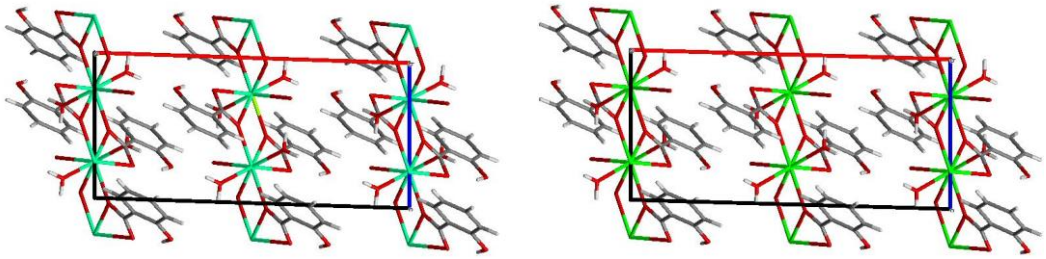

Figure 19: Unit cell contents of calcium salicylate (left) and strontium salicylate (right).

Although a limited amount of structural data on mixed metal organic salts were found in the CSD, no relevant studies examining solubility test data were found in the literature. The work described in this chapter on the use of mixed metal forms of organic salts is thus thought to be the first study to show the potential to fine tune both the solid-state structure and the physicochemical properties of an organic material through altering the ratio of the two counterions present.

After successful synthesis and elucidation of mixed metal salts of salicylic acid the synthesis of similar solid state solutions of 4-nitrophenol were attempted (as mentioned in experimental page 50). Unfortunately here no crystalline material suitable for single crystal X-ray diffraction contained mixed cations. Instead other (organic) coformers were tested for the salt screening of 4-nitrophenol. This work is described in the following chapter.

3.2. NLO 4-nitrophenol materials

A set of salt forms of 4-nitrophenol are presented, 4-nitrophenol salts have previously been described in the literature to have a higher than average likelihood to form materials which crystallise in non-centrosymmetric space groups (See section 1.6), therefore this trend is further investigated.

Throughout this work a total of 89 different syntheses of salt forms of 4-nitrophenol were attempted, from these 20 samples were obtained which were suitable for Single Crystal X-ray Diffraction. Of these 20 samples, 13 gave previously unpublished structures and can be considered novel. Out of the remaining 69 attempted syntheses 31 failed to produce crystalline material and 38 crystallised as starting material (either 4-nitrophenol or coformer). Some of those which crystallised as starting material would have been expected to produce salt forms as discussed below, including such relatively strong bases as adamantylamine (pKa 10.4). Additionally, crystalline material was obtained for the salt of 4-nitrophenol and hexamine however difficulty was observed when attempting to elucidate this structure due to rotation of the symmetrical hexamine fragment. This structure was thus not included in the discussions below. A total of 50 crystal structures which contained 4-nitrophenol[NPOH] or 4-nitrophenolate[NPO] were found on the Cambridge Structural Database (CSD)[62]and will be used in analysis and comparison in this body of work. (Structures with R1>10 %, disorder present or no 3D coordinates were omitted from this dataset). Thus, with the newly determined structures, there are a total of 63 structures available for comparison.

Of the 13 new structures elucidated, 8 were salt forms where proton transfer had occurred from NPOH to the base, an example is ethanolamine 4-nitrophenolate [Figure 19]. Three were cocrystal forms where neutral NPOH occurs in the crystal with a neutral coformer, and two were cocrystals of salts where both NPOH and NPO species were present along with a cationic coformer, see for example isopropylamine-4-nitrophenolate-4-nitrophenol [Figure 20]. Of these 13 samples,

two can be classed as hydrate forms, both of which were salts. A further two structures contained other solvate molecules (MeCN). One of these MeCN solvates was a salt and the other a cocrystal. Similarly the 50 database samples can be divided as follows: 23 cocrystals, 10 salts and 17 cocrystals of salts. Of these 50 structures 9 were hydrates, 1 of which was a cocrystal, 6 were salts and 2 were cocrystals of salts. Two other structures contained other solvent molecules (1 MeCN, 1 DCM) 1 of which was a salt form and the other a cocrystal.

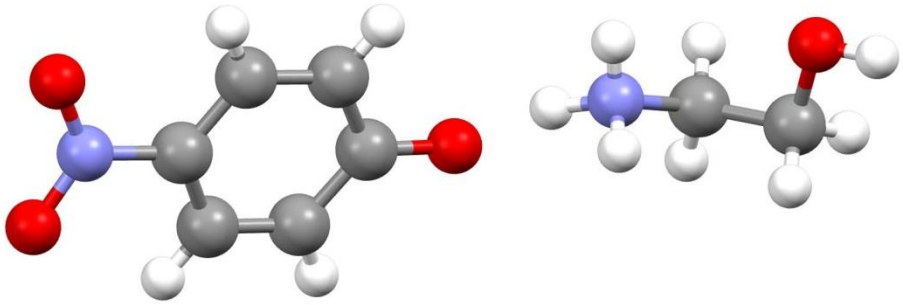

Figure 20: Contents of the asymmetric unit of the salt ethanolamine-4-nitrophenolate.

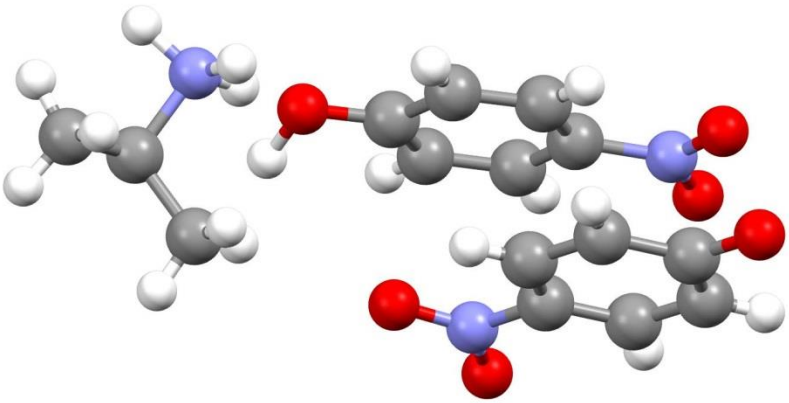

Figure 21: Contents of the asymmetric unit of the cocrystal of the salt formed from isopropylamine and 4-nitrophenol.

3.2.1 Analysis of pKa values of coformers

Due to the desirable properties of the salt forms of 4-nitrophenol found in the literature, a better understanding of the factors leading to salt formation of 4-nitrophenol was pursued. One of the key factors commonly associated with salt formation is the difference in pKa between the coformers.

In the literature it is stated that a salt form can generally be assumed to form when the ΔpKa between the two coformers is greater than 2 [66]. For this work all pKa values were obtained from MarvinSketch [137] and the pKa of NPOH was taken to be 7.16. The ΔpKa for each sample pairing was calculated as follows:

$$\Delta\mathrm{pKa} = \mathrm{pKa}_{\mathrm{Coformer}} - \mathrm{pKa}_{\mathrm{NPOH}}$$

The ΔpKa for all samples can be seen in [Figure 21].

From data collected on salt forms that resulted from protonation of a neutral molecule it is observed that 14/16 (87.5 %) salt forms were produced from coformers with ΔpKa ≥ 2 with an average ΔpKa of 2.78 for successfully formed salts.

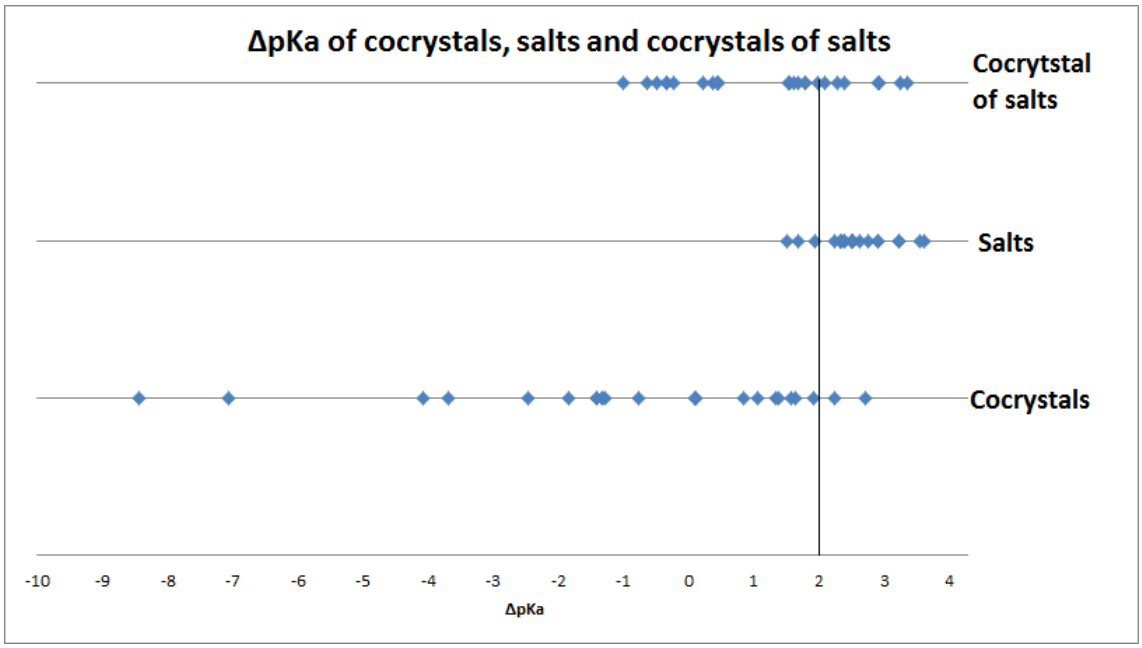

Figure 22: Spread of ΔpKa values for NPOH structures analysed.

As can be seen in Figure 21 all but two salt forms produced involved a ΔpKa between the coformer and NPOH that was greater than 2, the two coformers which do not lie within this trend are: (1S,2R)-(+)-methylephedrine and tris-2-amino-ethylenetriamine (pKa values of 8.86 and 8.68 respectively).

The ΔpKa values for the cocrystal of salts were more varied than the values for salts and indeed overlapped somewhat with the values found for salt forms, however only 7/19 (36.8 %) had values greater than 2. The graph shows this more spread range of ΔpKa values for cocrystal of salt samples with the majority of samples having ΔpKa between 1.7 and 3.3, though a number of cocrystals of salts were formed from reagents with ΔpKa less than 1. The examples with –ve values are interesting as they imply that the NPO anion can be isolated in the solid state even where the coformer is formally more acidic than NPOH (e.g. such coformers as VONYOO, 2-(methylamino)-pyridine). This illustrates nicely that pKa values, which are based on aqueous phases, are not always good guides to protonation/deprotonation behaviour in the solid state.

Finally a large range can be seen for the ΔpKa between reagents used to form binary cocrystalline samples. However, all but two were formed from materials with ΔpKa < 2. The two coformers that have a ΔpKa < 2 are LAQXIM and NUDLON (pKa values of 9.84 and 10.33 respectively) though both of these form zwitterions and the deprotonation occurs at other sites than the NPOH proton. In summary, it seems that which of our three categories of product (salt, cocrystal of salt or cocrystal) forms for a given coformer with NPOH is broadly related to the difference in pKa, but is not entirely governed by this.

3.2.2 Molecular structure of coformers studied

A large amount of crystal structures were found in the literature, these were combined with those elucidated in this project and split into the following categories which are listed below; cocrystals, salts and cocrystal of salt structures.

The cocrystal structures elucidated in this body of work are as follows: 2-amino-3-pyridinecarboxaldehyde –NPOH, 4-acetylpyridine-NPOH and rhodamine B-NPOH.2MeCN. The molecular structures of these coformers together with those found on the CSD for cocrystal forms of NPOH are shown below [Table 8].

Table 7: Molecular structures of coformers involved in formation of NPOH cocrystals.

2-amino-3-pyridinecarboxaldehyde	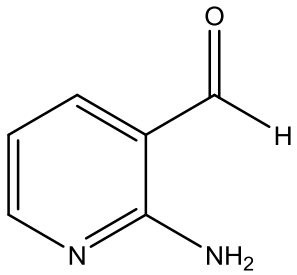
4-acetylpyridine	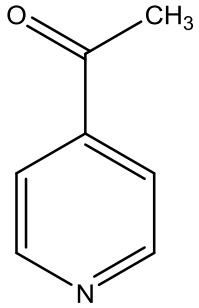
Rhodamine B	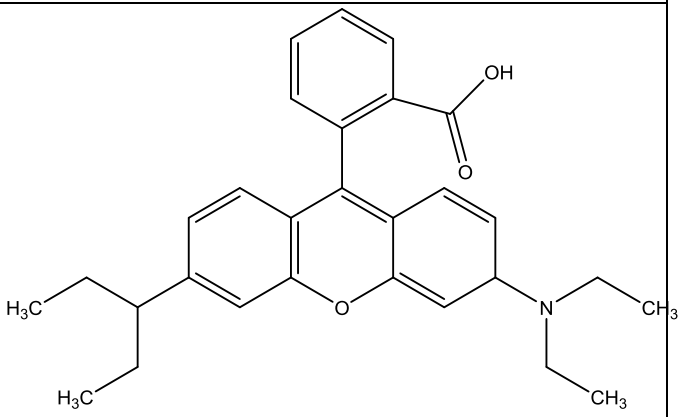

AFIGED	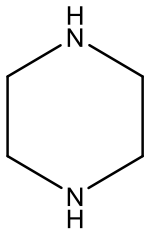
CAXNOE	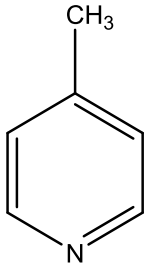
DICCUP	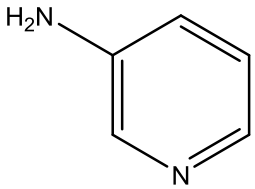
FIQBAJ	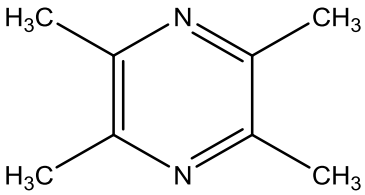
GAVHUH	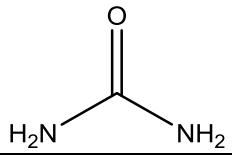
GOBYOL	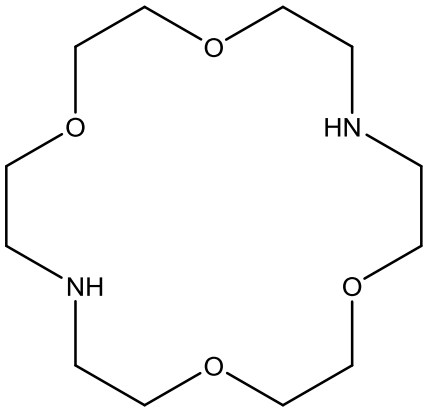

JUDNAX	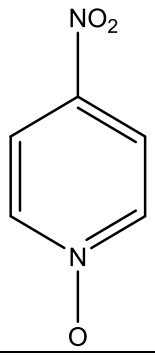
LAQXIM	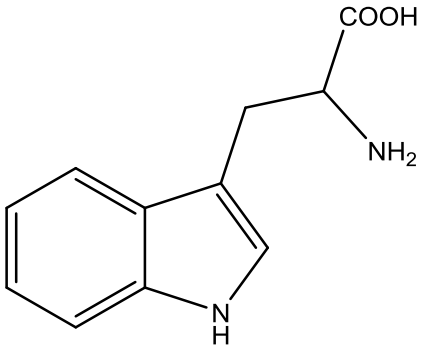
LOCHOB	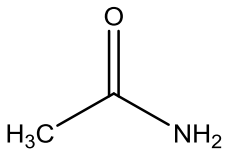
MIZMIT	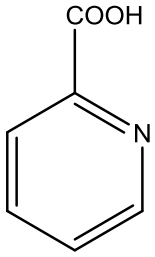
NILZOX	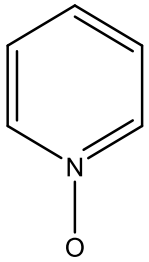
NITPOL	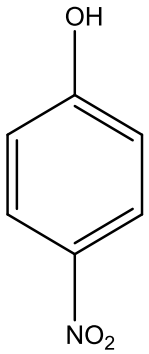

NUDLON	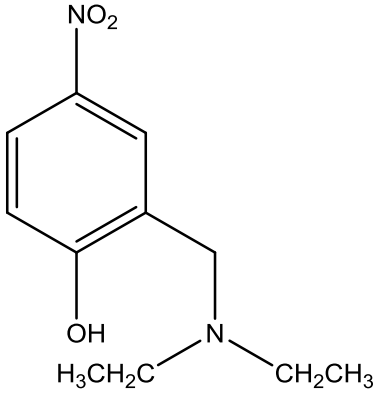
OFUGUR	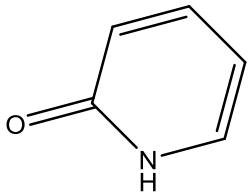
PECQOF	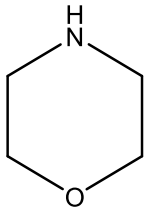
QIRNUC	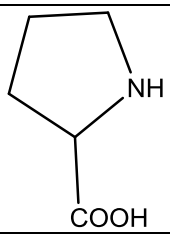
SUBZIY	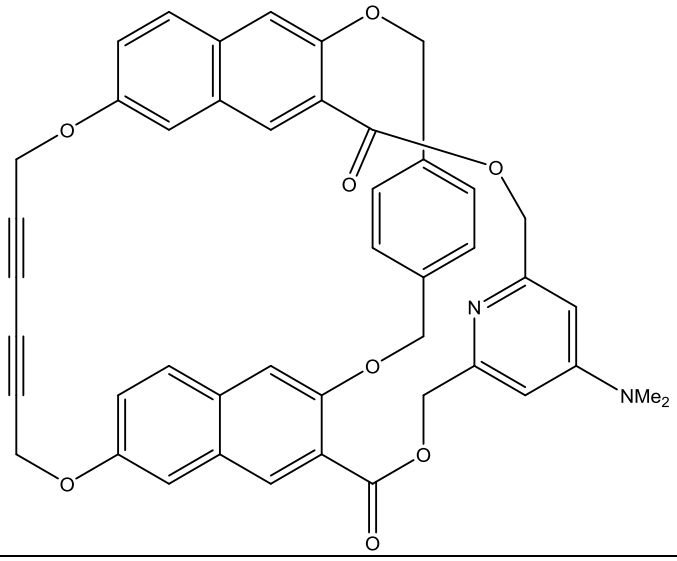

TOPPNP	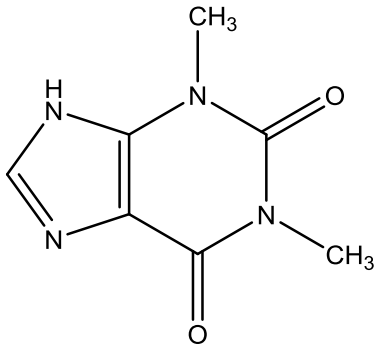
VIVYUU	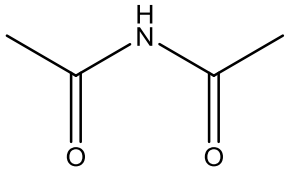
VIVZAB	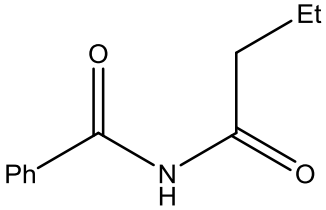
WIRWID	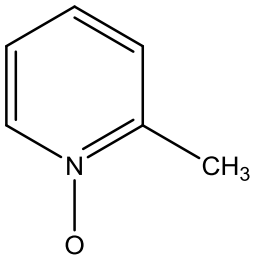
XECBEO	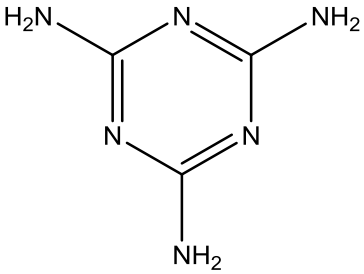
XETLIS	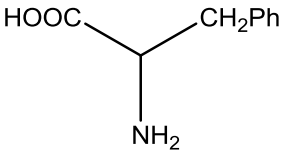

The new salt structures produced in this body of work were as follows: 2-aminobenzylamine-NPO, 1,4-diaminobutane-NPO, dimethylpiperidine-NPO.H_2O, dipropylenetriamine-NPO, (1S,2R)-(+)-ephedrine-NPO.2MeCN, ethanolamine-NPO, (1S,2R)-(+)-methylephedrine-NPO, tris-2-amino-ethylenetriamine-NPO.2H_2O. The structure of these coformers and those found of salt forms of NPO found on the CSD are shown below [Table 9].

Table 8: Molecular structure of coformers involves in salt formation of NPO.

2-aminobenzylamine	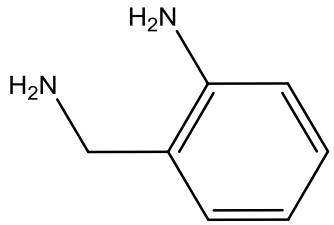
1,4-diaminobutane	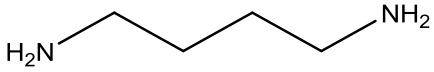
tetramethylpiperidine	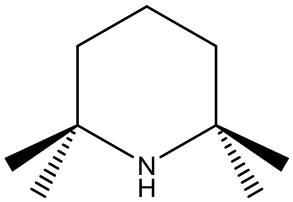
Dipropylenetriamine	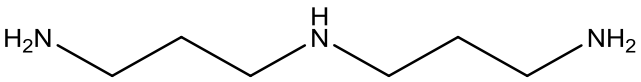
(1S,2R)-(+)-ephedrine	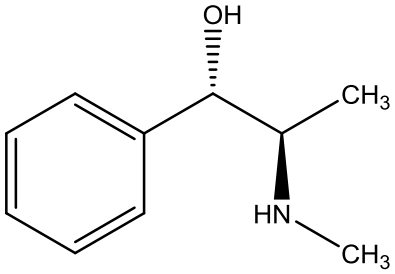
Ethanolamine	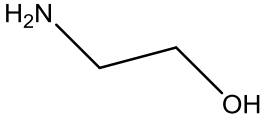

(1S,2R)-(+)-methylephedrine	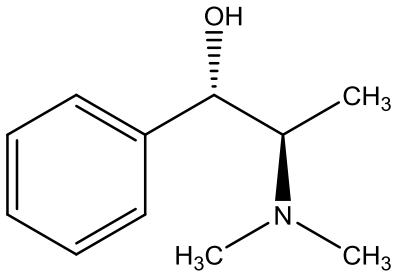
Tris-2-amino-ethylenetriamine	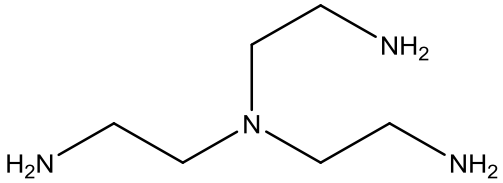
FIRNEA	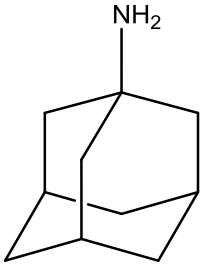
FITZEN	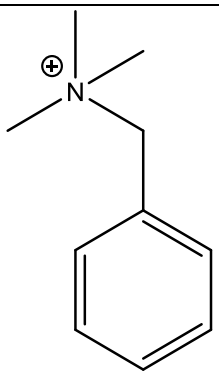

NEDDEF	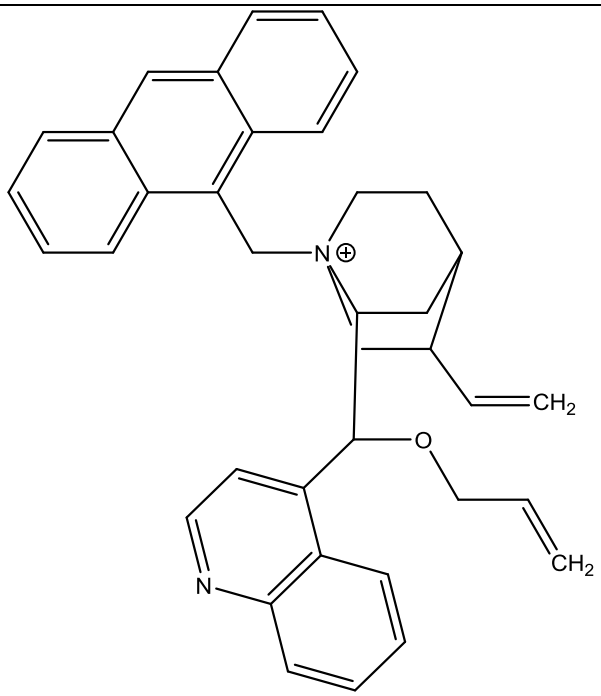
NUZKAU	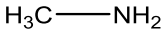
OFIWUW	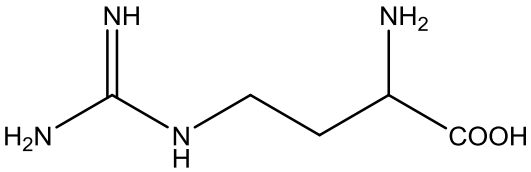
POKBIC	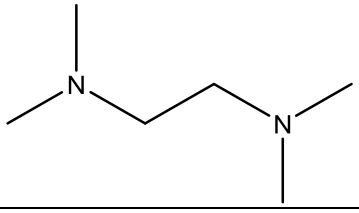
UQAXOA	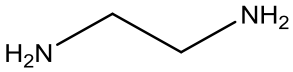
XUTCAQ	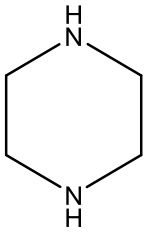
XOVSIM	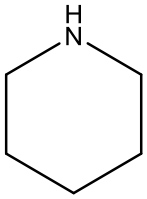
XOVSOS	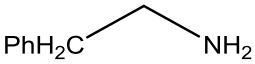

The new cocrystal of salt forms produced were as follows: isopropylamine-NPO-NPOH.H_2O, n-methylpyrollidine-NPO-NPOH. The structures of both of these coformers and those of other cocrystal of salt forms found on the CSD are shown in Table 10.

Table 9: Molecular structure of coformers involved in formation of cocrystal of salt forms of NPO.

Isopropylamine	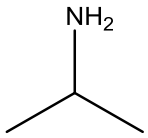
N-methylpyrrolidine	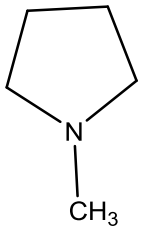
BORGEW	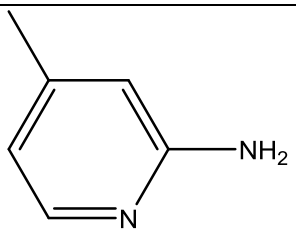
DICCOJ	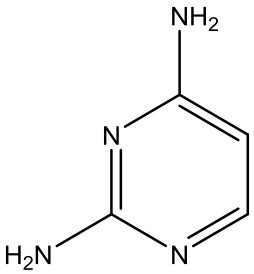
DICDAW	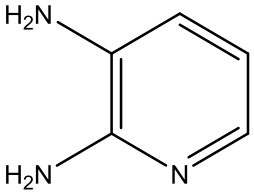
DICDEA	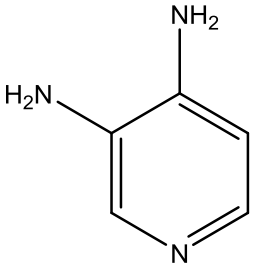

DICDIE	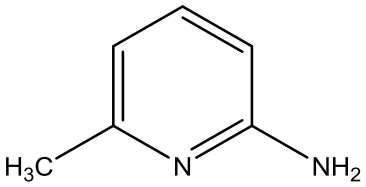
DICDOK	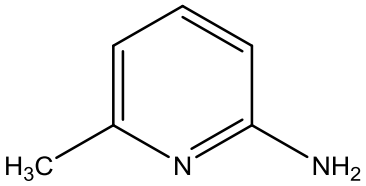
HILMAR	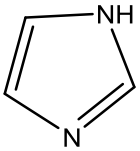
JOYJOY	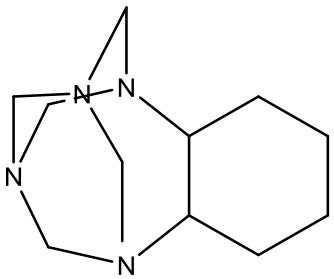
KAPFEN	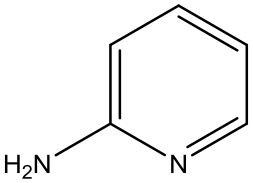
KAPFIR	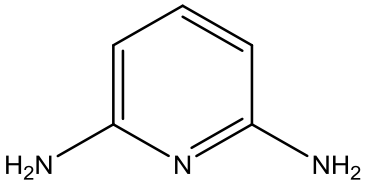
KUSWOL	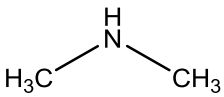
PUMQAP01	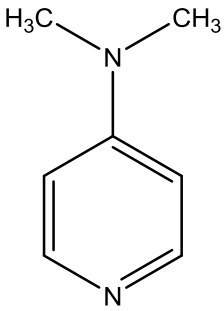

QUYZOA	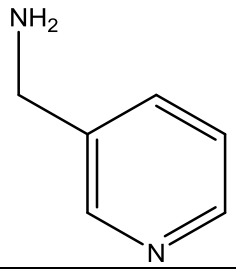
VONYII	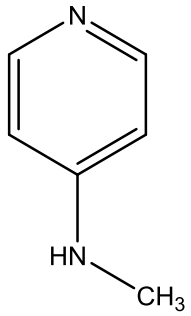
VONYOO	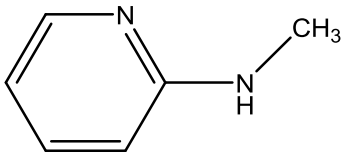
ZUGZIM	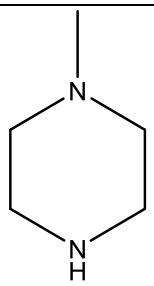

3.2.3 Structural evaluation of 4-nitrophenol complexes

As mentioned in section 3.2.1, factors that influence salt formation were studied. As a large number of crystal structures containing 4-nitrophenol had previously been published this allowed a study of the influence molecular structure on salt formation. These molecular structural features are summarised below:

A total of 10 of the above coformers were non-cyclic aliphatic amines, 8 of these were involved in the production of salt forms and only 2 formed cocrystal of salt species. From this information it appears that non-cyclic aliphatic amines make an excellent option for salt formation of NPOH. 10 of the coformers were alicyclic amine species, the complexes formed with these were evenly spread throughout the three classes adopted with: 3 cocrystals, 4 salts and 3 cocrystal of salt species. The 4 amide coformers were found to form cocrystals with 4-nitrophenol. This last result is expected as only limited examples of protonated amides are found in the literature and these exclusively form under extremely acidic conditions not available here [138].

One common feature of a number of the coformers studied is that presence of a pyridine ring. 21 of the coformers studied contain pyridine or closely related heteroaromatic ring systems, interestingly none of these form binary salt systems with 4-nitrophenol. Instead 11 form cocrystals of salt species and the remaining 10 form cocrystal species.

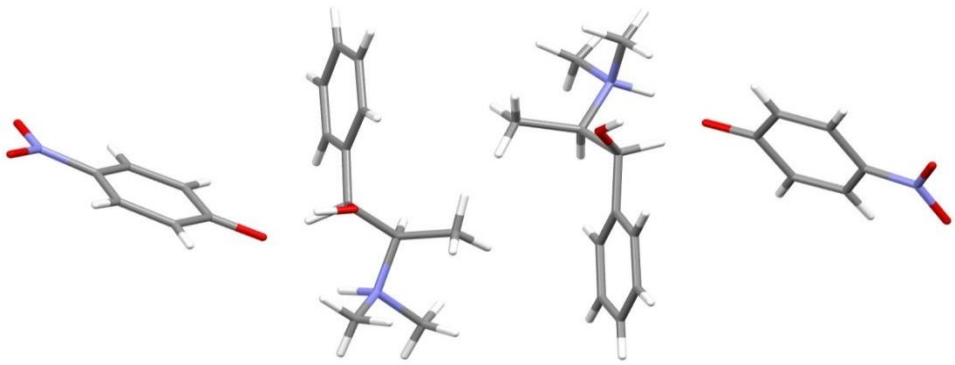

Figure 23: Structure of (1S,2R)-(+)-methylephedrine salt of NPO in the P1 space group.

3.2.4 Overview of intermolecular interactions

While a number of intermolecular interactions occur in the structures, the main focus of analysis in this body of work will be to investigate hydrogen bonding. The NPOH coformer is constant in all structures presented and a summary of its role as a hydrogen bond donor and acceptor is given below. In terms of hydrogen bonding, all classical hydrogen bonding donors present in the structures studied were either amine or hydroxyl groups (and for Rhodamine B, a carboxylic acid group). An initial analysis showed that non-classical donors such as sp^2 C-H groups were rarely involved in short range interactions and so these were not considered further. Acceptors were more variable, but were typically nitrogen or oxygen atoms as components of groups such as amines, hydroxyl/hydroxide, ketones and nitro groups. While nitro groups are typically not considered reliable receptor groups they are investigated in this work due to their consistent involvement in hydrogen bonding motifs present in the studied structures. In 61 out of the 63 structures all hydrogen bond donors formed classical interactions. The 2 donor groups which are not involved in classical hydrogen bond interactions are both N-H fragments of NH_2 groups where one proton is not used. One of these groups is involved in interactions with a π system, thus leaving only GAVHUH as an outlier to Etter's rules [59].

Whilst most potential donors are utilised, the situation with respect to hydrogen bond acceptors is more complicated. A summary of hydrogen bond acceptor behaviour for the different acceptor types available can be seen in Table 11. Of the potential acceptors present in large numbers of structures, only water and the phenoxide and phenol groups are reliable acceptors.

Table 10: Summary of hydrogen bond acceptors.

Acceptor	Number of structures acceptor is involved in H-bonding	%age structures acceptor is involved in H-bonding
NPOH	34	77.2 %
NPO^-	36	100 %
Nitro (both O accept)	17	26.9 %
Nitro (only one O accepts)	15	23.8 %
O (H_2O)	11	100%

3.2.5 Overview of hydrogen bonding

One common hydrogen bonding motif found in many of the cocrystal of salt structures is that formed from the interaction between the phenol and phenoxide groups in those structures where both NPOH and NPO are present [Figure 25]. This hydrogen bonding motif is found in 17/19 cocrystal of salt structures studied (with EMUROU and ZUGZIM being the two cocrystal of salt structures to not make this interaction). Similar motifs are also observed in two related structures found on the CSD (ref codes JUDNAX and NUDLON). Both feature NPOH and a “pseudo-NPO” phenoxide like group, one involves hydrogen bonding between 4-nitropyridine-N-oxide and 4-nitrophenol [Figure 26] and the other hydrogen bonding between 2-(N,N-diethylamino)methyl-4-nitrophenolate 4-nitrophenol. The 17 NPO-NPOH hydrogen bonds all display very short donor-acceptor O to O distances ranging from 2.416 to 2.681 Å (with an average distance of 2.556 Å), this suggests these hydrogen bonds are particularly strong [139]. Timofeeva et. al. also report this hydrogen bonding motif and make a claim that it is responsible for the acentricity of salts formed [113], though this will be further investigated later in this body of work. This more general claim followed earlier work by Prakash and Radhakrishnan who had claimed that the combination of a short NPO-NPOH hydrogen bond together with an *ortho*-aminopyridine fragment was favourable for, and indeed caused adoption of non-centrosymmetric structures [140].

3.2.6 Analysis of NPOH-NPO planar angles

The cocrystal of salt structures discussed in this body of work appear to display a higher likelihood to crystallise in non-centrosymmetric space groups than the salt or cocrystal structures. One common component found in these structures is the NPO-NPOH unit. The structure of this unit was studied by analysing the coplanarity of the two components, a summary of this is presented below.

The planarity of the hydrogen bonded NPO-NPOH units found in the cocrystal of salt structures was compared after splitting these structures into two groups, those that crystallise in centrosymmetric space groups and those that crystallise in non-centrosymmetric space groups. The calculations were done using the program Mercury, by defining the plane of each aromatic ring using the positions of the six aromatic carbon atoms [141] [Figure 24]. The angle calculated is the angle between the NPOH and NPO planes.

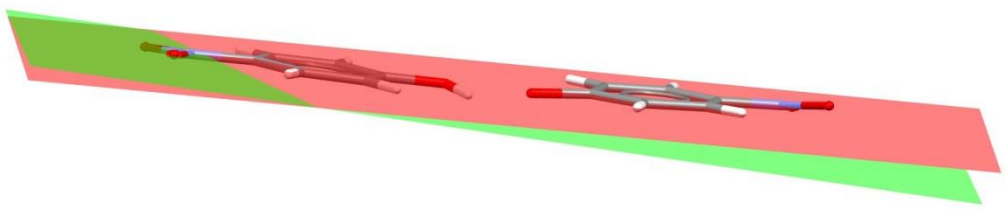

Figure 24: Defined planes of NPOH (green) and NPO (red).

An immediate observation can be made in that the structures that crystallise in non-centrosymmetric space groups tend to have a much more planar relationship between NPO and NPOH than those that crystallise in centrosymmetric space groups. The angle between planes found in 8 of the 11 non-centrosymmetric structures are all less than 10 °, indicating near coplanarity of the two rings. Of the remaining three structures, DICDOK has a modest inter-planar angle of 16.77 ° and

JOYJOY has a clearly different orientation with a near perpendicular 83.33 ° [tables 12 and 13]. Note that the coformer of JOYJOY is much bulkier than any other coformers in the cocrystal of a salt group. In contrast none of the 8 centrosymmetric structures have inter-planar angles of less than 10, with only 2 structures even approaching coplanarity (VONYII and ZUGZIM at 20.03 and 11.52 °respectively). The other 6 structures give values of between 30.21 and 81.22 °, Tables 12 and 13.

Table 11: Non-centrosymmetric structures, NPO-NPOH inter-planar angles (°).

JOYJOY	83.33
PUMQAP	0.76
KAPFIR	2.48
KAPFEN	2.97
EMUROU	9.10
DICDOK	16.77
DICDIE	7.10
DICDEA	4.70
DICDAW	5.10
BORGEW	3.74
NP_isopropylamine	45.68

Table 12: Centrosymmetric structures, NPO-NPOH inter-planar angles (°).

NP-n-methylpyrollidine	72.52
VONYII	20.03
VONYOO	40.54
DICCOJ	81.22
HILMAR	45.54
KUSWOL	73.30
QUYZOA	30.21
ZUGZIM	11.52

Another interesting note is that the non-centrosymmetric structures which contained a pyridine based or similar coformer typically displayed a more planar NPO-NPOH unit than others that did not with an average angle of 5.85 ° for these structures.

NPOH cocrystals that contain pyridine N-oxide coformers were also examined, these structures form a similar motif to the NPO-NPOH motif studied. A similar observation can be made from the planarity of these structures where one structure is found to crystallise in a non-centrosymmetric space group (JUDNAX which crystallises in $Pna2_1$) and has an angle of 7.22 ° between the two planes. The other two pyridine-N-oxide cocrystals (NILZOX and WIRWID) both crystallise in the centrosymmetric space group $P2_1/c$. The angles found between planes for these structures are 41.30 and 87.52 ° respectively. This follows the trend of non-centrosymmetric structures showing a more planar relationship between the two rings.

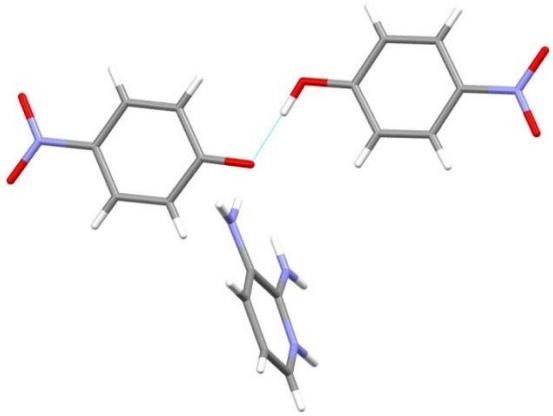

Figure 25: Hydrogen bonding between 4-nitrophenol and 4-nitrophenolate found in the structure DICDAW.

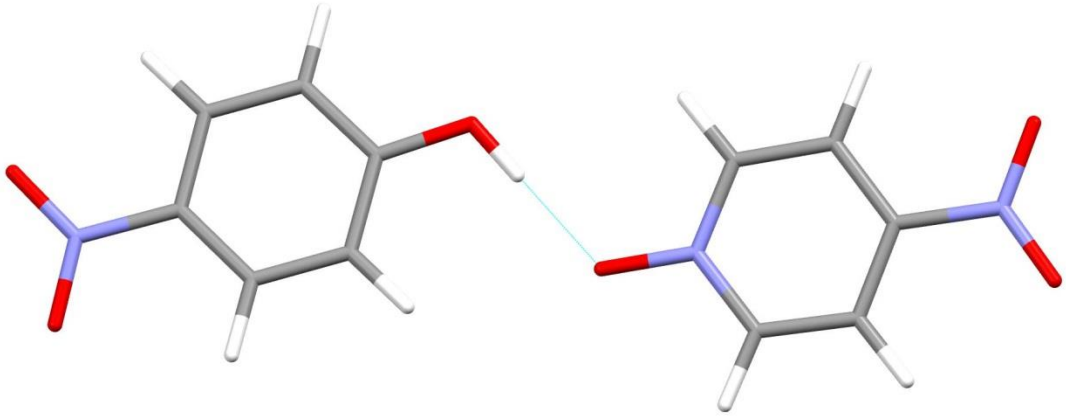

Figure 26: Hydrogen bonding between 4-nitrophenol and 4-nitropyridine-N-oxide found in the structure JUDNAX.

3.2.7 Analysis of hydrogen bond donor-acceptor ratios

Following on from the basic analysis of hydrogen bonding the ratio between hydrogen bond donors and acceptors is studied. In this project the hydrogen bonding donor : acceptor ratio is used in attempt to predict the ionisation state of the final product.

When looking at hydrogen bonding within the structures studied a number of general observations can be made. The first is that all structures which contain at least one hydrogen bond donor group form hydrogen bonds between both coformer species of the complex. Another general observation is that in structures that contain solvent water molecules, all water molecular protons are utilised as hydrogen bond donors and all but one water molecule were involved in classical hydrogen bonding interactions as acceptors, with the remaining otherwise non-utilised acceptor forming hydrogen bonds with an sp^2 carbon centre.

When examining hydrogen bond donor and acceptor ratios three different methods of comparison were utilised. The first involved using no prior knowledge where a 1:1 ratio of 4-nitrophenol and the coformer was assumed, the second involved examining the ratio of donor and acceptor groups found in the asymmetric unit of the crystal and the third involved the sum of donor and acceptors in the asymmetric unit.

All structures were divided into three categories; salts, cocrystals and cocrystals of salts and the average values for each of the three methods of comparisons were taken. Looking at the average values obtained from method 1, salt and cocrystal of salt structures appear to have similar average donor to acceptor ratios (0.81 and 0.72 respectively) with cocrystals having a lower average ratio of 0.43.

As expected the most noticeable difference between the ratios calculated by the first two methods of comparison is seen in cocrystal of salt structures, as the first method of comparison would not account for acceptor and donor groups present on the

uncharged nitrophenol species. This results in the average D:A for these species dropping to 0.45, this new value is closer to that of cocrystals rather than salts (0.46 and 0.80 respectively). Finally when looking at the sum of donors and acceptors (i.e. D + A) present in the asymmetric unit the average value is similar for cocrystals and salts (10.22 and 10.59 respectively). However, as expected cocrystal of salt samples with the extra molecular unit present have slightly higher average values (12.65).

3.2.7.1 Analysis of hydrogen bond donor-acceptor ratios of hydrate structures

The addition of water molecules into the crystal structure provides an additional two hydrogen bond donors and one acceptor. The relationship between hydrogen bond acceptor: donor ratio and likelihood of hydrate formation is discussed.

When studying hydrogen bonding of hydrate structures it is noted that the data set contains 11 such structures, 7 of which are salts, 1 a cocrystal and 3 cocrystal of salt forms. The salt form hydrates have a slightly higher average D:A ratio than the anhydrous salt forms (0.87 and 0.75 respectively). Note these values do not include the donor and acceptor groups of the solvent water molecules present in the structure. The D:A of the cocrystal hydrate is also higher than the average value of anhydrous cocrystals (0.67 and 0.39) though only limited conclusions can be drawn here as only a single data point is present. Finally a higher D:A is also seen for cocrystal of salt samples (0.74 and 0.67 respectively). Thus all three categories of hydrate species display a higher D:A than the anhydrous structures, this suggests that a higher D:A ratio can lead to an increased likelihood of hydrate formation. This is perhaps an expected result as the solvate water molecule provides two reliable hydrogen bond acceptors capable of forming strong hydrogen bonds with unused donor groups.

3.2.8 Crystal structure analysis

A primary objective of this project was to link molecular and structural features to the likelihood for a material to crystallise in a non-centrosymmetric space group. An overview of the structures elucidated in house and those collected from the literature is given below describing the number of each form produced and the percentage of each that crystallised in non-centrosymmetric space groups.

Out of the 63 structures examined, 24 formed in non-centrosymmetric space groups and thus are potentially NLO active. For the new structures in this body of work, 2 of the non-centrosymmetric structures are salt forms while one is a cocrystal of a salt. The non-centrosymmetric CSD derived structures consisted of 4 salt forms, 11 cocrystals of salts and 6 cocrystals.

However, of the 63 coformers examined 5 were enantiopure, namely (1S,2R)-(+)-methylephedrine, (1S,2R)-(+)-ephedrine, L-phenylalanine, L-tryptophan and L-arginine . Structures containing enantiopure components may only crystallise in the class of crystallographic space groups known as Sohncke space groups. These 65 space groups involve only symmetry operations based on translation and/or rotation and are thus non-centrosymmetric and therefore of interest to this study due to their potential to be NLO active.

Not considering cases where use of enantiopure bases forced the result, 1 of the 11 structures (9.1 %) newly synthesised and elucidated in this body of work and 19 out of 56 (33.9 %) of the structures found on the data base were found to be non-centrosymmetric. Out of a total of 754897 organic structures found on the CSD 124574 (21.9 %) crystallised in non-centrosymmetric space groups. This statistic included all organic structures found on the CSD including those containing enantiopure material which can only crystallise in non-centrosymmetric space groups. Therefore the “true” likelihood of a random achiral material crystallising in a non-centrosymmetric space group would be lower than the reported value of 21.9 %. Indeed, Etter and Huang estimate that only 11 % of achiral materials

crystallise in non-centrosymmetric space groups [112]. Working in the opposite direction, it is often claimed that salt forms of achiral materials in general have a higher than normal chance of crystallising in non-centrosymmetric space groups. The argument here is that neutral but polar organic molecules (e.g. NPOH) have a tendency to form centrosymmetric dimers that maximise dipole to dipole interactions. These dimers are inherently centrosymmetric. Introducing charges and counterions allows stronger ionic interactions to swamp the dipole to diploe contribution and lessen the chances of a centrosymmetric structure. Despite these arguments, no numerical estimate was found as to how much more likely salt forms were to adopt non-centrosymmetric structures [133].

Whatever estimate is used, those structures of 4-nitrophenol complexes found in the literature do appear to have a higher tendency to form in non-centrosymmetric space groups, as has been claimed [111]. However, the statistics for the structures newly elucidated in this body of work are much lower, being less than or equal to the general probability of an acentric species forming in a non-centrosymmetric space group. With relatively small numbers of “new” structures it is hard to make a conclusive statement. However, it should be noted that these figures are what would be expected if the high percentage of non-centrosymmetric structures reported for literature NPO and NPOH structures came about not for good structural reasons, but merely because of a reporting bias favouring the reporting of potentially active structures over inactive centrosymmetric ones.

3.2.9 Crystal packing similarity

Following the structural analysis in section 3.2.8 the search for isostructural units was carried out, this search contained both structures elucidated in house and those gathered from the literature. This search was carried out using the Mercury Crystal Packing Similarity software package.

The Mercury Crystal Packing Similarity [141] program allows analysis of a set of structures by comparing the packing of a single consistent molecule or molecular fragment throughout a data set of multiple structures that all contain the consistent molecule (in this case 4-nitrophenoxide fragments in a dataset of nitrophenoxide salt forms and nitrophenol cocrystals). The process involves searching for groups in which the studied molecule packs in geometrically similar clusters through cluster sizes of: 2, 3, 4, 6, 8, 12 and 15 molecules. For the purpose of this body of work only the packing of $HO(C_6H_4)NO_2$ was analysed and the counterions or coformer molecules present were ignored. The results of this analysis were then plotted on the tree diagram shown below [Figure 27]:

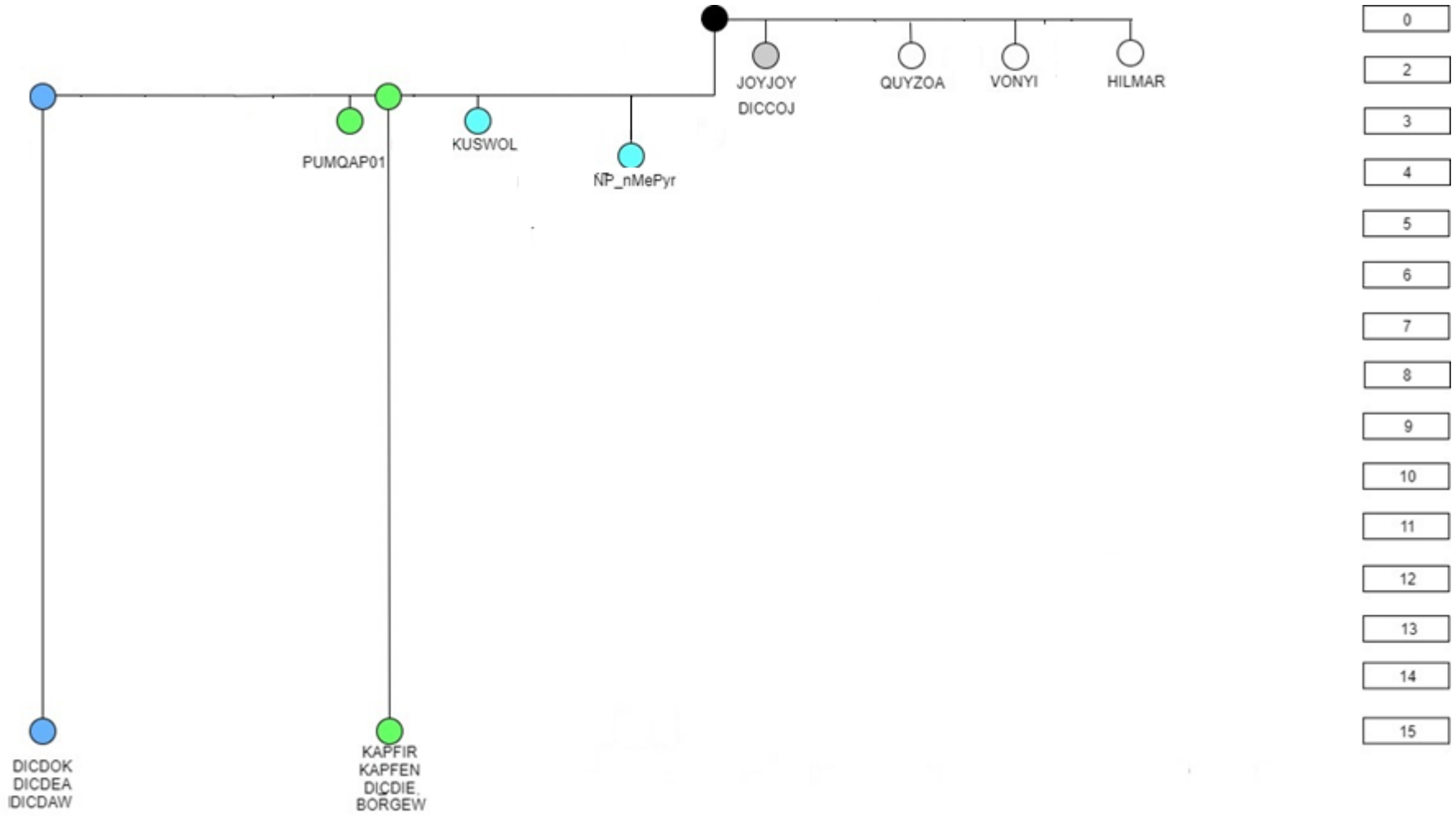

Figure 27: Packing diagram for cocrystal of salt 4-nitrophenol materials studied.

As can be seen in figure 26, two groups are found. The structures in each group have identical packing behaviour of NPOH fragments at least up to cluster sizes of 15 molecules. They are thus said to be isostructural with respect to NPOH packing. All structures not part of these three groups are highly individual, with no high level packing similarities. The isostructural groups both contain only cocrystal of salt type structures and will be described as group 1 (DICDOK, DICDEA and DICDAW) and group 2 (KAPFIR, KAPFEN, DICDIE and BORGEW). The structures of the coformers of each of these are shown below [Tables 14 and 15]. It should be noted that only the cocrystal of salt structures displayed any packing similarity and therefore only these structures are shown in the tree diagram, also 4 cocrystal of salts did not display any packing similarity and therefore do not appear in the figure.

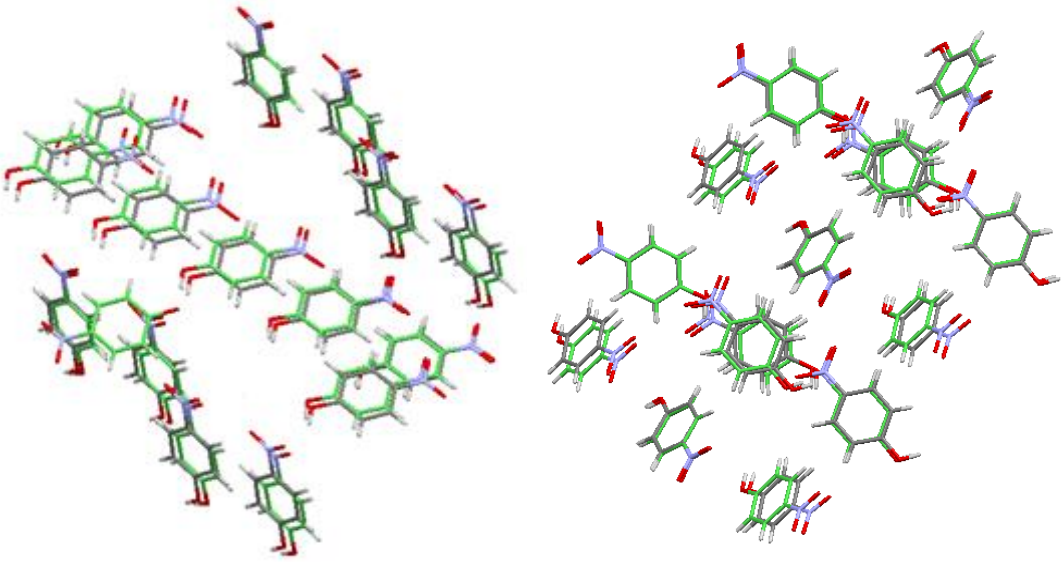

Figure 28: Packing diagram showing isostructural units for group 1 (left) and group 2 (right).

Table 13: Structures of coformers involved in group 1.

Group 1	
DICDOK	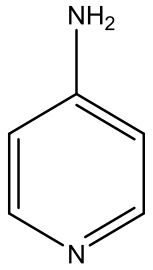
DICDEA	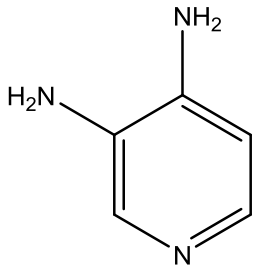
DICDAW	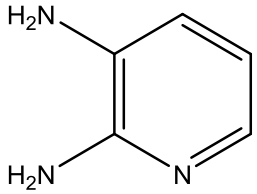

Table 14: Structures of coformers involved in group 2.

KAPFIR	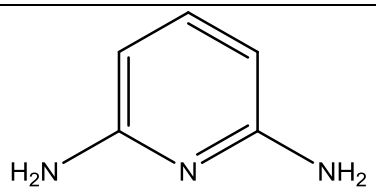
KAPFEN	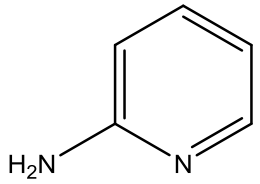
DICDIE	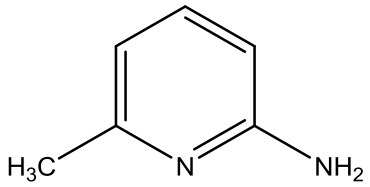
BORGEW	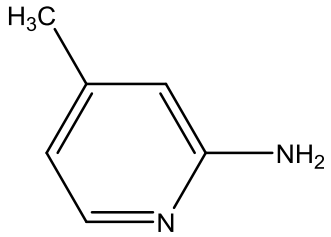

One interesting observation is that all 7 of these structures crystallise in polar (non-centrosymmetric) space groups. These are $P2_1$ and $Pna2_1$ for the group 1 and 2 structures respectively. These are therefore all potentially SHG active. Each group also consists of isomorphous structures, that share similar unit cell parameters (Group one approx. *a* = 5 *b* = 15 *c* = 11 Å, group two approx. *a* = 13 *b* = 11 *c* = 12 Å). Note that there is no need for an isostructural packing group to consist solely of structures with the same symmetry and similar unit cells [142].

Other similarities between the structures in groups 1 and 2 are obvious. Chemically it should be noted that all 7 of these structures contain amino-pyridine coformers with all members of group 2 featuring *ortho* substituted primary amines. Similar coformers such as picoline (methyl pyridine, CAXNOE) where the amine substituted pyridine system is not present, do not crystallise in polar space groups. Thus perhaps suggesting that the amino pyridine system leads to a higher possibility of crystallising in such space groups. One amino-

pyridine coformer that does not share crystal packing similarity with group 1 or group 2 is 3-aminopyridine (DICCUP). Despite dissimilar packing behaviour, this NPOH cocrystal form (as opposed to the cocrystal of salt forms found for the other aminopyridines) does crystallise in the polar, SHG active $P2_1$ space group. It should also be noted that the closely related pyridine alkylamine pyridine-3-methylamine (QUYZOA) does not share the same packing or crystallise in a polar space group (here P-1) which perhaps suggests an influence from the planar geometry of the above mentioned coformers. A final structural comparison is that between the above coformers and 2,3-diaminopyrimidine (DICCOJ) which has a similar molecular structure to KAPFIR but with the presence of a second aromatic nitrogen. This complex is a cocrystal of a salt but does not share similar packing and again does not crystallise in a polar space group (P-1). From the perspective of chemical identity, it can this be stated that aminopyridine species are likely to form polar, SHG active compounds with NPOH, whilst even closely related congeners do not favour such structures.

As all 7 structures form cocrystal of salt species with NPOH, this leads to the possibility that it is the short NPO-NPOH hydrogen bonding interactions that are a dominant attractive force in these structures and that are common throughout them is somehow favourable to non-centrosymmetric packing. As mentioned above Timofeeva et. al have reported a link between this particular hydrogen bonding motif and crystallisation of these species in polar space groups [113] and this structural feature is observed in all 7 structures. The one new cocrystal of salt structures elucidated in this body of work that crystalizes in a non-centrosymmetric space group also fits with this observation, resulting in a high fraction of 12 out of 19 (63.3 %) structures which contain this structural feature crystallising in polar space groups.

While hydrogen bonding is the main focus of this analysis other short contacts present in the above isostructural groups were also examined. Both groups of structures contained π-π interactions between 4-NPOH and the coformer. All of the group 1 structures contained edge (coformer) to face (NPOH) π interactions (3.493 Å shortest C···C contact) while all of the structures of group 2 formed face

(NPOH) to face (coformer) π interactions (3.377 Å shortest C···C contact). An example of both of these interaction types can be seen in figure 29.

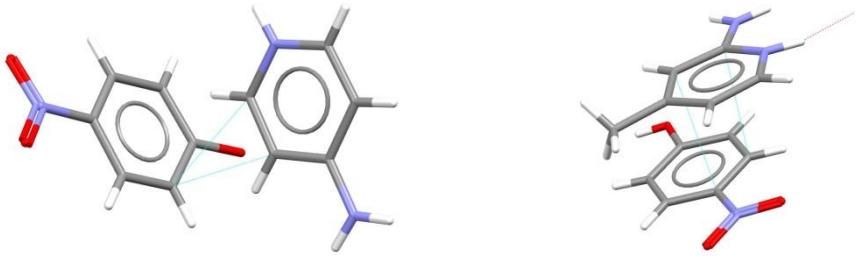

Figure 29: Edge to face (left) and face to face (right) π interactions found in the structures DICDOK and BORGEW respectively.

Finally a comparison between NPO-NPOH hydrogen bond length and bond angle was examined and plotted for the structures of group 1 and group 2 [Figure 30]. The O to O distance was chosen to represent bond length as this is measured more accurately than H to O distances. One reason the group 1 O···O distances may be shorter than those seen in group 2 is because the NPOH and NPO oxygen atoms make less interactions with neighbouring groups than those in group 2 (with group 1 making contact with the proton of an amine each and group 2 making 2).

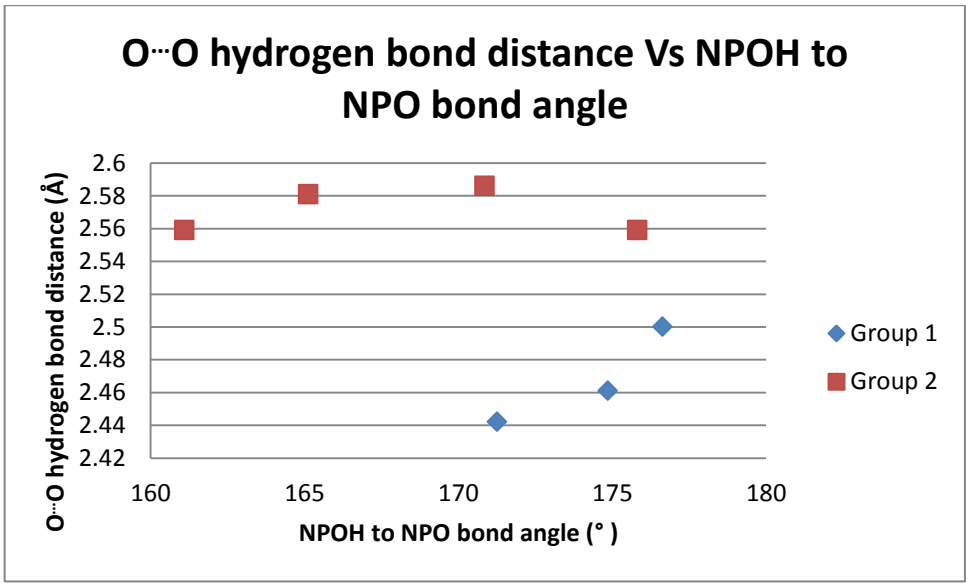

Figure 30: plot of hydrogen bond distance Vs bond angle for the NPOH to NPO hydrogen bond in the 7 structures of groups 1 and 2.

All of the structures in both groups 1 and 2 have O···O distances that are shorter than the typical 2.75 to 2.85 Å found for other structures [143-144] with O-H···O hydrogen bonds. It is known that hydrogen bonds involving charged species and those where H atoms are in equilibrium between to O atoms have typically short O···O distances and this is usually assumed to indicate strong, attractive interactions [145-146]. One interesting detail which can be observed from this plot is that the structures of group 1 form shorter hydrogen bonds between NPOH and NPO. The bond angles for the group 1 structures are also very close to linearity. This suggests a stronger hydrogen bond has formed in these group 1 structures though all O···O distances are relatively short suggesting that in all cases this hydrogen bonding motif is typically strong, as might be expected for charge assisted hydrogen bonding [143].

3.2.10 Graph set analysis

The hydrogen bonding motifs found within the structures studied were identified using the calculate graph set function in Mercury 2.0. The common motifs found in salt, cocrystal and cocrystal of salt forms are discussed.

Hydrogen bonding was examined in greater detail than previously discussed with the goal of finding common hydrogen bonding motifs and crystal structural features using graph set analysis, as originally suggested by Etter et. al. [112]. Typically graph set notation is written in the following form $G^a_d(r)$ where G is the pattern designator, a and d are respectively the number of acceptors and donors present, and r is the degree which refers to the size of a ring formed or the repeating length of a chain. G is used to describe the pattern of hydrogen bonding, consisting of 4 possible descriptors: S, C, R and D. Of these descriptors, S describes an intramolecular interaction, C describes intermolecular chains that propagate infinitely, R refers to ring structures such as the carboxylic acid dimer seen in Figure 31 which commonly forms and D refers to noncyclic dimers and other finite hydrogen bonding patterns.

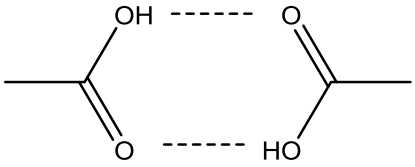

Figure 31: Carboxylic acid dimer ($R_2^2(8)$).

The hydrogen bonding of the nitrophenol structures were inspected in greater detail to determine the presence of more complex hydrogen bonding networks and to identify any common motifs between sets of structures. The first subset of structures to be examined are the cocrystals. An initial observation that can be made from these structures is that a large number of the cocrystals that crystallise in centrosymmetric space groups do not form any complex hydrogen bonding networks as 7/20 of these only form $D^1_1(2)$ discrete units between NPOH and the coformer whereas all but one of the non-centrosymmetric cocrystal structures form complex hydrogen bonding networks(the exception is JUDNAX where only one acceptor and donor group are present which then form a $D^1_1(2)$ discrete unit with each other). A common motif found in the 13 remaining centrosymmetric structures that do form complex hydrogen bonding networks is small ring geometries formed from coformer···coformer hydrogen bonds. Such examples involve $R^2_2(8)$ and $R^2_2(10)$[such as those seen in Figure 32] interactions. These rings are seen in 8 structures that crystallise in centrosymmetric space groups whilst no non-centrosymmetric cocrystal examples form these motifs. A summary of these ring motifs can be seen in table 16.

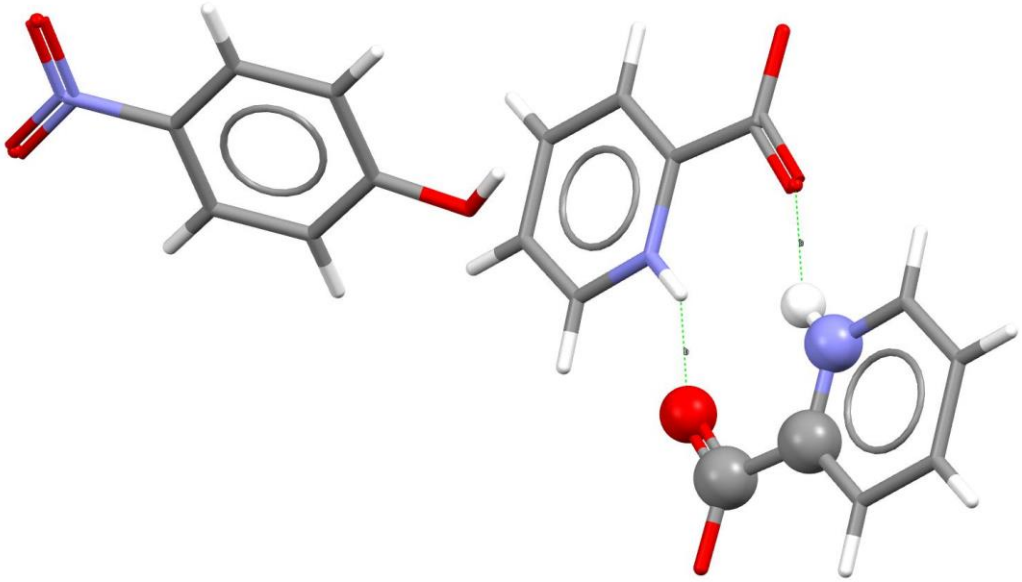

Figure 32: $R_2^2(10)$ ring network between two coformers found in the structure MIZMIT, a cocrystal which crystalizes in the centrosymmetric space group P-1.

Table 15: Summary of ring motifs formed within centrosymmetric cocrystal structures.

Structure	Hydrogen bonding interaction a	Hydrogen bonding interaction b	Graph set notation
[NPOH]-2-amino-3-pyridinecarboxaldehyde	NH_2···C=O	NH_2···C=O	$R^2_2(12)$
GAVHUH	NH_2···C=O	NH_2···C=O	$R^2_2(8)$
LOCHOB	NH_2···C=O	NH_2···C=O	$R^2_2(8)$
MIZMIT	NH···COO	NH···COO	$R^2_2(10)$
OFUGUR	NH···C=O	NH···C=O	$R^2_2(8)$
VIVZAB	NH···C=O	NH···C=O	$R^2_2(8)$
VIVYUU	NH···C=O	NH···C=O	$R^2_2(8)$
XECBEO	NH_2···N (triazine)	NH_2···N (triazine)	$R^2_2(8)$

A final structural motif seen in the non-centrosymmetric cocrystals is the presence of short chain motifs (e.g. $C^1_1(5)$, $C^1_1(6)$) [Figure 33]. These chain motifs propagate through coformer repeat units. These chain motifs are observed in 4 of the 5 non-centrosymmetric cocrystals which show complex hydrogen bonding networks. These chains formed through coformer-coformer interactions are found in two centrosymmetric cocrystals (NUDLON and PECQOF).

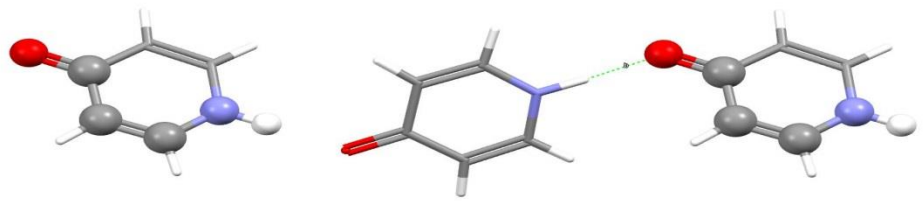

Figure 33: $C^1_1(6)$ chain propagating through coformer···coformer contacts found in the non-centrosymmetric cocrystal PUMQET.

The next set of structures we will examine is the salt forms of nitrophenol. One observation that can be made is the presence of large ring motifs in centrosymmetric structures ($R^4_4(20)$ and $R^4_4(26)$ these involve interactions typically between sets of coformers and NPO anions [Figure 34]. These ring networks are seen in 8/14 salts that crystallise in centrosymmetric space groups whereas this motif is not seen in any of those which crystallise in non-centrosymmetric space groups. A similar interaction occurs in the structure XUTCAQ where water molecules bridge the NPO molecules instead of coformers resulting in a $R^2_4(8)$ interaction.

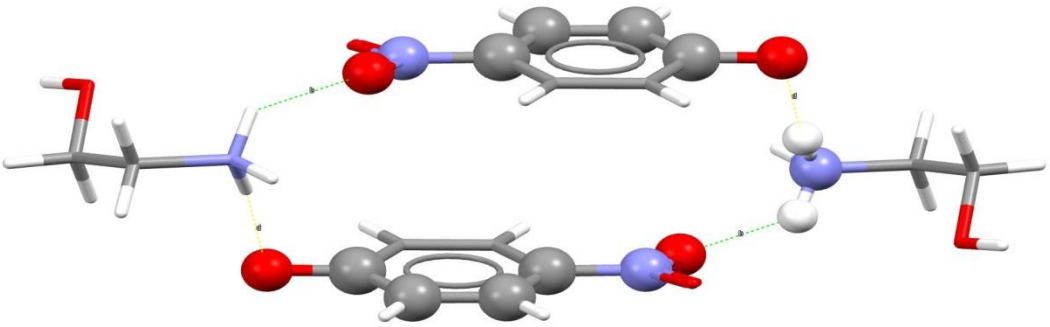

Figure 34: $R^4_4(20)$ ring network between coformers and NPO found in the centrosymmetric salt formed from 4-nitrophenol and ethanolamine.

Another feature of the salts which crystallise in non-centrosymmetric space groups is the tendency to form small chain motifs such as $C^1_2(4)$, $C^1_2(6)$ and $C^1_2(7)$ interactions between two coformers and NPO, as seen in figure 35. These interactions are present in all of the non-centrosymmetric salts but are found in only 4/14 centrosymmetric salt forms.

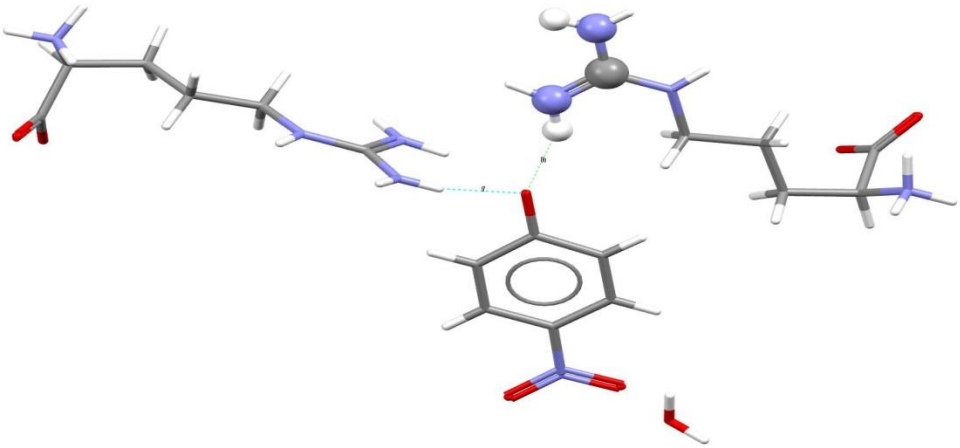

Figure 35: $C^1_2(6)$ chain formed between coformers and NPO (Example shown is found in the non-centrosymmetric salt OFIWUW).

The final set of structures to be examined is the cocrystals of salts. As discussed above, one common hydrogen bonding motif found in both centrosymmetric and non-centrosymmetric structures is the hydrogen bond interaction between NPOH and NPO and the coformer. In graph set notation this is a discrete $D^1_2(3)$

motif (as seen in figure 36) and it is found in 7/8 centrosymmetric structures and 10/11 non-centrosymmetric structures. Neither of the two structures (ZUGZIM and EMUROU) that do not form this discrete unit form the common phenoxide to phenol NPO-NPOH interaction described throughout this section. However, ZUGZIM does form a $D^1_2(3)$ unit between coformer···NPO···H_2O. Thus here water takes the structural role of phenol.

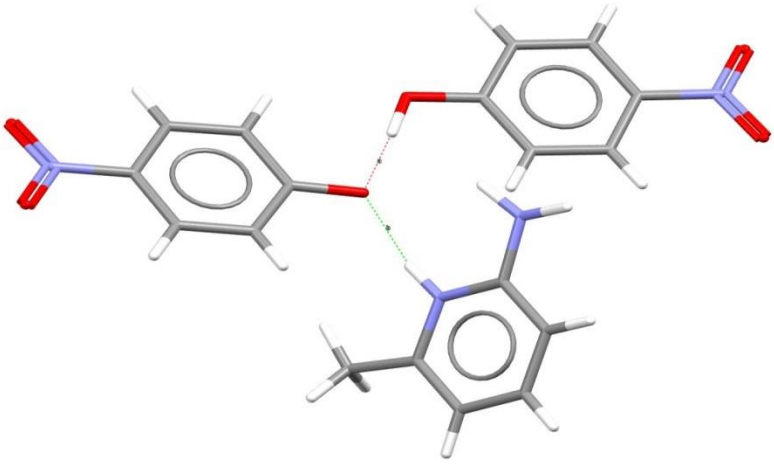

Figure 36: $D^1_2(3)$ interaction between coformer…NPO…NPOH (example shown above is found in the non-centrosymmetric cocrystal of salt structure DICDIE).

Another common feature of the non-centrosymmetric structures is small ring networks formed through $R^1_2(6)$ and $R^2_1(4)$ motifs, typically between coformer···NPO and coformer···NO_2 respectively as seen in figure 37. The $R^2_1(6)$ interaction between coformer and NPO is seen in 5/11 structures and the $R^2_1(4)$ interaction is present in 5/11, contrastingly both of these are each found in only one centrosymmetric structure (DICCOJ and VONYII respectively).

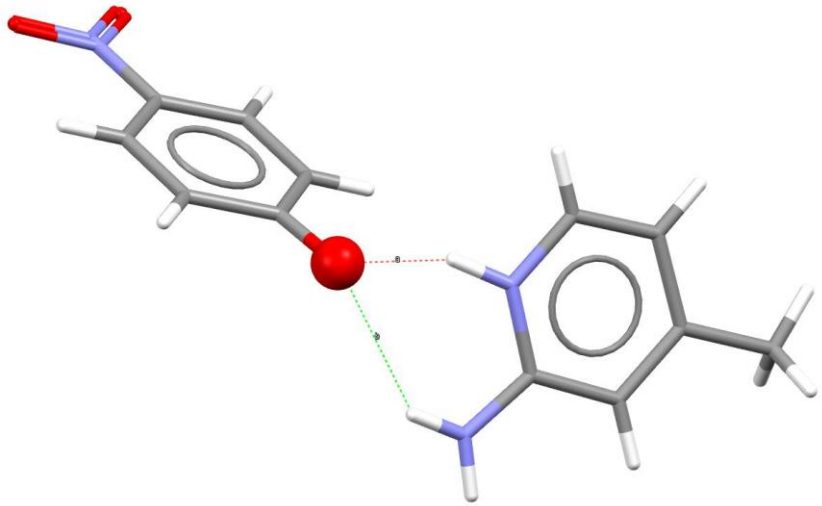

Figure 37: $R^1_2(6)$ ring motif found in the cocrystal of salt structure BORGEW.

The final motifs to be discussed are the chains that form between NPO···Coformer···NO_2 ($C^2_2(10)$, $C^2_2(12)$ and $C^2_2(13)$) as seen in figure 38. These chain networks are found in 8/11 non-centrosymmetric structures but are only found in two of eight centrosymmetric structures. The two centrosymmetric structures which this motif is found in are KUSWOL and DICCOJ. DICCOJ is particularly interesting as the coformer (2,3-diaminopyrimidine) is molecularly similar to a number of coformers identified as giving families of related structures which crystallise in non-centrosymmetric space groups (including those of isostructural packing groups 1 and 2 discussed previously). It should also be noted that DICCOJ also contains a $R^4_4(20)$ ring motif which is described above as a common hydrogen bonding motif found in structures that crystallise in centrosymmetric space groups.

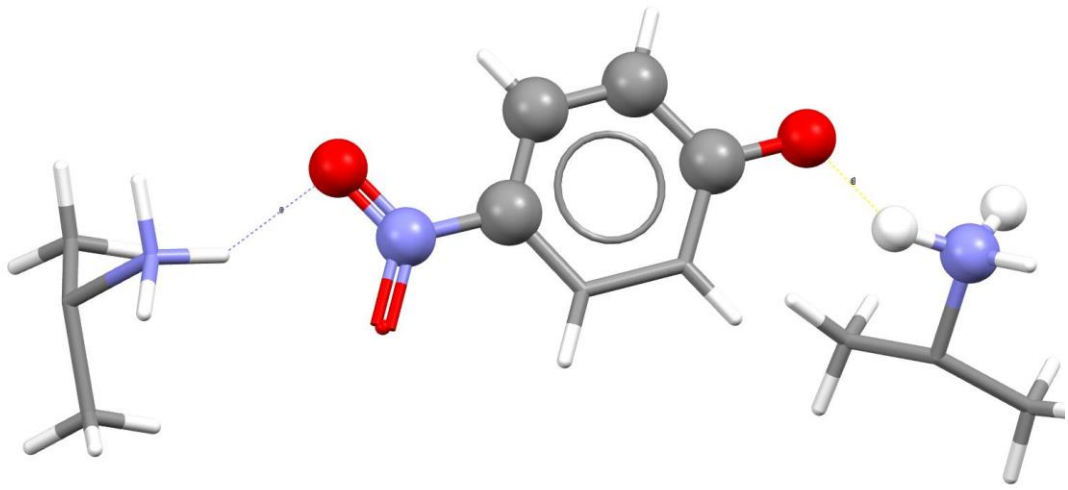

Figure 38: $C^2_2(10)$ chain propagating through coformer…NPO…coformer contacts (example shown above is found in the non-centrosymmetric cocrystal of salt structure NP_isopropylamine).

3.2.10.1 Comparison of crystal packing groups to all cocrystal of salt structures

Upon further examination a number of common hydrogen bonding motifs are seen to be shared between members of isostructural group 2 (BORGEW, DICDIE, KAPFEN and KAPFIR). Note that as here the isostructural packing refers to the packing of the NPOH units, there is no strict need for the structures to share hydrogen bonding motifs. Two motifs which are present in all 4 members of group 2 are the NPOH···NPO interaction and the hydrogen bond formed between the protonated pyridine nitrogen and the deprotonated hydroxide group of NPO. In all 4 structures these two interactions combine to form a discrete hydrogen bonded unit through a $D^1_2(3)$ motif, as seen in figure 39 which results in a NPOH-NPO-coformer unit. This interaction is also seen in all but two of the general set of cocrystals of salts studied above, thus it cannot be said to be a driver to adoption of non-centrosymmetrical structures. However, a difference is observed in that all four of the structures in group 2 make this interaction through the protonated pyridine nitrogen whereas a variety of donor groups are involved in the remaining structures.

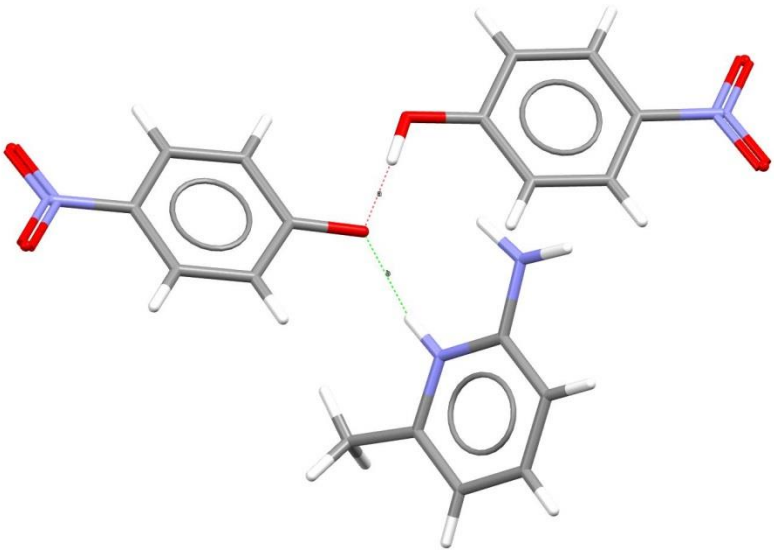

Figure 39: $D^1_2(3)$ graph set formed between NPO, NPOH and coformer. Similar clusters are found in all group 2 structures (example shown above is found in the non-centrosymmetric cocrystal of salt structure DICDIE).

A third hydrogen bonding interaction found in the group 2 structures is that formed between the *ortho* substituted primary amine of the coformer and the nitro group of NPOH. This hydrogen bonding interaction is involved in further hydrogen bonding networks including both of the previously mentioned (NPOH···NPO and Pyridine N···NPO) hydrogen bonding motifs. These two hydrogen bonding networks involve the formation of discrete groups through $D^2_2(7)$[Figure 40] and $D^2_2(10)$ interactions. The $D^2_2(7)$ group is formed from hydrogen bonding interactions between the meta-substituted primary amine of the coformer and the nitro group of NPOH and the interaction between NPO and the protonated pyridine nitrogen. This interaction is not present in any other non-centrosymmetric cocrystal of salt structure outwith the members of group 2. The $D^2_2(10)$ interaction occurs from hydrogen bonding interactions between the *ortho* substituted primary amine of the coformer and the nitro group of NPOH and the interaction between NPO and NPOH, this interaction however is also seen in two other non-centrosymmetric structures (DICDOK and NP-isopropylamine). A similar interaction to $D^2_2(7)$ is seen in one centrosymmetric structure (VONYII) where a para-substituted amine is involved in a $D^2_2(9)$ motif, but the $D^2_2(7)$ motif itself is not seen in this group. This interaction is thus potentially a driver to adoption of non-centrosymmetric

structures. However, the $D^2_2(10)$ interaction is observed in 5/8 centrosymmetric structures and is thus of less interest here.

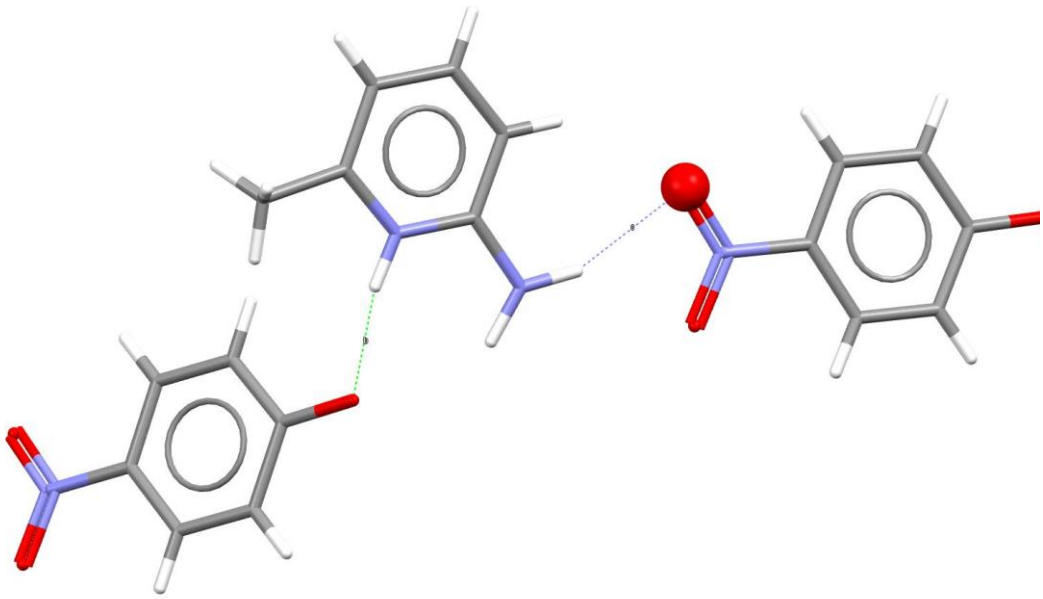

Figure 40: $D^2_2(7)$ discrete unit observed in all members of group 2 (example shown above is found in the non-centrosymmetric cocrystal of salt structure DICDIE).

A final hydrogen bonding network is seen in the structures which do not contain a coformer with para substitution present, this involves the cations and anions and involves formation of a chain structure (as seen in figure 41) through a $C^2_2(12)$ interaction. While these chains are present in a total of 8 non-centrosymmetric structures, all structures in group 2 propagate in this way through *ortho* substituted primary amines and protonated pyridine hydrogen bonds. While this motif is seen in 2 centrosymmetric cocrystal of salt structures neither involve aminopyridine coformers nor propagate along the same crystallographic axis as those observed in group 2.

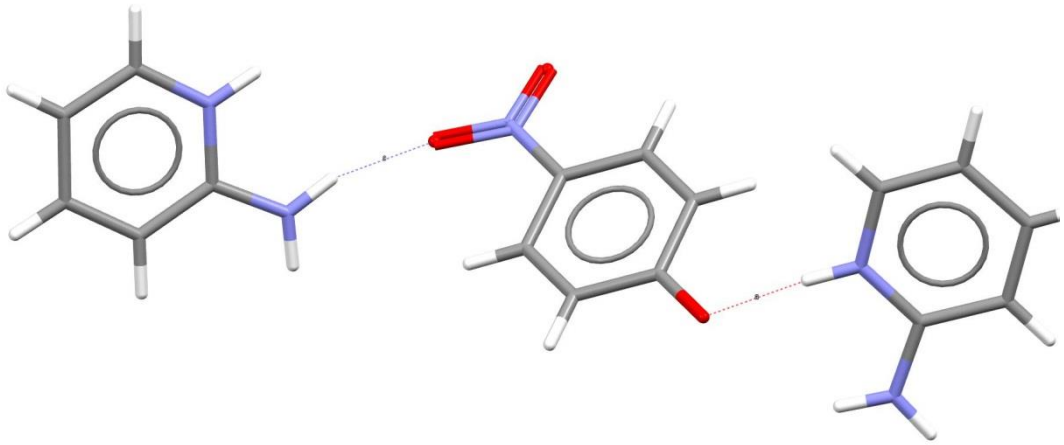

Figure 41: $C^2_2(12)$ chain seen in all members of group 2 (Example shown above is found in the non-centrosymmetric cocrystal of salt structure BORGEW).

Upon examination of the group 1 structures, they do not appear to share as many common hydrogen bonding motifs as those found in group 2. A complication is the apparent equilibrium seen for the proton of the NPO-NPOH bond of DICDEA [114] as seen in figure 42. This was modelled half way between the two O atoms meaning that the NPO and NPOH groups cannot be differentiated and so makes any comparison of this particular hydrogen bonding motif difficult. The common motifs observed in the group 1 structures are generally more complex in nature than the motifs seen for group 2 above.

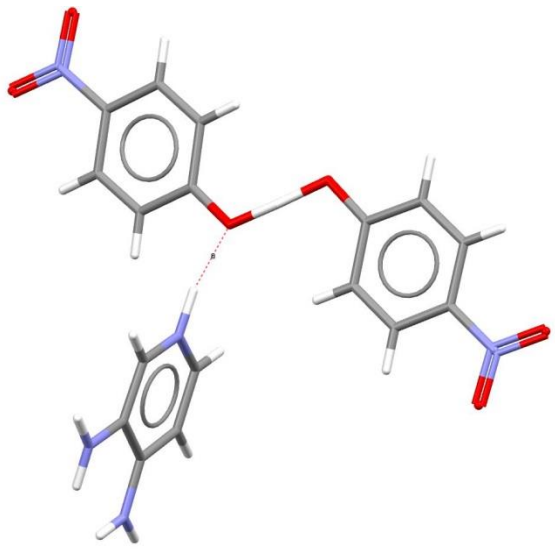

Figure 42: Asymmetric unit of DICDEA with the H atom of the NPO-NPOH unit shown in equilibrium position.

All three structures are seen to form interactions between primary amine groups and the NPO-NPOH units, although the amine groups involved are found at different substitution positions on the pyridine rings. Indeed one of the structures (DICDEA) contains an interaction between both the *meta* substituted primary amine and one of the NPOH/NPO oxygen atoms and an interaction between the *para* substituted primary amine and the other NPOH/NPO oxygen atom. All three of the structures also share common interactions between primary amines and nitro groups which form chains which are also linked by the interactions between nitrophenoxide and primary amines mentioned above. This results in a chain which can be described with a $C^2_2(10)$ notation which propagates along the crystallographic *b* axes (as seen in figure 43) this chain motif is only seen in one centrosymmetric cocrystal of salt (KUSWOL), which also propagates along the crystallographic *b* axis. Two of the structures (DICDEA and DICDOK) contain hydrogen bonding between the protonated pyridine nitrogen and the nitrophenoxide oxygen atom. The third structure (DICDAW) with no such interaction between the pyridine nitrogen and the NPO-NPOH contains interactions between the *meta* substituted primary amine and NPOH.

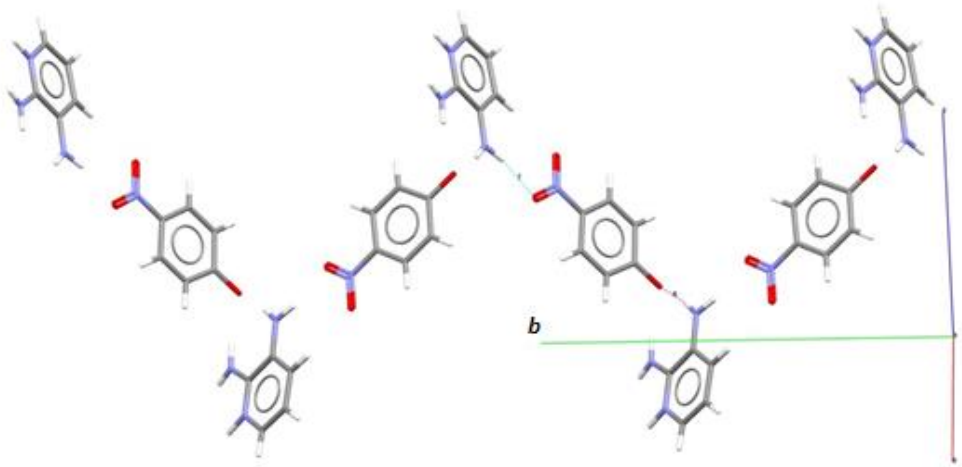

Figure 43: $C^2_2(10)$ chain which propagates along the crystallographic b axis (Example shown is found in the non-centrosymmetric cocrystal of salt structure DICDAW).

3.3 Summary of NPOH material structural analysis

When the NPOH materials are split into the three categories: salts, cocrystals and cocrystals of salts, it can be observed that the cocrystal of salts are much more likely to crystallise in a polar space group (57.8 %, 11/19) than the others. The equivalent figures for cocrystals and salts are 23.1 and 33.3 % respectively. It is likely that these structures still display a higher likelihood to crystallise in polar space groups than a random achiral organic molecule, but the added likelihood is not nearly as significant as seen in the cocrystal of salt structures.

This indicates that when designing a NLO material using NPOH and organic coformers, the formation of cocrystal of salt forms is desirable. Timofeeva et. al. state that 3 component formulation is favourable for the formation of non-centrosymmetric materials [113], though no further explanation is given as to why this should be. One way to preferentially prepare the desirable cocrystal of salt forms may be through control of the pKa difference between the two coformers. From analysis of pKa differences it was observed that cocrystal of salts are likely to form when a pKa range of 1.7-3.3 is present though this has a significant overlap with the range of pKa differences that salt forms have a tendency to form over. When hydrogen bonding donor/acceptor ratios were examined the pre-product values (1:1 coformer:NPOH) were similar for salts and cocrystal of salts, therefore there appears to be no driver for structural engineering here. Cocrystal forms however are favoured by small pKa differences and low donor/acceptor ratios, so perhaps the use of coformers that match these criteria should be avoided.

One common category of coformers found in the structures studied are the aminopyridines. There are 9 aminopyridine coformers in the data set. 8 of these form cocrystal of salt structures and one forms a salt. 8 of the structures which contain an aminopyridine coformer crystallise in non-centrosymmetric space groups (7 of these are cocrystal of salts and the remaining 1 is a salt). These coformers are thus attractive for the synthesis of NLO materials. Prakash Et. Al.

believed that *ortho*-aminopyridine substituents acted is a “hinge” between linear NPOH-NPO units and thus favoured the formation of helix structures [140] (which themselves favour non-centrosymmetric structures). This argument is too restrictive as more general aminopyridines with other substitution patterns also form non-centrosymmetric structures. In contrast the argument made by Timofeeva et. al. that a simple 3 component make up is all that is required to favour non-centrosymmetry [113] is too general. There does however appear to be a driver for non-centrosymmetric structures when aminopyridine coformers are used.

In looking for a structural driver as to why aminopyridines show a high likelihood to form non-centrosymmetric structures several observations were made. The NPOH-NPO unit previously described by Timofeeva et.al [113] is a common hydrogen bonding motif in both centrosymmetric and non-centrosymmetric structures, this unit tends to have two coplanar aromatic rings in non-centrosymmetric structures, whilst for centrosymmetric structures these are non-coplanar. Two hydrogen bonding motifs were found to be common for non-centrosymmetric cocrystal of salts and largely absent from centrosymmetric cocrystal of salts. These are small ring motifs and C(10) and C(13) chains. Five non-centrosymmetric cocrystal of salts formed helical structures through $R^1_2(6)$ motifs and the NPOH···NPO interaction, as seen in figure 44. The formation of helical structures is desirable for this work as they are a chiral structure which favours non-centrosymmetry.

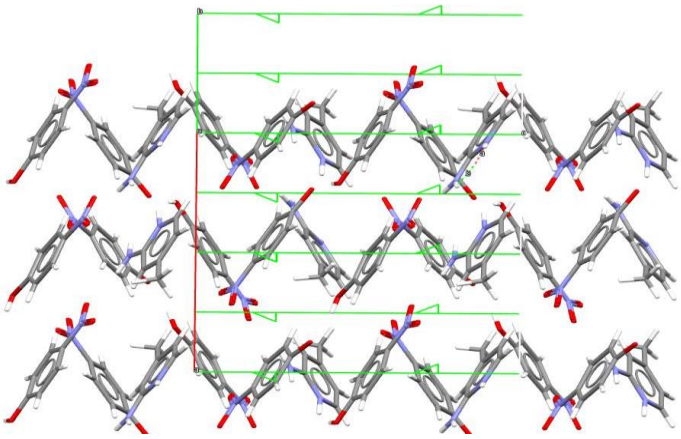

Figure 44: Helical structures formed through hydrogen bonding motifs found within the non-centrosymmetric cocrystal of salt BORGEW.

These helical structures formed through R and C motifs appear in a large percentage of non-centrosymmetric cocrystal of salt structures. Coformers unable to form such interactions can therefore be considered undesirable.

4. Conclusion

As discussed in section 1 the properties of a solid material are governed by the intermolecular interactions that arise from the packing arrangement of the molecules in the solid state. The most common method for altering the molecular packing and thus the properties of the solid state is salt formation. Two separate methods of salt formation were successfully attempted; the formation of isostructural mixed metal salts and the formation of organic salts of NPOH. The latter was done in an attempt to generate a series of NLO active materials for a structural study of factors which influence the likelihood of NPOH materials crystallising in non-centrosymmetric space groups, a condition which is required for second order NLO activity such as SHG as mentioned in section 1.6.

The synthesis of mixed metal salts of salicylic acid was attempted. Ten of these containing calcium and strontium anions sharing a crystallographic site with the chemical formula [$Ca_{(1-x)}Sr_x(C_7H_5O_3)_2(OH_2)_2$] were prepared. The structures elucidated in this body of work had the following values for x: 0, 0.041, 0.083, 0.165, 0.306, 0.529, 0.632, 0.789, 0.835 and 1. The single-crystal diffraction structures of these were successfully elucidated and refined. The strontium and calcium content of the bulk materials were also calculated through Atomic Absorption Spectroscopy. A further isostructural barium/strontium mixed metal salt of salicylic acid was prepared and its structure was solved and refined, the Ba/Sr salt had the chemical formula [$Ba_{0.27}Sr_{0.73}(C_7H_5O_3)_2(OH_2)_2$] however samples containing Mg could not be prepared. Solubility tests were then carried out on each sample where a trend of increasing aqueous solubility with increasing strontium content was observed. As expected from previous work the sample containing barium and strontium had a higher solubility than the calcium/strontium salts [85]. Systematic trends were also found in the unit cell dimensions of these species, with *a* and *c* growing as expected but *b* decreasing

slightly. Thus it has been shown that using mixed-metal salts can give systematic changes in both crystal structure and in material property.

Next the preparation of mixed metal salts of 4-nitrophenol was trialled in an attempt to create a series of NLO active materials, however no crystalline samples suitable for single crystal x-ray diffraction were obtained. The formation of organic salts of 4-nitrophenol (NPOH) was then pursued, from this 13 previously unpublished structures were synthesised and had their crystal structures solved and refined. The structures of an additional 50 relevant organic NPOH materials were found on the CSD, which were added to the structures produced in this body of work for analysis. Comparative structural analysis was carried out on these 63 structures including studying hydrogen bonding, graph set analysis, crystal packing analysis and analysis of difference in pKa values between NPOH and coformers.

It is stated in the literature that a salt form can generally be assumed to form when the difference in pKa between the two coformers is greater than 2 [66]. The samples investigated followed this observed trend with 14/16 salt forms containing coformers with pKa values at least 2 greater than NPOH. The cocrystal of salt structures in this dataset displayed a more spread range of pKa values and indeed showed some overlap with the values found for salt forms with 7/19 having ΔpKa values greater than 2. The majority of ΔpKa values for the cocrystal of salt structures however lay between 1.7 and 3.3. While the ΔpKa values for cocrystals of salts were varied a much larger range of ΔpKa values was observed in the cocrystal structures with only two coformers having ΔpKa values of 2 or greater (LAQXIM and NUDLON, both of which were zwitterions). From this it seems that which of the three categories of product described (salt, cocrystal of salt or cocrystal) forms from NPOH with a given coformer is broadly related to the difference in pKa between the two, however it is not entirely governed by this.

Of the three forms of NPOH materials examined (salts, cocrystals and cocrystals of salts) the cocrystal of salt structures had a significantly higher probability to

crystallise in non-centrosymmetric space groups than that of a random organic material (57.8 % vs approximately 13 %). Both other forms of NPOH materials also showed higher probability of crystallising in non-centrosymmetric space groups than random organic materials however this difference was not as significant as that seen in the cocrystal of salt structural group. While a number of hydrogen bonding motifs were observed for each category of product two interesting motifs found in non-centrosymmetric cocrystal of salt structures, these were small ring motifs such as $R^1_2(6)$ interactions and C(10) and C(13) chains. In 5 non-centrosymmetric cocrystal of salt structures these interactions were involved in the formation of helical structures which favour the formation of non-centrosymmetric structures.

When the hydrogen bonding of the NPOH structures was examined it was noted that all hydrogen bond donors were involved in hydrogen bonding interactions and thus follow Etters' rules. Both the neutral and anionic oxygen atoms of the NPOH and NPO molecules acted as reliable acceptor groups and while the nitro group is not traditionally considered a reliable hydrogen bond acceptor, a large number of NPOH/NPO structures featured hydrogen bonding interactions involving this group. One particular hydrogen bonding motif highlighted in this study to be of particular interest is the NPOH-NPO interaction, this had previously been discussed as a potential driver for crystallisation in non-centrosymmetric space groups by Timofeeva et. al. [113] though conclusions drawn in that particular study could be considered vague. It was found that while the NPOH-NPO hydrogen bond is a common structural feature in both centrosymmetric and non-centrosymmetric cocrystal of salt structures the NPOH-NPO unit tends to contain coplanar aromatic rings in non-centrosymmetric structures, while these tend to be non-coplanar in centrosymmetric structures.

While carrying out crystal packing analysis, two isostructural groups were found when comparing the packing of NPOH fragments. These two groups contained coformers which were shared similar molecular structures (aminopyridines). As mentioned in section 3.3 these aminopyridines appear to have a higher

likelihood to crystallise in non-centrosymmetric space groups with Prakash et. al. claiming that *ortho* substituted aminopyridines formed helical structures [140](which in themselves are a chiral structure) leading to an increased likelihood of crystallising in non-centrosymmetric space groups. This conclusion is perhaps too specific, however 5 structures that crystallised in polar space groups did form these helical structures.

Further work:

An area for further investigation stemming from this study would be the expansion of the work on mixed metal salt forms. This could be pursued through two paths; the first would be through the use of other metal cations, the second would be attempted synthesis of mixed metal salts of other functional materials. This could be further developed with continued analysis of any materials successfully synthesised including: solubility tests, analysis of mechanical properties and thermal analysis.

Further investigation of the work in this study covering NPOH materials can also be expanded by further increasing the sample size of the data being analysed. This extended data set could be further expanded through structural analysis similar to that carried out in this study, allowing further investigation into the structural features that favour crystallisation in non-centrosymmetric space groups. Finally the NPOH materials studied in this work should have their SHG properties measured in order to gauge their functionality as NLO materials.

References

1. C. B. Aakeroy, *J. Am. Chem. Soc*., 2009, **131**, 17048
2. N. Arunkumar, M. Deecaraman, C. Rani, *Asian J. Pharm.,* 2009, **9**, 168
3. L. Infantes, S. Motherwell, *Chem. Commun.,* 2004, **0**, 1166
4. J. Th. H. Van Eupen, R. Westheim, M.A. Deij, H. Meekes, P. Bennema, E. Vlieg., *Int. J. Pharm*., 2009, **368**, 146
5. M. J. Zaworotko, *Cryst. Growth Des.,* 2012, **12**, 2147
6. C. Brough, R. O. Williams, *Int. J. Pharm*., 2013, **453**, 157
7. J. W. Steed, *Trend Pharm. Sci.*, 2013, **34**, 185
8. R. R. Pfeiffer, K. Yang, M. A. Tucker, *J. Pharm. Sci*., 1970, **59**, 1809
9. S. R. Byrn, *Solid State Chemistry of Drugs*, *Academic Press, New York,* 1982
10.. N. Kaneniwa, T. Yamaguchi, N. Watari, M. Otsuka, *Yakugaku Zasshi, 1984,* ***104****, 184*
11. H. G. Brittain, *Polymorphism in Pharmaceutical Solids, Marcel Dekker Inc., New York,* 1999
12. J. Aaltonen, M. Alleso, S. Mirza, V. Koradia, K. C. Gordon, J. Rantanen, *Eur. J. Pharm. Biopharm.*, 2009, **71**, 23
13. T. L. Threlfall, *Analyst*, 1995, **120**, 2435
14. Y. Koboyashi, S. Ito, S. Itai, K. Yamamoto, *Int. J. Pharm.,* 2000, **193**, 137
15. C. P. Price, A. L. Grzesiak, J. W. Kampf, A. J. Matzfer, *Cryst. Growth Des*., 2003, **23**, 1021
16. M. L. Verdonk, J. C. Cole, M. J. Hartshorn, C. W. Murray, R. D. Taylor, *Proteins*, 2003, **52**, 609
17. B. Hancock, G. Zografi, *J. Pharm. Sci*., 1997, **86**, 1
18. A. M. Healy, Z. A. Worku, D. Kumar, A. M. Madi, *Adv. Drug Del. Rev*., 2017, **117**, 25

19. S. R. Byrn, R. R. Pfeiffer, J. G. Stowell, *Solid-State Chemistry of Drugs*, SSCI., West Lafayette, 1999
20. J. Bauer, S. Spanton, R. Henry, J. Quick, W. Dziki, W. Porter, J. Morris, J. Deming, P. Bauer, J. Donaubauer, B.A Narayanan, M. Soldani, D. Riley, K. Macfarland, *Org. Process Res. Dev.*, 2000, **4**, 413
21. R. J. Choi, J. Y. Yoo, H-S. Kwak, B. Uk Nam, J. Lee, *Curr. Appl. Phys.,* 2005, **5**, 472
22. R. J. Choi, J. Y. Yoo, N. H. Sandhu, A. W. Malick, H. Zia, *J. Pharm. Sci*., 2008, **97**, 2286
23. E. R. Cooper, *J. Control*., 2010, **141**, 300
24. A.M. Gualandi-Signorini, G. Giorgi, *Eur. Rev. Med. Pharm. Sci*., 2001, **5**, 73
25. K. B. Pfeiffer, P. Langguth, P. Grass, H. Hausler, *Eur. J. Pharm. Bio*., 2003, **56**, 393
26. A. Dahan, J. M. Miller, G. L. Amidon, *AAPS J*, 2009, **11**, 740
27. B. C. Hancock, M. Parks, *Pharm. Res*., 2000, **17**, 397
28. M.M. Crowley, F. Zhang, M.A.Repka, S. Thumma, S.B. Upadhye, S. Battu Kumar, J.W.McGinity, C. Martin, *Drug Del. Ind. Pharm*., 2007, **33**, 909
29. Guidance for industry, ANDAs: Pharmaceutical Solid Polymorphism; Food and Drug Administration: Silverspring, 2007
30. J. Th. H. Van Eupen, R. Westheim, M.A. Deij, H. Meekes, P. Bennema, E. Vlieg, *Int. J. Pharm*., 2009, **368**, 146
31. P. York, *Int. J. Pharm*., 1983, **14**, 1
32. J. Haleblian, W. McCrone, *J. Pharm. Sci*., 1969, **58**, 911
33. P. Lang, V. Kiss, R. Ambrus, P.Szabó-Révész, Z. Aigner, E. Várkonyi, *J. Pharm. Bio. Analysis*, 2013, **84**, 177
34. E. H. Lee, *Asian J. Pharm. Sci.*, 2014, **9**, 163
35. Y. Kobayashi, S. Ito, S. Itai, K. Yamamoto, *Int. J. Pharm.*, 2000, **193**, 137
36. N. Kaneniwa, T. Yamaguchi, N. Watari, M. Otsuka, *Yakugaku Zasshi*, 1984, **104**, 184
37. M. Haisa, S. Kashino, H. Maeda, *Acta Cryst. Sect. B*, 1974, **30**, 2510
38. M. Haisa, S. Kashino, R. Kawai, *Acta Cryst. Sect. B*, 1976, **32**, 1283

39. L. H. Thomas, C. Wales, L. Zhao, *Cryst. Growth Des*., 2011, **11**, 1450
40. P. D. Martino, P. Conflant, M. Dranche, *J. Therm. Anal.,* 1997, **48**, 447
41. M. Szelagiewicz, C. Marcolli, S. Cianferani, *J. Therm. Anal.*, 1999, **57**, 23
42. W. Herbst, K. Hunger, G. Wilker, H. Ohleier, R. Winter, Industrial Organic Pigments: Production, Properties, Applications, Wiley word press, 2005
43. A. R. Kennedy, C. McNair, W. E. Smith, G. Chisholm, S. J. Teat, *Angewandte Chemie Int. Ed.*, 2000, **39**, 638
44. Z. Hao, A. Iqbal, *Chem. Soc. Rev.*, 1997, **26**, 203
45. J. Bauer, S. Spanton, R. Henry, J. Quick, W. Dziki, W. Porter, J. Moris, *Pharm. Res.*, 2001, **18**, 859
46. T. Threlfall, *Org. Process Res. Dev*., 2003, **7**, 1017
47. C. P. Price, A. L. Grzesiak, J. W. Kampf, A. J. Matzger, *Cryst. Growth Des.*, 2003, **3**, 1021
48. S. Chen, I. A. Guzei, L. Y. Yu, *J. Am. Chem. Soc*., 2005, **127**, 9881
49. J. C. Castro, M. Warzechna, A. R. Kennedy, C. J. McHugh, A.J. McLean, *Cryst. Growth Des*., 2014, **14**, 4849
50. R.M. Vrcelj, J.N. Sherwood, A. R. Kennedy, H.G. Gallagher, T. Gelbrich, *Cryst. Growth Des*., 2003, **3**, 1027
51. W. Jones, *Cryst. Growth Des*., 2009, **9**, 1621
52. J. D. Dunitz, *Cryst. Eng. Comm*., 2003, **5**, 506
53. J. A. Bis, *Mol. Pharmaceut*., 2007, **4**, 401
54. O. Almarsson, M. J. Zaworotko, *Chem. Commun.,* 1997, **86**, 1
55. *Guidance for Industry: Regulatory Classification of Pharmaceutical Co-crystals; Food and Drug Administration*: Silver Spring, MD, Dec 2011
56. A. S. Tayi, *Nature*, 2011, **488**, 485
57. K. S. Huang, *J. Mater. Chem.,* 1997, **7**, 713
58. M. C. Etter, S. M. Reutzel, *J. Am. Chem. Soc*., 1991, **113**, 2586
59. M. C. Etter, *J. Am. Chem. Soc.*, 1990, **112**, 8415
60. A. V. Trask, *Mol. Pharmaceutics*, 2007, **4**, 301

61. J. D. Wuest, *Nat. Chem.*, 2012, **4**, 74
62. C. R. Groom, I. J. Bruno, M. P. Lightfoot, S. C. Ward, *Acta Cryst.*, 2016, **B72**, 171
63. L. Infantes, J. Chisholm, S. Motherwell, *Cryst. Eng. Comm.*, 2003, **5(85)**, 480
64. L. Infantes, S. Motherwell, *Cryst. Eng. Comm*., 2002, **4**, 454
65. P. Van der Sluis, J. Kroon, *J. Cryst. Growth*, 1989, **97**, 645
66. Y. Xu, L. Jiang, Y. Huang, J. R. Wang, X. Mei, *J. Pharm. Sci*., 2014, **103**, 3588
67. L. Infantes, L. Fabian, S. Motherwell, *Cryst. Eng. Comm.*, 2007, **9**, 65
68. C. Saal, A. Becker, *Eur. J. Pharm. Sci.*, 2013, **49**, 614
69. T. S. Wiedmann, A. Naqwi, *Asian J. Pharm. Sci*., 2016, **11**, 722
70. E. Nelson, *J. Am. Pharm. Assoc.*, 1957, **46**, 607
71. E. Nelson, *J. Am. Pharm. Assoc*., 1958, **47**, 297
72. E. C. Ware, D. R. Lu, *Pharm. Res.*, 2004, **21**, 177
73. S. L. Morissette, O. Almarsson, M. L. Peterson, J. F. Remenar, M. J. Read, A. V. Lemmo, S. Ellis, *Adv. Drug Deliv. Rev*., 2004, **56**, 275
74. R. J. Bastin, M. J. Bowker, B. J. Slater, *Org. Process Res. Dev.*, 2000, **4**, 427
75. Orange Book for Approved Drug Products, U.S Deperatment of Health and Human Services, Food and Drug Administration, 2018
76. S. Paulekuhn, J. B. Dressman, C. Saal, *J. Med. Chem.*, 2007, **50**, 6665
77. A. T. M. Serajuddin, *Adv. Drug Del. Rev*., 2007, **59**, 603
78. H. B. Callen, *Thermodynamics and an Introduction to Thermostatistics*, John Wiley and Sons Ltd, Chichester, UK, 1985
79. S. Li, S.M. Wong, S. Sethia, H. Almoazen, *Pharm. Res.*, 2005, **22**, 628
80. S. Li, P. Doyle, S. Metz, A. E. Royce, A. T. M. Serajuddin, *J. Pharm. Sci.,* 2005, **94**, 2224
81. S. Sweetana, M. J. Akers, *J. Pharm. Sci.*, 1996, **50**, 330
82. H. S. Gwak, J. S. Choi, H. K. Choi, *Int. J. Pharm.*, 2005, **297**, 156
83. S. L. Lin, C. J. Schwartz, C. F. Huebner, *J. Pharm. Sci.*, 1972, **61**, 1418

84. M. B. Hursthouse, *Cryst. Rev.*, 2004, **10**, 85

85. J. B. Arlin, A. J. Florence, A. Johnston, A. R. Kennedy, G. J. Miller, K. Patterson, *Cryst. Rev.,* 2011, **11**, 1318

86. H. Bock, E. Heigel, *Z. Naturforsch*, *B: Chem. Sci.*, 2000, **55**, 785

87. J. Landmann, J. A. P. Springer, M. Hailmann, V. Bernhardt-Pitchougina, H. Willner, N. Ignat'ev, E. Bernhardt, M. Finze, *Angewandte Chemie, Int. Ed.*, 2015, **54**, 11259

88. A. R. Kennedy, J. B. A. Kirkhouse, L. Whyte, *Inorg. Chem.,* 2006, **45**, 2965

89. K. L. Hull, I. Carmichael, B. C. Noll, K. W. Henderson, *Chem. Eur. J.,* 2008, **14**, 3939

90. M. Matsui, T. Watanabe, N. Kamijo, R. L. Lapp, R. A. Jacobsen, *Acta Cryst.,* 1980, **B36**, 1081

91. W. Hume-Rothery, H. M. Powell, *Z. Kristallogr.,* 1935, **91**, 23

92. U. Mizutani, *In Hume-Rothery Rules for structurally complex alloy phases*. Boca Raton, FL.: CRC Press- Taylor & Francis group

93 S. Suresh, A. Ramanand, D. Jayararman, P. Mani, *Rev. Adv. Mater. Sci.*, 2012, **30**, 175

94. S. J. Lalama, A. F. Garito, *Phys. Rev. A*, 1979, **20**, 1179

95. P. A. Franken, A. Hill, C. W. Peters, G. Weinrich, *Phys. Rev. Lett.*, 1961, **7**, 118

96. X. liu, Z. Yang, D. Wang, H. Cao, *Crystals*, 2016, **6**, 158

97. T. F. Krauss, T. Baba, *J. Quantum Electron.*, 2002, **38**, 724

98. R. M. Delarue, *J. Quantum Electron.*, 2002, **34**, 1

99. L. R. Dalton, P. Gunter, M. Jazbinsek, O. P. Kwon, P. A. Sullivan, *Organic Electro-Optics and Photonics: Molecules, Polymers and Crystals*; Cambridge University Press: Cambridge, UK, 2015

100. L. R. Dalton, P. A. Sullivan, D. H. Bale, *Chem. Rev.,* 2010, **110**, 25

101. B. J. Coe, S. P. Foxon, M. Helliwell, D. Rusanova, B. S. Brunschwig, K. Clays, G. Depotter, M. Nyk, M. Samoc, *Chem. Eur. J.,* 2013, **19**, 6613

102. B. E. A. Saleh and M. C. Teich, *Fundamentals of Photonics*, Wiley, New York, 1991.

103. N. J. Long, Angew. Chem., *Int. Ed. Engl*., 1995, **34**, 21

104. I. C. Khoo, Liquid Crystals. *Physical Properties and Nonlinear Optical Phenomena*, Wiley, New York, 1995.

105. P. N. Prasad and D. J. Williams, Introduction to Nonlinear Optical E*ff*ects in Molecules & Polymers, Wiley, New York, 1991.

106. L. Li, H. J. Cui, Z. Yang, X. T. Tao, X. S. Limn N. Ye, H. Yang, *Cryst. Eng. Comm.*, 2012, **14**, 1031

107. P. J. Skabara, *Organic second-order nonlinear optical materials.* In: Functional Organic and Polymeric Materials. John Wiley & Sons Ltd, Chichester, UK, pp. 295-325, 2000

108. S. K. Kurtz, T. T. Perry, *J. Appl. Phys.*, 1968, **39**, 3798

109. B. F. Levine, C. G. Bethea, C. D. Thurmond, R. T. Lynch, J. L. Bernstein, *J. Appl. Phys.*, 1972, **43**, 2765

110. B. F. Davydov, S. G. Kotovshchikov, V. A. Nefedov, *Sov. J. Quantum Electron*., 1977, **7**, 129

111. *CSD Space group Statistics – Space group Frequency Ordering 2018*

112. M. C. Etter, K. S. Huang, *Chem. Mater.*, 1992, **4**, 824

113. S. Muralidharan, P. Nagapandiselvi, T. Srinivasan, Y. Vidyalakshmi, D. Velmurugan, R. Gopalakrishnan, *Asian J. Chem.*, 2013, **25**, 10107

114. Sergiu Draguta, Marina S. Fonari, Artëm E. Masunov, Joel Zazueta, Shannon Sullivan, Mikhail Yu. Antipin, Tatiana V. Timofeeva, *Cryst. Eng. Comm*, 2013, **15**, 4700

115. B. Dhanalakshmi, S. Ponnusamy, C. Muthamizhchelvan, *J. Cryst. Growth,* 2010, **313**, 30

116. W-S. Guo, F. Guo, *Z. Kristallogr.*, 2004, **219**, 383

117. G. L. Butt, M. F. Mackay, R. D. Topsom, *Acta Cryst.*, 1987, **C43**, 1092

118. T.B.Poulsen, L.Bernardi, J.Aleman, J.Overgaard, K.A.Jorgensen, *J. Am. Chem. Soc.*, 2007, **129**, 441

119. V.H.Rodrigues, M. R.Costa, E.de M. Gomes, M. S. Belsley, *Acta Cryst.*, 2007, **E63**, 4031
120. A. Rivera, J.M. Uribe, J. Ríos-Motta, H.J. Osorio, M. Bolte, *Acta Cryst.*, 2015, **C71**, 284
121. M. J. Prakash, T. P. Radhakrishnan, *Cryst. Growth Des.*, 2005, **5**, 721
122. J-M. Xiao, *Acta Cryst.*, 2010, **E66**, 791
123. E. J. Corey, F. Xu, M. C. Noe, *J. Am. Chem. Soc.*, 1997, **119**, 12414
124. Y. Le Fur, R. Masse, *Z. Kristalogr.*, 1998, **213**, 430
125. P. Srinivasan, Y. Vidyalakshmi, R. Gopalakrishnan, *Cryst. Growth Des.*, 2008, 8, 2329
126. P. Nagapandiselvi, C. Baby, R. Gopalakrishnan, *RSC Adv.*, 2014, **4**, 22350
127. L. Lui, C. He, H. Wang, Z. Li, S. Chang, J. Sun, X. Zhang, S. Zhang, *J. Mol. Struct.*, 2011, **989**, 136
128. C. C. Evans, M. Bagieu-Beucher, R. Masse, J.-F. Nicoud, *Chem. Mater.*, 1998, **10**, 847
129. Y. Zhang, M. T. Han, *Acta Cryst.*, 2010, **E66**, 1649
130. S. Draguta, A. A. Yakovenko, M. S. Fonari, T. V. Timofeeva, *Cryst. Growth Des.*, 2014, **14**, 3423
131. N.S. Sowmya, S. Sampathkrishnan, S. Sudhahar, G. Chakkaravarthi, R.M. Kumar, *Acta Cryst.*, 2014, **E70**, 559
132. Y. Xiong, T. An, C. He, Y. Liu, J. Chen, C. Zha, H. T. Karlsson, X. Chen, *J. Chem. Cryst.*, 2002, **32**, 219
133. K. S. Haung, D. Britton, M. C. Etter, S. R. Byrn, *J. Mater. Chem.*, 1997, **7**, 713
134. X. Sheldrick, G. M. (2015). *Acta Cryst.* C**71**, 3
135. A. Altomare, G. Cascarano, C. Giacovazzo, A. Guagliardi, M. C. Burla, G. Polidori, M. Camalli, *J. Appl. Cryst.*, 1994, **27**, 435
136. L. J. Farruga, *J. Appl. Cryst.*, 2012, **45**, 849

137. MARVIN version 5.11.5 (2013). Chemaxon (<http://www.chemaxon.com>).

138. D. Trzybinksi, S. Domagala, M. Kubsik, K. Wozniak, *Cryst. Growth Des*., 2016, **16**, 1156

139. I. D. Brown, *Acta Cryst.*, 1976, A**32**, 24e31

140. M. J. Prakash, T. P. Radhakrishnan, *Cryst. Growth. Des.*, 2005, **5**, 721

141 C. F. Macrae, I. J. Bruno, J. A. Chisholm, P. R. Edgington, P. McCabe, E. Pidcock, L. Rodriguez-Monge, R. Taylor, J. van de Streek and P. A. Wood, *J. Appl. Cryst*., 2008, **41**, 466

142. L. S. de Moraes, D. Edwards, A. J. Florence, A. Johnston, B. F. Johnston, C. A. Morrison, A.R. Kennedy, *Cryst. Growth Des.*, 2017, **17**, 3277

143. R. S. Clark, J. Reid, *Acta Cryst*., 1995, A**51**, 887

144. Ichikawa, *J. Mol. Struct*., 2000, **63**, 554

145. A. R. Eberlin, M. D. Eddleston, C. S. Frampton, *Acta Cryst*., 2013, C**69**, 1260

146. A. R. Buist, A. R. Kennedy, K. Shankland, N. Shankland, M. J. Spillman, *Cryst. Growth Des.*, 2013, **13**, 5121

Appendix 1: Crystallographic and refinement details for structures elucidated in this study.

Sample ID	NP_1S,2R-(+)-methyl ephedrine	NP_ NP_1S,2R-(+)-ephedrine	NP_2-amino-3-formaldehydepyridine	NP_4-acetylpyridine
Empirical formula	C_{17} H_{22} N_2 O_4	$C_{20}H_{26}N_4O_4$	C_{12} H_{11} N_3 O_4	C_{13} H_{12} N_2 O_4
Formula weight	318.36	386.45	261.24	260.25
Temperature	123(2) K	123(2) K	123(2) K	123(2) K
Wavelength	1.5418 Å	1.5418 Å	1.5418 Å	1.54184 Å
Crystal system	Monoclinic	Monoclinic	Monoclinic	Monoclinic
Space group	P 1	C2	C2/c	$P2_1/c$
a	5.6890(5) Å	22.4074(9) Å	25.445(2) Å	14.1089(10) Å
b	11.8661(11) Å	6.6784(2) Å	3.8552(5) Å	6.9669(3) Å
c	12.9754(13) Å	13.6595(5) Å	24.305(3) Å	13.5344(9) Å
α	99.057(8)°	90°	90°	90°
β	100.409(8)°	92.019(4) °	95.1228(9)°	115.723°
γ	103.142(8)°	90°	90°	90°
Volume	820.73(14) $Å^3$	2042.81(13) $Å^3$	2374.7(5) $Å^3$	1198.53(15) $Å^3$
Z	2	4	8	4
Density (calculated)	1.288 gcm^{-3}	1.257 gcm^{-3}	1.461 gcm^{-3}	1.442 gcm^{-3}
Absorption coefficient	0.757 mm^{-1}	0.729 mm^{-1}	0.950 mm^{-1}	0.914 mm^{-1}
Reflections collected	5312	3015	3588	4145
Independent reflections	3662 [R(int) = 0.1066]	2237 [R(int) = 0.0104]	2236 [R(int) = 0.0473]	2354
Data/ restraints/ parameters	3662/ 5/ 427	2237 / 2/ 270	2236/ 0/ 184	2354/ 0/ 177
Goodness-of-fit	1.083	1.122	1.067	1.082
Final R indices [I>2sigma(I)]	R1 = 0.0933 wR2 = 0.3317	R1 = 0.0313 wR2 = 0.0878	R1 = 0.0839 wR2 = 0.2482	R1 = 0.0438 wR2 = 0.1253
R indices (all data)	R1 = 0.1416 wR2 = 0.2355	R1 = 0.0313 wR2 = 0.0878	R1 = 1.064 wR2 = 0.2143	R1 = 0.0477 wR2 = 0.1216
Largest diff. Peak and hole	0.444 and -0.576 e.$Å^{-3}$	0.147 and -0.205 e.$Å^{-3}$	0.420 and -0474 e. $Å^{-3}$	0.249 and -0.292 e. $Å^{-3}$

Sample ID	NP_amino-benzylamine	NP_tetramethyl-piperidine	NP_dipropylene triamine
Empirical formula	C_{13} H_{15} N_3 O_3	C_{15} H_{26} N_2 O_4	C_{24} H_{32} N_6 O_9
Formula weight	261.28	298.38	548.55
Temperature	123(2) K	123(2) K	123(2) K
Wavelength	1.54184 Å	1.54184 Å	1.54184 Å
Crystal system	Triclinic	Triclinic	Triclinic
Space group	P-1	P-1	P-1
a	9.6358(6) Å	6.3390(5) Å	9.4608(5) Å
b	10.8511(6) Å	10.6794(9) Å	11.5992(6) Å
c	12.8730 Å	12.8859(9) Å	13.0699(4) Å
α	103.262(5)°	100.229(7)°	76.370(3)°
β	101.757(5)°	97.982(6)°	82.766(4)°
γ	90.436(5)°	105.428(7)°	67.555(5)°
Volume	1280.52(13) $Å^3$	811.45(11) $Å^3$	1287.25(11) $Å^3$
Z	4	2	2
Density (calculated)	1.355 gcm^{-3}	1.221 gcm^{-3}	1.415 gcm^{-3}
Absorption coefficient	0.815 mm^{-1}	0.722 mm^{-1}	0.925 mm^{-1}
Reflections collected	9783	10550	10145
Independent reflections	4999 [R(int) = 0.0263]	3203 [R(int) = 0.0498]	5022 [R(int) = 0.0257]
Data/ restraints/ parameters	4999/ 0 / 383	3203/ 0 / 210	5022/ 0 / 384
Goodness-of-fit	1.132	1.098	1.060
Final R indices [I>2sigma(I)]	R1 = 0.0452 wR2 = 0.1302	R1 = 0.0500 wR2 = 0.1405	R1 = 0.0448 wR2 = 0.1208
R indices (all data)	R1 = 0.0544 wR2 = 0.1259	R1 = 0.0658 wR2 = 0.1925	R1 = 0.0503 wR2 = 0.1208
Largest diff. Peak and hole	0.398 and -0.230 e. $Å^{-3}$	0.238 and -0.233 e.$Å^{-3}$	0.295 and -0.335 e.$Å^{-3}$

Sample ID	NP_ethanolamine	NP_tris(2-amino) ethylamine	NP_N-methyl-pyrollidine
Empirical formula	$C_8 H_{12} N_2 O_4$	$C_{24} H_{37} N_7 O_{11}$	$C_{17} H_{21} N_3 O_6$
Forumula weight	200.20	599.60	363.37
Temperature	150(2) K	123(2) K	123(2) K
Wavelength	0.71073 Å	1.54184 Å	1.54184 Å
Crystal system	Monoclinic	Orthorhombic	Triclinic
Space group	$P2_1/c$	Pbca	P-1
a	11.7724(8) Å	19.3947(9) Å	6.3665(3) Å
b	11.5486(7) Å	14.3114(6) Å	7.6372(4) Å
c	7.0535(6) Å	21.0361(9) Å	18.1238(9) Å
α	90°	90°	91.210(4)°
β	105.856(8)°	90°	90.534(4)°
γ	90°	90°	99.903(4)°
Volume	922.47(12) $Å^3$	5838.9(4) $Å^3$	867.82(8) $Å^3$
Z	4	8	2
Density (calculated)	1.441 gcm^{-3}	1.364 gcm^3	1.391 gcm^{-3}
Absorption coefficient	0.117	0.923 mm^{-1}	0.895 mm^{-1}
Reflections collected	10025	13830	5582
Independent reflections	1728 [R(int) = 0.0643]	5748 [R(int) = 0.0678]	3380 [R(int) = 0.0173]
Data/ restraints/ parameters	1728/ 0/ 143	5748/ 0/ 431	3380/ 0/ 244
Goodness-of-fit	1.079	1.027	1.065
Final R indices [I>2sigma(I)]	R1 = 0.0411 wR2 = 0.0970	R1 = 0.0561 wR2 = 0.1756	R1 = 0.0419 wR2 = 0.1174
R indices (all data)	R1 = 0.0597 wR2 = 0.0870	R1 = 0.0699 wR2 = 0.1499	R1 = 0.0438 wR2 = 0.1157
Largest diff. Peak and hole	0.167 and -0.209 e.$Å^{-3}$	0.308 and -0.301 e.$Å^{-3}$	0.241 and -0.232e$Å^{-3}$

Sample ID	NP_rhodamine B	NP_isopropylamine	NP_1,4-diaminobutane
Empirical formula	C_{42} H_{43} N_5 O_9	$C_{14}H_{14}N_2O_4$	$C_{10}H_{17}N_3O_3$
Formula weight	761.81	274.27	227.14
Temperature	123(2) K	150 (2) K	298(2) K
Wavelength	1.54184 Å	0.71073 Å	0.71073
Crystal system	Monoclinic	Monoclinic	Monoclinic
Space group	$P2_1/c$	Pn	$P2_1/c$
a	22.821(2) Å	7.133(5) Å	12.5622(14) Å
b	9.8713(7) Å	5.923(5) Å	7.7582(7) Å
c	36.161(2) Å	19.454(5) Å	11.1110(12) Å
α	90°	90°	90°
β	105.611(8)°	95.803(5)°	111.887(12)°
γ	90°	90°	90°
Volume	7686.6(11) $Å^3$	817.7(9) $Å^3$	1004.8(2) $Å^3$
Z	8	2	4
Density (calculated)	1.317 gcm^{-3}	1.114 gcm^{-3}	1.330 gcm^{-3}
Absorption coefficient	0.771 mm^{-1}	0.083 mm^{-1}	0.107 mm^{-1}
Reflections collected	29363	8774	9998
Independent reflections	14528[R(int) = 0.0449]	3671[R(int) = 0.0564]	2793 [R(int) = 0.392]
Data/ restraints/ parameters	14528/ 1/ 1051	3671/ 2/ 235	2793/ 0/ 147
Goodness-of-fit	1.038	1.111	1.010
Final R indices [I>2sigma(I)]	R1 = 0.0643 wR2 = 0.1870	R1 = 0.0582 wR2 = 0.1959	R1 = 0.0483 wR2 = 0.1322
R indices (all data)	R1 = 0.0953 wR2 = 0.1598	R1 = 0.0818 wR2 = 0.1487	R1 = 0.0713 wR2 = 0.1139
Largest diff. Peak and hole	0.482 and -0.398 $e.Å^{-3}$	0.370 and -0.230 $e.Å^{-3}$	0.186 and -0.201 $e.Å^{-3}$

Sample ID	BaSrSal	CaSal100	CaSrSal9010
Empirical Formula	C_{14} H_{14} $Ba_{0.27}$ O_8 $Sr_{0.73}$	C_{14} H_{14} Ca O_8	C_{14} H_{14} $Ca_{0.96}$ O_8 $Sr_{0.04}$
Formula weight	411.35	350.33	352.27
Temperature	150(2) K	150(2) K	150(2) K
Wavelength	0.71073 Å	0.71073 Å	0.71073 Å
Crystal system	Monoclinic	Monoclinic	Monoclinic
Space group	C2/c	C2/c	C2/c
a	16.8381(7) Å	16.4233(14) Å	16.4335(7) Å
b	11.4349(5) Å	11.5002(9) Å	11.4974(4) Å
c	7.9433(3) Å	7.6203(6) Å	7.6301(3) Å
α	90°	90°	90°
β	91.280(4)°	91.914(7)°	91.778(4)°
γ	90°	90°	90°
Volume	1529.04(11) $Å^3$	1438.5(2) $Å^3$	1400.96(10) $Å^3$
Z	4	4	4
Density(calculated)	1.787 gcm^{-3}	1.618 gcm^{-3}	1.624 gcm^{-3}
Absorption coefficient	3.314 mm^{-1}	0.478 mm^{-1}	0.612 mm^{-1}
Reflections collected	10452	6630	16338
Independent reflections	1754 [R(int) = 0.0330]	1638 [R(int) = 0.0272]	1640 [R(int) = 0.0363]
Data/ restraints/ parameters	1754/ 0/ 118	1638/ 2/ 117	1640/ 0/ 118
Goodness-of-fit	1.167	1.083	1.066
Final R indices [I>2sigma(I)]	R1 = 0.0207 wR2 = 0.0439	R1 = 0.0267 wR2 = 0.0676	R1 = 0.0211 wR2 = 0.0552
R indices (all data)	R1 = 0.0227 wR2 = 0.0434	R1 = 0.0305 wR2 = 0.0653	R1 = 0.0220 wR2 = 0.0545
Largest diff. peak and hole	0.350 and -0.315 e.$Å^{-3}$	0.343 and -0.204e.$Å^{-3}$	0.228 and -0.207 e.$Å^{-3}$

Sample ID	CaSrSal8020	CaSrSal7030	CaSrSal6040
Empirical Formula	C_{14} H_{14} $Ca_{0.92}$ O_8 $Sr_{0.08}$	C_{14} H_{14} $Ca_{0.83}$ O_8 $Sr_{0.17}$	C_{14} H_{14} $Ca_{0.69}$ O_8 $Sr_{0.31}$
Formula weight	354.25	358.18	364.90
Temperature	150(2) K	150(2) K	150(2) K
Wavelength	0.70173 Å	0.71073 Å	0.71073 Å
Crystal system	Monoclinic	Monoclinic	Monoclinic
Space group	C2/c	C2/c	C2/c
a	16.4344(3) Å	16.4921(10) Å	16.5626(13) Å
b	11.4853(2) Å	11.5345(8) Å	11.4921(10) Å
c	7.641(2) Å	7.6679(16) Å	7.7041(7) Å
α	90°	90°	90°
β	91.785(2)°	91.838(6)°	91.558(8)°
γ	90°	90°	90°
Volume	1441.70(5) $Å^3$	1457.90(16) $Å^3$	1465.8(2) $Å^3$
Z	4	4	4
Density(calculated)	1.632 gcm^3	1.632 gcm^{-3}	1.653 gcm^{-3}
Absorption coefficient	0.750 mm^{-1}	1.011 mm^{-1}	1.465 mm^{-1}
Reflections collected	16552	3241	9041
Independent reflections	1642 [R(int) = 0.0304]	1659 [R(int) = 0.0324]	1656 [R(int) = 0.0347]
Data/ restraints/ parameters	1642/ 0/ 118	1659/ 0/ 118	1656/ 0/ 118
Goodness-of-fit	1.079	1.084	1.107
Final R indices [I>2sigma(I)]	R1 = 0.0211 wR2 = 0.0527	R1 = 0.0364 wR2 = 0.0931	R1 = 0.0238 wR2 = 0.0559
R indices (all data)	R1 = 0.0224 wR2 = 0.0521	R1 = 0.0418 wR2 = 0.0931	R1 = 0.0257 wR2 = 0.0550
Largest diff. peak and hole	0.305 and -0.230 e.$Å^{-3}$	0.367 and -0.377 e.$Å^{-3}$	0.278 and -0.204 e.$Å^{-3}$

Sample ID	CaSrSal5050	CaSrSal4060	CaSrSal3070
Empirical Formula	C_{14} H_{14} $Ca_{0.47}$ O_8 $Sr_{0.53}$	C_{14} H_{14} $Ca_{0.23}$ O_8 $Sr_{0.77}$	C_{14} H_{14} $Ca_{0.37}$ O_8 $Sr_{0.63}$
Formula weight	375.48	386.72	380.38
Temperature	150(2) K	150(2) K	150(2) K
Wavelength	0.71073 Å	0.71073 Å	0.71073 Å
Crystal system	Monoclinic	Monoclinic	Monoclinic
Space group	C2/c	C2/c	C2/c
a	16.5994(10) Å	16.6758(16) Å	16.6319(6) Å
b	11.4832(6) Å	11.4670(11) Å	11.4995(4) Å
c	7.7650(5) Å	7.8096(7) Å	7.7729(3) Å
α	90°	90°	90°
β	91.555(5)°	91.542(8)°	91.599(4)°
γ	90°	90°	90°
Volume	1479.57(15) $Å^3$	1492.8(2) $Å^3$	1486.05(9) $Å^3$
Z	4	4	4
Density(calculated)	1.686 gcm^{-3}	1.721 gcm^{-3}	1.700 gcm^{-3}
Absorption coefficient	2.168 mm^{-1}	2.904 mm^{-1}	2.489 mm^{-1}
Reflections collected	8207	10263	16351
Independent reflections	1691 [R(int) = 0.0464]	1711 [R(int) = 0.0893]	1704 [R(int) = 0.0357]
Data/ restraints/ parameters	1691/ 0/ 118	1711/ 2/ 118	1704/ 0/ 118
Goodness-of-fit	1.118	1.068	1.060
Final R indices [I>2sigma(I)]	R1 = 0.0270 wR2 = 0.0577	R1 = 0.0463 wR2 = 0.1167	R1 = 0.0208 wR2 = 0.0519
R indices (all data)	R1 = 0.0316 wR2 = 0.0563	R1 = 0.0544 wR2 = 0.1114	R1 = 0.0228 wR2 = 0.0509
Largest diff. peak and hole	0.251 and -0.284 $e.Å^{-3}$	1.186 and -1.436 $e.Å^{-3}$	0.488 and -0.256 $e.Å^{-3}$

Sample ID	CaSrSal2080	CaSrSal1090	SrSal100
Empirical Formula	C_{14} H_{14} $Ca_{0.21}$ O_8 $Sr_{0.79}$	C_{14} H_{14} $Ca_{0.17}$ O_8 $Sr_{0.83}$	C_{14} H_{14} O_8 Sr
Formula weight	387.85	390.00	397.87
Temperature	150(2)	150(2) K	150(2) K
Wavelength	0.71073 Å	0.71073 Å	1.5418 Å
Crystal system	Monoclinic	Monoclinic	Monoclinic
Space group	C2/c	C2/c	C2/c
a	16.6650(11) Å	16.6603(9) Å	16.7182(6) Å
b	11.4816(7) Å	11.4865(7) Å	11.4644(4) Å
c	7.8105(5) Å	7.8446(4) Å	7.8627(3) Å
α	90°	90°	90°
β	91.576(6)°	91.510(5)°	91.660(3)°
γ	90°	90°	90°
Volume	1493.90(16) $Å^3$	1501.50(14) $Å^3$	1506.37(9) Å
Z	4	4	4
Density(calculated)	1.724 gcm^{-3}	1.725 gcm^{-3}	1.754 gcm^{-3}
Absorption coefficient	2.977 mm^{-1}	3.106 mm^{-1}	5.364 mm^{-1}
Reflections collected	6802	8538	2454
Independent reflections	1716 [R(int) = 0.0414]	1720 [R(int) = 0.0440]	1272 [R(int) = 0.0162]
Data/ restraints/ parameters	1716/ 0/ 118	1720/ 0/ 118	1272/ 3/ 118
Goodness-of-fit	1.064	1.075	1.159
Final R indices [I>2sigma(I)]	R1 = 0.0243 wR2 = 0.0533	R1 = 0.0274 wR2 = 0.0645	R1 = 0.0273 wR2 = 0.0735
R indices (all data)	R1 = 0.0277 wR2 = 0.0521	R1 = 0.0322 wR2 = 0.0624	R1 = 0.0276 wR2 = 0.0733
Largest diff. peak and hole	0.311 and –0.317 e.$Å^{-3}$	0.699 and -0.479 e.$Å^{-3}$	0.685 and -0.493 e.$Å^{-3}$

Publications arising during MPhil year

The following papers were published during the year this MPhil project was carried out:

Structural study of salt forms of amides; paracetamol, benzamide and piperine.

A.R. Kennedy, N.L. King, I.D. Oswald, D.G. Rollo, R. Spiteri & A. Walls

J. Mol. Structure (2018), **1154**, 196-203.

Aqueous solubility of a series of mixed Ca/Sr salt forms of salicylic acid.

J.-B. Arlin, A. R. Kennedy & A. Walls.

Acta Crystallogr. Section C (2018), **74**, 131,-138

Other publications

Ag(I) bipyridyl coordination polymers containing functional anions.

C.A. Dodds, C.L. Hobday, A.R. Kennedy, S.C. Mckellar, K. Smillie & A. Walls.

New J. Chem. (2017) **41**, 1574-1581